PhD degree in Systems Medicine

Curriculum in Molecular Oncology

European School of Molecular Medicine (SEMM),

University of Milan and University of Naples “Federico II”

Settore disciplinare: MED/04

A GUT PATCH FOR OBESITY
superabsorbent hydrogel as a novel therapeutic intervention

Alessandra Silvestri

Humanitas Clinical and Research Center – IRCCS, Rozzano (Milan)

Tutor: Prof. Alcalay Myriam

European Institute of Oncology (IEO) - Milan

Co-Tutor: **Prof. Maria Rescigno**

Humanitas Clinical and Research Center – IRCCS, Rozzano (Milan)

PhD Coordinator: Prof. Giuseppe Viale

Anno accademico 2019 – 2020

TABLE OF CONTENTS

ABBREVIATIONS LIST

AJs - Adehrens Junctions
BAT – Brown Adipose Tissue
BMI – Body Mass Index
CMC – CarboxyMetyl Cellulose
EAT – Epididymal Adipose Tissue
EMA – European Medicines Agency
EVOC – Ex Vivo Organ Culture
FA – Fatty Acids
FDA- U.S Food and Drug Administration
FFA – Free Fatty Acids
FMT – Fecal Microbiota Transplantation
GLP-1 – Glucagon Like Peptide 1
GTT – Glucose Tolerance Test
HFD – High Fat Diet
HOMA IR – Homeostatic Model Assessment of Insulin Resistance
IBD – Intestinal Bowel Disorder
IBS – Intestinal Bowel Syndrome
IEB – Intestinal Epithelial Barrier
IF – Immuno Fluorescence
IHC – Immuno Histo Chemistry
IL-6 – Interleukin 6
IR – Insulin Resistance
ITT – Insulin Tolerance Test
JAM-A – Junctional Adhesion Molecule-A
LFD- Low Fat Diet
LPS – Lipopolysaccharide
MAC - Microbiota-accessible carbohydrates
MLCK – Myosin Light Chain Kinase
NAFLD – Non-Alcoholic Fatty Liver Disease
NASH – Non-Alcoholic Steato Hepatitis
ORO – Oil Red O
PYY- Peptide YY
SCFAs – Short Chain Fatty Acids
T2M – Type 2 Diabetes
TJs – Tight Junctions
TLR-4 – Toll Like Receptor 4
TNF-α - Tumor Necrosis Factor-alpha
VLDL – Very Low Density Lipoproteins
WAT – White Adipose Tissue
ZO-1 – Zonula Occludens-1

FIGURES INDEX

EXPERIMENTAL SCHEMES INDEX

ABSTRACT

The intestinal barrier is the first line of defense against pathogens that separates our body from the external environment. Its function is to maintain intestinal tissue homeostasis, regulating the passage of molecules and protecting from harmful microbes. This barrier is made up by the mucus layer, critical for limiting the exposure to the gut microbiota, and by intestinal epithelial cells sealed by inter-epithelial tight junctions. A strong cause-effect relation between intestinal permeability alterations and both intestinal and systemic diseases (like obesity, type 2 diabetes and NAFLD) is becoming evident, suggesting that restoring proper gut permeability by targeting the intestinal epithelial barrier could represent a successful intervention. The present study proposes the use of a naturally-derived superabsorbent hydrogel to restore gut permeability, likely acting on the intestinal epithelial barrier, either directly or indirectly.

In a mouse model of HFD-induced obesity, hydrogel diet supplementation prevented early development of adiposity, hepatic steatosis and intestinal barrier perturbations, mainly reinforcing intestinal epithelial TJ and inhibiting bacterial LPS translocation and endotoxemia. In long-term HFD experiments, both prophylactic and therapeutic hydrogel administration reduced body weight, adipose tissue deposition and improved metabolic parameters; notably, this was paralleled by the restoration of intestinal barrier permeability, thus limiting endotoxemia, as well as the reshaping of the gut microbiota composition despite dysbiosis associated to HFD feeding. Indeed, both dysbiosis and low-grade inflammation are hallmarks of metabolic diseases.

Collectively our data show the potentiality of this superabsorbent hydrogel as a completely naturally-derived and non-invasive therapeutic tool for the treatment of obesity and metabolic disorders.

Keywords:

Intestinal barrier, obesity, metabolic disorder, superabsorbent hydrogel, tight junctions, endotoxemia, gut microbiota

INTRODUCTION

1. Obesity and metabolic disorders

Obesity is a major health and economic issue worldwide, associated with excess mortality and morbidity. Obesity is defined by the World Health Organization (WHO) as "an abnormal or excessive fat accumulation that presents a risk to health". Over the past 50 years, the prevalence of obesity has increased worldwide to pandemic proportions[1]. According to recent studies, providing trends for all countries in the world, based on body weight and height data measured from 128.9 million people, obesity prevalence increased over 18% between 1975 and 2016 worldwide[2]. With more than 1.9 billion adults (over 18 years old) overweight and among these over 650 million obese in 2016 (data from WHO). Obesity is directly linked to common conditions and metabolic alterations encompassing insulin resistance, low HDL cholesterol, high triglycerides and high blood pressure (hypertension) collectively known as "*metabolic syndrome*", a serious health condition that increases the risk of type 2 diabetes (T2D) and cardiovascular disease[3]. In addition, obesity might lead to reduced quality of life, unemployment, lower productivity and social disadvantages, thus creating and economic burden[1]. Therefore, insights in the pathogenesis of obesity and associated metabolic disorders are important to identify novel prevention and treatment strategies.

1.1 Pathogenesis of obesity

The fundamental cause of obesity is a long-term energy imbalance between excessive calories consumption and defective calories expenditure[4]. Dysfunctional accumulation of energy leads to the formation of fat depots and body weight gain[5]. In turn, a chronic excess of body fat promotes unbalanced energy homeostasis as well as the onset of an impairment in glucose, lipid and protein metabolism that can trigger chronic low-grade inflammation[6] and cardiometabolic diseases[7] .

However, obesity is a disease with a more complex multifactorial etiology, involving interactions among genetics, environmental factors and hormones. All these factors affect food intake, nutrient turnover, thermogenesis and lipids utilization[5].

Several genes have been implicated in the pathogenesis of obesity, but findings relating specific genes to obesity, in humans, are inconsistent[8]. Whereas, multiple hormones were shown to be involved in the regulation and pathophysiology of obesity, including gut-related hormones and adipokines[9,10].

Among the hormones regulating food intake and obesity, ghrelin, a circulating peptide hormone derived from the stomach, is the only known peripherally acting orexigenic hormone and is responsible for stimulating appetite[11].

Differently, all other gut-derived hormones function as anorectic agents, responsible for limiting food intake, achieving optimal digestion and absorption while preventing consequences of overfeeding, like hyperinsulinemia and insulin resistance[12].

Among gut-derived anorectic hormones, peptide YY (PYY) secreted by L cells of distal small intestine and colon, is released postprandially and it has the function of delaying gastric emptying and reducing gastric secretions. Indeed, administration of PYY before meals results in decreased food consumption[13]. L cells also secrete oxyntomodulin, another gut-derived hormone, regulating meal termination. A single infusion of oxyntomodulin was shown to suppress appetite and reduce food intake over a 12 hours period, in association with a reduction in fasting ghrelin levels[13,14]. Other hormone secreted by enteroendocrine L-cells and certain neurons, upon food consumption, is Glucagon-Like Peptide-1 (GLP-1), a long peptide deriving from specific posttranslational processing of the proglucagon peptide. GLP-1 is an in incretin hormone, with the ability of decreasing blood sugar levels in a glucose-dependent manner by enhancing insulin secretion[15]. GLP-1 has also other functions, encompassing slowdown of gastric emptying, inhibition of food intake, increase of natriuresis and diuresis, and modulation of β-cell proliferation[16]. GLP-1 receptor agonists are extensively proposed and used for the treatment of T2D and administration of high doses of liraglutide (GLP1-R agonist) is FDA approved as a pharmacologic treatment for obesity and overweight in patients with comorbidities[17]. However, high costs as well as tolerability, remain significant barriers in prescribing these medications[18].

Other key players in obesity are adipokines, hormones produced by the adipocytes. Adipokines are a family of cytokines secreted by the adipose tissue including tumor necrosis factor-alpha (TNF-α), interleukin-6 (IL-6), leptin and adiponectin. The role of TNF-α in obesity has been linked to insulin-resistance development through reduction of adiponectin synthesis and impairment of insulin signaling. Obese mice lacking either TNF-α or its receptor showed protection against developing insulin resistance[19]. Therefore, targeting TNF-α and/or its receptors has been suggested as a promising treatment for insulin resistance and type 2 diabetes[20].

IL-6 is a pleiotropic circulating cytokine proposed to be one of the main trigger of low-grade inflammation in obesity. Many studies described elevated IL-6 levels in obese patients and the role of adipocytes and adipose tissue macrophages in producing IL-6. In

obese patients, IL-6 acts by inhibiting insulin receptor signal transduction in hepatocytes, increasing circulating free fatty acids from adipose tissue and reducing adiponectin secretion[21].

Adiponectin is an insulin sensitizing, anti-inflammatory and antiatherogenic hormone. In contrast to other adipokines, adiponectin levels are reduced in adipose tissue in obese and diabetic individuals, and adiponectin levels are restored to normal levels after weight loss[22].

Studies showed that adiponectin administration in humans and mice has insulin-sensitizing, anti-atherogenic, and anti-inflammatory effects, and in certain settings, also decreases body weight[3]. Therefore, adiponectin in humans may be a potential therapeutic target in the treatment of obesity, insulin resistance,T2D, and atherosclerosis[23].

Another adipokine produced by both adipocytes and enterocytes in the small intestine is leptin. Leptin regulates energy balance by inhibiting hunger and in turn it diminishes fat storage in the adipose tissue. It acts as a dominant long-term signal in the brain where it binds to specific receptors on appetite-modulating neurons in the arcuate nucleus in the hypothalamus, inhibiting appetite. Leptin-deficient mice that lack leptin receptors have been shown to be hyperphagic and obese. Furthermore, leptin deficiency reduces energy expenditure[24]. Leptin deficiency in humans is rare and obese individuals are, in part, leptin-resistant[25].

Therefore, increased visceral fat results in increased levels of pro-inflammatory IL-6 and TNF-α as well as reduced levels of adiponectin and interleukin-10, resulting in a proinflammatory milieu that leads to insulin resistance culminating in the metabolic syndrome, T2D and atherosclerosis. Hence, visceral adiposity is key regulators of inflammation and playing a major role in the development of obesity and its related co-morbidities.

1.2 Adipose tissue in Obesity and Metabolic Syndrome

Adipose tissue is classified in two major types: white adipose tissue (WAT) and brown adipose tissue (BAT), both having a crucial role in sensing and responding to changes in systemic energy balance[26]. Adipocytes in brown adipose tissue contribute to energy expenditure via thermogenesis, mainly maintaining body temperature, while adipocytes in the white adipose tissue act as energy storage and are also responsible for the secretion of bioactive substances (i.e. adipokines). Indeed, in addition to adipocytes, WAT contains macrophages, leukocytes, fibroblasts and endothelial cells, that are responsible for the great variety of signaling molecules secreted by WAT under varying conditions.

The white adipose tissue is distributed over the entire body and has different compartments that vary in terms of cell size, metabolic activity, and its potential role in insulin resistance and other complications associated with obesity [27]. White adipose tissue depots are classified into subcutaneous adipose tissue and visceral adipose tissue based on their location in the body. Visceral adipose tissues include intra-abdominal (mainly mesenteric adipose tissue), pericardial and perirenal adipose tissue. Indeed, researchers and clinicians have been mostly interested in intra-abdominal adipose tissue, as its accumulation in obesity was shown to be closely correlated with the development of the constellation of metabolic abnormalities commonly referred to as the metabolic syndrome[26].

Although the list of clinical outcomes associated with obesity is rather extensive, the number and severity of obesity-associated complications seem to be dependent on the presence of excess fat stores in inner adipose deposits (i.e. abdominal and visceral adipose tissue), and deposits inside and surrounding normally lean tissues, such as the heart, the liver and the kidneys, generating a phenomenon referred to as ectopic fat deposition[28]. Reports have shown that the way adipose tissue manages the energy surplus, i.e. by the pathological growth of the adipocytes, has a profound effect on an individual's insulin sensitivity and dyslipidemia (manifested as high levels of triglycerides or low levels of high-density lipoprotein cholesterol)[29]. Indeed, the subcutaneous adipose tissue handles energy excess by causing adipose tissue hyperplasia - tissue growth characterized by an expansion in cell number – and expanding adipose tissue will then act as a 'metabolic reserve', protecting lean tissues (i.e. the heart, liver, pancreas and kidneys) against harmful ectopic fat deposition[29]. Conversely, if subcutaneous adipose tissue cannot expand through fat cell hyperplasia, triglyceride molecules accumulation is buffered through adipocyte hypertrophy, characterized by an enlargement of individual cells; once the adipocytes size reaches saturation and cells are no longer able to expand, their rupture stimulates macrophage invasion, with increased release of pro-inflammatory adipokines and decreased anti-inflammatory adipokines[29]. These phenomena create a pro-inflammatory milieu making the tissue prone to develop insulin-resistance. Furthermore, when the expanding capacity of hypertrophied adipocytes becomes saturated, the excess triglyceride molecules must be stored at unconventional sites, such as the liver, heart, kidneys and pancreas, generating an atherogenic, diabetogenic and inflammatory environment in the cell of these tissues[30]. Accordingly, reports have shown that visceral obesity is often accompanied by excessive fat in the liver, heart and kidneys, whereas this association is less evident for subcutaneous obesity[31]. Excess visceral adipose tissue and

excess of fat in the liver often co-occur; however some individuals with extensive visceral adipose tissue do not show fatty liver, and vice versa[32]. Clearly, local drivers of regional differences in ectopic fat deposition (i.e. genetic, hormonal and environmental) must be further explored for the development of targeted treatments.

1.3 Insulin Resistance in Obesity

Insulin has many physiological activities, among which reducing blood glucose is its primary function. Insulin is able to control glycemia by inducing glucose uptake in insulin-sensitive tissues like skeletal muscle, heart and fat, while it is able to inhibit glucose production (gluconeogenesis) in liver, kidney and small intestine. Insulin resistance occurs when insulin-sensitive tissues lose their ability to respond to insulin, and is accompanied by: hyperinsulinemia and hyperglycemia in fasting condition, increased glycosylated hemoglobin (HbA1c), postprandial hyperglycemia, hyperlipidemia, impaired glucose and insulin tolerance, increased hepatic glucose production, loss of first phase secretion of insulin, hypoadiponectinemia, and increased inflammatory markers in plasma[33]. Both obesity and type 2 diabetes are associated with insulin resistance[34].

Insulin resistance in obesity has extensively been linked to inflammation of both adipose tissue and liver. In turn, inflammation inhibits the insulin signaling activity in adipocytes and hepatocytes through several mechanisms. As previously described, visceral adipose tissue secrete specific cytokines, such as leptin and adiponectin, but also pro-inflammatory cytokines such as TNF-α and IL-6, monocyte chemoattractant protein-1 (MCP-1) and additional products of macrophages and other cells that populate adipose tissue, believed to have a major role in the development of insulin resistance[33]. TNF-α and IL-6 act through classical receptor-mediated processes, stimulating both the c-Jun amino-terminal kinase (JNK) and the IκB kinase-β (IKK-β)/nuclear factor-κB (NF-κB) pathways, resulting in upregulation of potential mediators of inflammation that can lead to insulin resistance[34]. Furthermore, in humans, the size of the visceral adipose depot and adipocyte size is linked to systemic insulin resistance, as well as increased expression of chemokines and cytokines by immune cells in the tissue[35]. These reports suggest that the propensity of visceral adipose tissue to inflammation and the subsequent secretion of cytokines, impairing in turn insulin signaling, may significantly contribute to the development of systemic insulin resistance in central obesity. Consistently with the concept that mild inflammation is causal in the development of insulin resistance,

treatment of obese mice with resolvins, endogenous lipid mediators that promote inflammatory resolution, improved glucose tolerance, decreased fasting blood glucose levels, and enhanced insulin signaling in adipose tissue[36]. This is in agreement with the positive effects reported for anti-inflammatory agents in controlling glucose levels in human affected by T2D further reinforcing this rational[37].

1.4 Hepatic steatosis and obesity

Obesity is associated with an increased risk of developing Non-Alcoholic fatty Liver Disease (NAFLD). Hepatic steatosis occurs when the amount of fatty acids in liver cells exceeds their consumption (i.e. triglycerides accumulate in the liver parenchyma) and is an hallmark of NAFLD [38]. This imbalance in intrahepatic deposit of triglycerides is the result of four main mechanisms: increased inflow of fatty acids (FA) from the peripheral circulation; increased hepatic synthesis of FA (*de novo* lipogenesis); reduced intrahepatic and peripheral FA oxidation; and reduced triglycerides release in the circulation through VLDL[39]. All these mechanisms contribute to the pathogenesis of hepatic steatosis driven by metabolic alterations. Therefore, an excessive load of intrahepatic triglycerides cause an imbalance between complex interactions of metabolic events.

Many players are involved in metabolic alterations related to NAFLD, encompassing adipose tissue, hepatic and systemic inflammation, leading to the development of insulin resistance and dyslipidemia. However, a key role has been ascribed to adipose tissue expansion and particularly to inflammatory cytokines release, involved in the pathogenesis of insulin resistance[39]. This condition also results in increased hepatic flux of FFAs and leads to the accumulation of triglycerides, mitochondrial dysfunction, reactive oxygen species production and eventually hepatic inflammation and fibrogenesis[40]. Therefore, in the context of obesity, accumulation of visceral adipose tissue becomes an important risk factor for the onset of NAFLD.

1.5 Current treatments for obesity

The management of obesity and its associated disorders has evolved in the recent years with a shift towards different strategies: dietary interventions, pharmacotherapies and surgical interventions[4].

Dietary interventions are mainly aimed at inducing weight loss. Weight loss can be achieved through a deficiency in the caloric intake, leading to a net energy deficit. Dietary therapies include: modifications in diets macronutrient composition, lowering of energy

dense macronutrients (i.e. fats and carbohydrates) intake; caloric restriction; meal replacement by low-calorie substitutes for daily meals and modifications of dietary habits (e.g. switch from Western Diet to Mediterranean-style diet)[4]. Currently available pharmacological options for obesity management are fairly limited, with most licensed for weight loss maintenance in patients with BMI (Body Mass Index) of >27 kg/m^2 with associated risk factors, or those with BMI of ≥30 kg/m^2. However, pharmacological treatment for weight loss can have adverse events and must be associated to a reduced-calorie diet and physical exercise[4]. Finally, surgical interventions comprehend: placement of an intragastric balloon, consisting of an endoscopically-deployed silicone balloon which is filled with saline and inflated in the stomach for a duration of 6 months; and bariatric surgery, considered as the treatment of choice when all other intervention have failed[4]. Several anti-obesity treatment options alone or in combination are available. However, the therapeutic benefit of these anti-obesity strategies is limited by their marginal efficacy, variable tolerability and safety profiles, and poor patient's compliance. Hence, novel, safe and effective therapeutic approaches are required to address the growing obesity epidemic.

2. Intestinal barrier

The intestine is not only the main organ involved in nutrient uptake, but it constitutes the major barrier that separates our body from the external environment[41]. The intestinal barrier allows protection against exogenous harmful and toxic substances, entering the body mainly in the form of dietary contaminants[42]. Trillions of bacteria reside in the gastro-intestinal tract constituting the so called "gut microbiota". Under normal conditions, the gut microbiota lives in symbiosis with the host, playing a vital role providing several benefits encompassing: energy harvest, protection against pathogens and regulation of host immunity. However, intestinal microbes can also represent a potential risk of infection[43]. Therefore, the intestinal mucosa has the complex assignment to act as a semi-permeable mucosa, allowing nutrients absorption and immune sensing, while limiting direct contact and passage of potentially harmful antigens and microorganism mounting an immune response, and counterbalancing growth of pathogenic bacteria[44]. The regulation of this "double faced" task is achieved by the interplay between structural components and molecular interactions, operating in a dynamic manner to maintain intestinal integrity and immune homeostasis. Accordingly, intestinal barrier has evolved as a function unit organized in a multilayered structure.

2.1 Anatomy of the intestinal barrier

The intestinal barrier is armed with a multilayer defense system working both simultaneously and sequentially. The multiple layers of this barrier from the intestinal lumen to the systemic circulation include: (1) the mucus layer, a physical barrier which prevents direct interactions between gut bacteria and intestinal epithelial cells; (2) the tight junctions, sealing juxtaposed epithelial cells, limiting paracellular transport of bacteria and of bacterial products to systemic circulation; and (3) the antibacterial proteins secreted by specialized intestinal epithelia cells, the Paneth cells, and IgA secreted by immune cells present in the lamina propria underlying the epithelial cell layer [45].

2.1.1 The mucus layer

The mucus is the first physical barrier encountered by bacteria in the gastrointestinal tract. It is made up by two layers: the outer mucus layer and the inner mucus layer. The outer mucus layer is a thicker and looser film harbored by commensal bacteria, while the inner

mucus layer is a thinner film, firmly attached to epithelial cells blocking bacteria penetration and contact with epithelial cells.

These two layers are both constituted by water and mucins, heavily glycosylated proteins secreted by specialized epithelial cells named goblet cells. Amount and composition of the mucus layer is the product of a balance between mucus secretion and degradation by bacteria[46].

Alterations in the mucus layer either by increased erosion and degradation or by deficient mucins synthesis has a major impact on intestinal barrier integrity, allowing for the penetration of bacteria and bacterial antigens and their consequent contact with epithelial cells. Consistently, reports show that Muc 2 $^{-/-}$ mice lacking MUC2 mucin, the major glycoprotein secreted by goblet cells, are characterized by increased bacterial adherence to the intestinal epithelium, a disrupted intestinal barrier and an enhanced susceptibility to colitis[47].

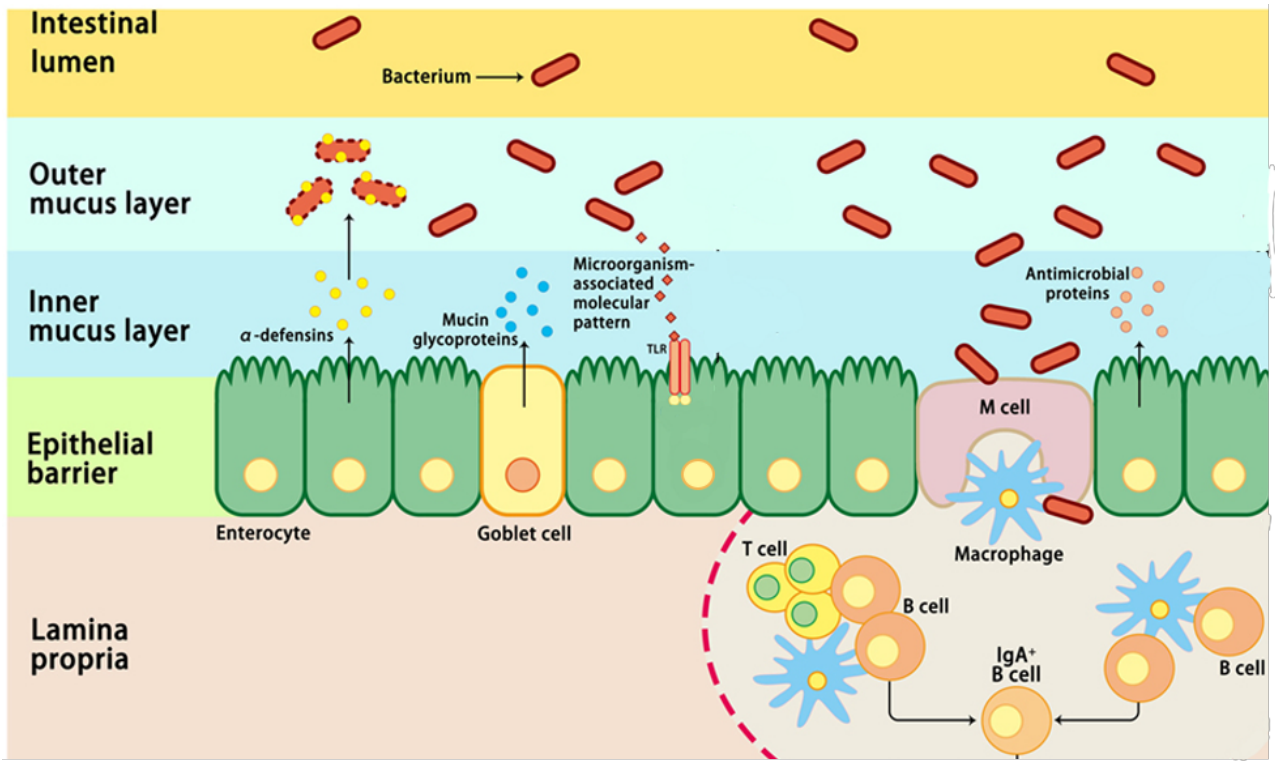

Adapted from Zang et al. "*Interactions between intestinal microbiota and Host Immune Response in Inflammatory Bowel Disease*" Frontiers in Immunology 8 (2017) 10.3389/fimmu.2017.00942

Figure 1. Intestinal Barrier a multilayer defence system.

A multilayer defence system working in cocert to the intestinal microbiota, contributing to intestinal homeostasis.

2.1.2 The intestinal epithelial layer

Underneath the mucus layer, the second level of protection of the intestinal barrier is represented by the intestinal epithelium, a continues and polarized single layer of epithelial cells that separates the lumen from the lamina propria, preventing the passage of harmful luminal components, while allowing translocation of water, electrolytes and essential dietary nutrients to the circulation.

The intestinal epithelial monolayer is composed of different types of specialized cells: enterocytes, Paneth cells, goblet cells, endocytes and microfold cells[45], each having a specialized function, but all originating from the same pool of pluripotent stem cells residing at the base of intestinal crypts[42]. The most represented cells are enterocytes, responsible for the maintenance of epithelial barrier integrity[48], followed by goblet cells, secreting mucus and resistin-like molecules, covering a central role in both repair and defense of epithelial layer and epithelial homostasis[49]. Paneth cells reside at the base of intestinal crypts and are key for stem niche maintenance and are responsible for secretion of anti-microbial peptides hindering microbial entry. Endocytes regulates antigens incoming and microfold (M cells) secreting IgA, which, in addition to goblet cells, participate in presenting bacterial antigens to dendritic cells[50].

Collectively all these cells are kept together to form a tight polarized barrier layer through virtue of intracellular tight junctions, adherens junctions and desmosomes. Molecular transport across this barrier happens through three major pathways: the paracellular pathway, characterized by passive diffusion between adjacent cells, the trans-cellular pathway, characterized by passive diffusion across cell membranes, and the carrier-mediated pathway, a type of trans-cellular pathway mediated by carrier proteins and receptors[51]. Regulation of the paracellular pathway is guaranteed by intracellular complexes localized at the level of apical-lateral cell membrane junctions and along the lateral membrane, allowing for the formation of a size-exclusive and charge selective semipermeable barrier. Hence, transport of molecules through paracellular spaces is usually referred to as “intestinal permeability”[52].

2.2 Intestinal epithelial junctions

The intestinal epithelium keeps its barrier function selective through the formation of protein-protein networks, mechanically sealing intercellular space linking adjacent cells. These protein-networks connecting epithelial cells are based on three adhesive complexes: adherens junctions, desmosomes and tight junctions[48], all together regulating paracellular pathways[53].

Adherens junctions (AJ) and desmosomes have a major role in the mechanical linkage of adjacent cells, consisting of transmembrane proteins connecting adjacent cells to the actin cytoskeleton via cytoplasmic scaffolding proteins [3]. Tight junctions (TJ) contribute to cell polarization and by sealing the intercellular space regulates paracellular transport[54].

2.2.1 Adherens junctions

The AJs accomplish multiple functions including: stabilization of cell-cell adhesion, regulation of actin cytoskeleton , intracellular signaling and transcriptional regulation[55].

AJs are composed of two protein complexes associated with cell–cell adhesion: the cadherin–catenin and the nectin–afadin complexes. The extracellular region of these proteins mediats cell-cell contacts between neighboring cells, while the intracellular domain is involved in signaling and control of AJ dynamic and interactions with the cytoskeleton[54].

2.2.2 Tight Junctions

Tight junctions marke the border between apical and basolateral cell surface domains. TJ have been proposed to have two exclusive functions: support the maintenance of cell polarity by preventing the mixing of membrane proteins between the apical and basolateral membranes, and a gate function regulating paracellular passage of ions and solutes in-between cells[55].

Main constituents of tight junctions include transmembrane proteins, like occludin, claudins and junctional adhesion molecules (JAM-A), and membrane-associated or cytoplasm proteins, like the ZO-1 family[56].

Occludin was the first TJ component to be identified; however its role remains somehow unclear[57]. It is reported to be involved in the regulation of paracellular permeability between cells, although occludin knockout mice show normal TJ strand formation and normal barrier function[58,59]. Together with occludin, claudins constitute TJ strands being the major components of this structures[60].

The claudin family consists of 27 members ranging from 20 to 27 kDa[61]. Claudin proteins play a crucial role in the formation of TJ and the preservation of epithelial barrier integrity, having also functions in cytoskeleton organization, vesicles transport and signaling pathways in direct association with scaffolding proteins.

Claudins are grouped according to their channel and barrier-forming properties into three main subgroups: cation-selective claudins (i.e. claudin 15, claudin 10b and claudin-2), anion-selective claudins (claudin 10a and claudin 17), and sealing claudins (i.e. claudin 1)[62].

The sealing group includes claudins that have not yet been associated with a specific type of molecule or ion but are thought to reduce their transport enhancing barrier functions[62]. Therefore, changes in the structure and the expression of claudins are related to alterations of intestinal barrier homeostasis contributing to the development of different disorders characterized by: decrease absorptive passage, increased secretory passages of small solutes and water and increased absorptive passage of macromolecules that can induce inflammatory processes[63]. Claudin proteins dysregulation have been correlated with increased intestinal permeability, activation of inflammation, epithelial-to-mesenchymal transition (EMT) and tumor progression in IBD as well as consequent colitis-associated colorectal cancer[61].

ZO proteins are cytoskeletal connectors of the tight junctions and scaffolding proteins of TJ [64]. ZO-1, ZO-2 and ZO-3 are members of the ZO-protein family characterized by binding domains to adherens junction proteins and the acting cytoskeleton. ZO-1 was one of the first tight junction protein identified, however its contribution to barrier function is still partly unclear, reflecting the complexity of ZO-1 interactions[65]. For instance, ZO-1 is able to bind to its related proteins ZO-2 and ZO-3, JAM-A, F-actin and various other cytoskeletal and regulatory proteins. Thus, ZO-1 knockdown models provide only limited information eliminating all these interactions together[66]. Complexity in understanding the precise functions of ZO-1 is also linked to functional redundancy among ZO proteins. However, reports show that depletion of both ZO-1 and ZO-2 in epithelial cell culture completely eliminated TJ barrier formation[67]. Moreover, in ZO-depleted cells, barrier-forming proteins (i.e. claudin and occludin) were unable to assemble into the characteristic strands found in the TJ, indicating ZO proteins are necessary for TJ assembly by acting as scaffold proteins[66].

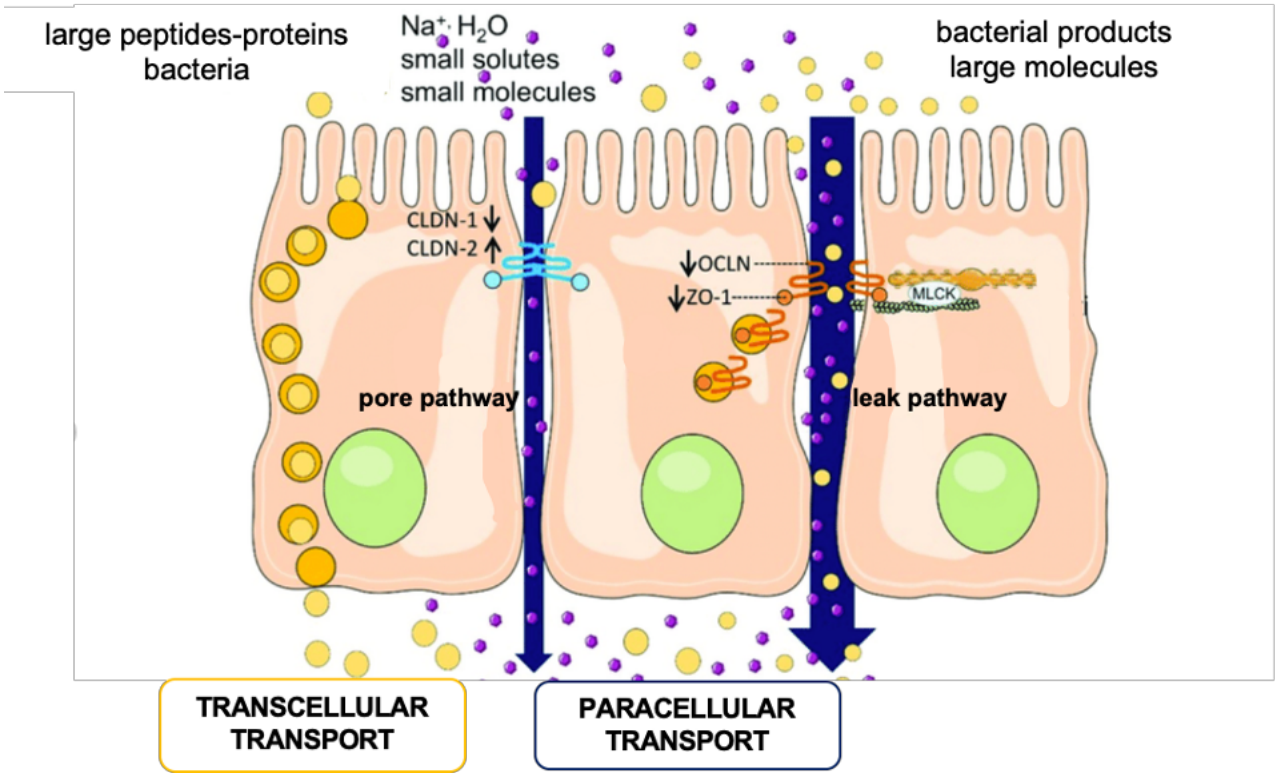

Adapted from Meijers et al. "*Intestinal Barrier Function in Chronic Kidney Disease*" Toxins. (2018) 10. 298. 10.3390/toxins10070298.

Figure 2. Paracellular-transcellular transport and tight junctions in intestinal epithelium.

Intestinal epithelial cells are tied together by tight junction complexes. Several transport pathway facilitate transport form the apical to the basolateral side encompassing: transcellular pathway, mediated by active transporters and paracellular transport trough either pore pathway or leak pathway.

3. Intestinal barrier alterations in disease

In the last two decades a number of different diseases encompassing intestinal and extraintestinal disorders, were associated with alterations in the intestinal barrier structure and permeability. Among these, intestinal bowel disorder (IBD), intestinal bowel syndrome (IBS)[68] together with celiac disease[69], and more recently obesity[70], type 2 diabetes[71] and metabolic diseases[72].

From the realization that intestinal barrier is so important in disease development, raises the question of what can disrupt the barrier. Recently, it is becoming more and more evident that beside nutritional factors also bacterial infections and toxins can play a role in the gut and affect distant organs[73].

3.1 Alteration of intestinal barrier in obesity and metabolic disorders

Loss of barrier integrity has been closely related to the onset of obesity and associated metabolic disorders, including T2D, NAFLD and NASH.

The hypothesis that such pathologies are related to alterations of intestinal barrier derives mainly form mouse studies[74,75]; however, evidence from human studies have been reported. Clinical studies, indeed, have shown a difference in gut permeability between individuals with and without T2D[71], together with an improvement in intestinal permeability in obese patients upon body weight reduction[76]. Moreover, growing evidences show that microbiota of obese and diabetic individuals is different from that of healthy population[77,78].

Diets rich in fat and sugars (i.e. Western Diet and High Fat Diet) are known to alter intestinal barrier, resulting in enhanced permeability and elevated endotoxin levels in the portal vein[79]. In agreement, tight junctions alterations have been found in animal models of High Fat Diet -induced obesity (DIO) and diabetes[80]. High Fat Diet (HFD) caused a reduction in occludin, claudin-1, claudin-3 and JAM-A expression levels in the small intestinal epithelium of rats, together with an increase level of plasma TNF-alpha[81]. Furthermore, HFD feeding changed gut microbiota composition in mice, suggesting that microbiota alterations and improved gut permeability can be associated with diet induced endotoxemia and metabolic syndrome[80]. Another study showed that alterations in gut microbiota composition in DIO mice are associated to inflammation and increased gut barrier permeability, mainly related to a reduction in the expression of ZO-1 and occludin genes.

Of note, antibiotics administration and prebiotic supplementation, prevented alterations of gut barrier functions found in obesity and diabetes[82]. Obesity-related fatty liver disorders, NAFLD and NASH, are also known to be associated with TJ dysfunction. Interactions between gut microbiota, gut-liver axis and obesity are emerging mechanisms related to the development of liver disorders often associated to obesity[83].

NAFLD patients exhibited altered intestinal morphology, increased TJ permeability and overgrowth of small intestinal bacteria. Indeed, increased intestinal permeability in NAFLD[84] mainly results from ZO-1 protein alteration[85].

Overall, it is clear that altered intestinal barrier has a role in metabolic disorders: disruption of TJ integrity[86] and subsequent translocation of bacteria and/or bacterial products from the intestine to the adipose tissue, the liver and other tissues[87,88] is the main cause of low-grade systemic inflammation, which has a central role in metabolic diseases patophysiology[89].

3.2 Bacteria and endotoxin transport through intestinal barrier

Generally, water soluble compounds of cross-sectional diameters inferior to 15 Å migrate from intestinal lumen to the circulation through intracellular spaces between epithelial cells, without involving membrane channels and transporters. Intracellular spaces are not of a sufficient dimension to allow passage of larger molecules, particulates or microorganisms, including bacteria having a cross-sectional diameter of more than 1000 Å[90].

Therefore, how bacteria and their endotoxins translocate across the intestine (i.e. transcellular vs paracellular) and whether bacteria or bacteria products can penetrate the intestinal epithelium in both baseline[91] and "stress" conditions, characterized by damaged intestinal barrier[92], are still open questions.

In vitro studies report that entire bacteria can penetrate monolayers of intestinal cell lines such as Caco-2 cells grown on permeable supports[93,94]; still, it is not clear if bacteria penetrate cells through paracellular spaces or are able to penetrate cells themselves[95]. These cell culture models, however, radically differ from the *in-vivo* situation, missing interactions with other specialized cell types, the immune system and other compartments like mucus, blood and lymphatic circulations and mesenteric nerves. Different authors have proposed the occurrence of bacteria translocation from the intestine in humans to explain sepsis and endotoxemia observed in patients with severe traumas, intestinal obstructions and liver diseases[96]. In these studies, sepsis is usually detected by the culture of enteric bacteria in the systemic circulation, in the mesenteric lymph nodes and in a

variety of extra-intestinal tissues and organs. Indeed, in these circumstances, bacteria able to reach the portal or lymphatic circulations may be then transported to multiple organs, fueling inflammation. Furthermore, studies have reported increase circulating LPS levels, and endotoxemia, in patients with sepsis[97]. Enhanced levels of LPS were also found in patients with obesity and metabolic syndrome[98,99], which might indicate bacterial translocation from the gut lumen to the circulation as a consequence of intestinal barrier function failure. In murine models, LPS circulating levels were also shown to be correlated to increased intestinal permeability.

In a recent study LPS-induced increase in intestinal permeability was mediated by TLR-4/MyD88 signal-transduction pathway up-regulation of MLCK[100]. Myosin light chain kinase (MLCK) is a Ca^{2+}/calmodulin-activated enzyme that catalyzes the myosin light chain phosphorylation, triggering actin/myosin contraction. LPS-induced increase in intestinal permeability was inhibited in MLCK$^{-/-}$ and TLR-4$^{-/-}$ mice[100]. This report is in line with another study showing that LPS causes an increase in intestinal tight junction permeability by inducing enterocyte membrane expression and localization of TLR-4 and CD14[101]. Therefore, endotoxemia itself can further promote bacterial translocation, possibly suggesting an amplification cascade.

Mechanisms by which bacteria and bacteria-derived endotoxins enter cross the intestinal epithelial barrier are still partially unclear. However, the majority of reported studies have shown a *correlative link* between alterations of intestinal epithelial barrier and endotoxemia and disease onset.

3.3 Therapeutic strategies to restore intestinal barrier

Reinforcing the intestinal barrier and in particular restoring the paracellular pathways stringency has recently been suggested as a therapeutic strategy to treat or prevent diseases driven by luminal antigens. Thus, addressing the integrity of the intestinal barrier, mainly targeting TJs, can be used as a potential therapeutic strategy to restore intestinal barrier homeostasis and prevent disorders associated to its impairment.

Two major regulators of intestinal barrier have been identified in diet - prebiotics, and secondly with intestinal microbiota – probiotics. Both players are related to lifestyle, suggesting that environmental factors might have an impact on intestinal barrier and gut health[102].

3.3.1 Dietary Intervention and Prebiotics

The only evidence for a dietary intervention helping in fortifying intestinal barrier function is the consumption of dietary fibers. High-fiber intake has been reported to be beneficial in numerous chronic diseases[103]. However, consumption of dietary fiber significantly alters the composition of the gut microbiota. Indeed, the concept of prebiotics is based on the possibility of favorable modulating the gut microbiota composition to maintain and/or promote health, using nutrients such as non-digestible and fermentable carbohydrates.

Microbiota-accessible carbohydrates (MAC), found within dietary fibers, are complex carbohydrates, resulting indigestible by the host, but fermentable by intestinal microbiota mainly in the colon. The association between consumption of non-digestible MAC and maintenance of functional intestinal barrier, is partially attributed to the production of short-chain fatty acids (SCFAs) and their release in the gut lumen. SCFAs are known to protect intestinal barrier integrity[104,105,106] and cell proliferation[107,108] through a combination of mechanisms. SCFAs, indeed, constitutes the primary energy source for colonocytes and are known to induce mucus secretion[109].

Mouse models have shown the importance of a balance between mucus secretion and erosion by the gut microbiota. Indeed, mucus consumption increases when dietary fibers become limited in the diet, and mucus is used as a backup food source by fiber-degrading microbes. In these cases, mucus becomes thinner and bacteria from the microbiota can enter in contact with intestinal epithelium, inducing inflammation and enhancing pathogen susceptibility[110]. Reports have shown the increase of both mucosal and systemic inflammatory markers in concomitance with low-fiber diets, and low fiber-diet induced mucosal thinning[111].These diet-driven modifications of the mucus layer and induction of inflammation are consistent with findings in mouse colitis models and in humans with inflammatory bowel diseases[112]. Similarly, HFD induced microbiota encroachment and low-grade inflammation in mice; process that were ameliorated when diet was supplementation with the dietary microbial-accessible carbohydrate inulin[113]. Furthermore, reports indicate that increased SCFAs production positively affects the host by exerting anti-obesity and antidiabetic effects[114]. Administration of non-digestible, fermentable carbohydrates in animals with a compromised gut barrier, consistently showed an improvement in colonic barrier functions, characterized by an increase expression of TJ proteins[115]. Indeed, dietary supplementation with SCFAs have positive results on intestinal permeability[116].

Other food-derived compounds have been shown to modulate intestinal barrier functions. For instance, zinc, an essential mineral for the survival and function of cells, has been identified as a food-derived compound able to modulate intestinal barrier. Indeed, zinc depletion was reported to impair TJs altering the expression of ZO-1, occludin, and F-actin filaments[117].

Finally, also some vitamins showed a protective effect on intestinal permeability. Vitamin D was shown to enhance the expression of TJs ZO-1 and claudin-1, and adherent junction (E-cadherin) proteins[118]. Furthermore, Vitamin A-deficient diet was shown to induce, within few weeks, alterations of gut commensals, and impairment of the intestinal barrier by changing mucin dynamics and expression of MUC2 and defensin 6[119].

3.3.2 Intestinal Bacteria and Probiotics

Several bacteria, including pathogens and commensals, have been found to directly or indirectly modulate intestinal barrier function. Therefore, the use of probiotic strains could be an important milestone in the management of gut dysfunction. Numerous studies reported the use of commensal bacteria and probiotics to promote intestinal barrier integrity *in vivo*[120,121].

Indeed, *Bifidobacterium infantis Y1*, one of the components of the probiotic product VSL3, has been shown to secrete metabolites leading to an increase in the expression of ZO-1 and occludin while reducing expression of claudin-2 leading to an amelioration of transepithelial resistance[122]. Another probiotic strain, from the VSL3, Lactobacillus plantarum MB452 was shown to induce transcription of occludin and cingulin genes[123]. Importantly, a recent report has shown that *L. plantarum* can regulate human epithelial TJ proteins *in vivo* and to confer protective effects against chemically induced disruption of the epithelial barrier in an in vitro model[124]. Administration of *L. plantarum* into healthy human volunteers was shown to significantly increase ZO-1 and occludin in TJ structures[124]. Therefore, probiotic mixtures (i.e. VSL3: L. casei, L. plantarum, L. acidophilus, L. delbrueckii, B. longum, B. infantis, *B. brevo and Streptococcus salivarius*) was reported to protect the intestinal epithelial barrier against acute colitis by preventing alterations of tight junction proteins, occludin, ZO-1 and claudins, together with an improvement of intestinal barrier function in Muc2 deficient mice[123,125]. Furthermore, inflammatory cytokines such as TNF-alpha and IFN-gamma, induced during infections and intestinal disorders (i.e. IBD) have been shown to increase intestinal permeability, while probiotics and commensal microbes were reported to revert these inflammatory dysfunctions, by improving barrier function[126].

Overall, probiotic administration and gut microbiota modulation can improve the stability of TJs in both humans and mice, and may attenuate their disruption induced by pathogens, pathogen derived antigens and inflammatory cytokine.

4 Gut Microbiota

The human intestinal tract harbors a diverse and complex microbial community, the so called "gut microbiota", which plays a central role in human health.

It has been estimated that our gut microbiota contains tens of trillions of microorganisms, including at least 1000 different species of known bacteria with 150 times more genes than humans[127,128,129].

Gut microbiota is commonly referred to as our hidden metabolic 'organ' due to its massive impact on human wellbeing. Intestinal bacteria establish a symbiotic relationship with the host shaping metabolism, physiology, nutrition and immune function[130]. Indeed, intestinal microbiota covers essential functions in body homeostasis acting both locally and systemically.

Under physiological conditions, gut bacteria contribute to the anatomy and function of the intestine: improving absorption, promoting cell renewal and participating to intestinal transit, while playing a variety of metabolic function. Gut microbiota, in fact, contributes to digestive process harvesting energy through hydrolysis of diet components as carbohydrates, proteins, and lipids and extracting essential nutrients, participating to vitamin synthesis and favoring the absorption of minerals (calcium, phosphorus, magnesium, and iron). Gut microbiota is also involved in immunomodulation and direct protection against pathogenic microorganisms[131]; trough the interaction with the immune system it favors immune cell maturation and contributes to toxin clearance[132].

Recent evidence indicated that gut microbiota coevolves with the host and that changes in gut microbial population can have major consequences, both beneficial and harmful for humans health[130]. Undeniably, it has been shown that alteration of gut microbiota, known as dysbiosis, play a key role in the development of pathological condition such as obesity[129,132], diabetes[128,133], NAFLD[134,135] and chronic inflammatory diseases such as inflammatory bowel disease (IBD), ulcerative colitis and Crohn's disease[136].

4.1 Gut Microbiota in Obesity and Metabolic disorders

Mechanisms by which gut microbiota promote metabolic alterations are still not well understood.

To date, leading theories about the mechanism include modifications in bacteria chemical signaling with local intestinal tissue and distant organs[137,138], together with increased energy harvesting by obesity associated gut microbiota.

The advance in techniques for bacteria DNA sequencing and bioinformatic tools have contributed to the identification of bacterial communities constituting gut microbiota[139]. Levels of classification are subsequentially divided in class, order, family, gender and species.

Modern tools allowed the identification of bacterial communities to species level allowing a better understanding of specific bacteria involvement in physiologic and pathologic processes.

The most predominant phyla in gut microbiota are represented by *Bacteroidetes* and *Firmicutes* together with *Actinobacteria*, *Proteobacteria* and *Verrucomicrobia*[140].

The obese microbiota is characterized by a decrease of taxa belonging to *Bacteroidetes* phylum and a proportional increase in members of the *Firmicutes* phylum, revealing an association with higher prevalence of enzymes for carbohydrates degradation and fermentation[129], improving ability to decompose the polysaccharides that cannot be digested by the host and an increase monosaccharide and short chain fatty acids production that in turn can induce lipogenesis and increase triglyceride stores[139]. Furthermore, recent studies indicated that gut microbiota alterations in obesity are probably related to a higher proportion of *Actinobacteria* and *Firmicutes* phyla, with a decrease in *Bacteroidetes*, *Verrucomicrobia* and *Faecalibaculum prausnitzii*[141]. Obese individuals experiencing weight loss display an increase of certain species of *Lactobacillus*, *Bacteroides* and *Prevotella* genus, paralleled by a reduction in species of *Bifidobacterium*, *Clostridium* and *Eubacterium* genus[142,143]. In addition, the relative proportion of *Bacteroidetes* and *Firmicutes* was augmented in obese individuals after weight loss, indicating that modulation of microbiota can be an effective means for weight management.

Furthermore, recent findings linked reduced level of *Akkermansia muciniphila*, a mucin-degrading bacteria, to both T2D and obesity[144,145]. An increase in *Akkermansia muciniphila* abundance was observed in association to an healthier metabolic state, and an improvement in lipid and carbohydrates metabolism and body fat distribution with a

decrease in waist circumference[146;147]. Together these data underline the importance of gut microbiota in the pathogenesis of obesity and metabolic disorders.
However, gut microbiota has effects beyond local tissue. Growing evidence suggest that gut microbiota contributes to metabolic disorders participating to changes in endotoxemia, bowel permeability and insulin resistance.

4.2 Obesity Induced Dysbiosis, Insulin Resistance and Endotoxemia

Several reports over the past decades have linked obesity-associated gut microbiota to insulin resistance through alterations in LPS [148].
LPS, is a major component of the outer membrane of gram-negative bacteria contributing to structural integrity, identified as a strong activator of toll-like receptor 4 (TLR4), receptor expressed in most cells and macrophages. The binding between LPS and TLR4, in turn, is known to activate extensive cell signaling pathways inducing inflammation[149].
Inflammation is considered a key component in the pathogenesis of insulin resistance and metabolic syndrome. In obesity pro-inflammatory cytokines, released by organ resident macrophages in adipose tissue, are believed to be responsible of insulin resistance development through inhibition of insulin transduction signaling[150]. Indeed, obese patients displaying insulin resistance show significantly higher number of macrophages in visceral adipose tissue in comparison to insulin sensitive ones[151]. However, factors at the base of the development of obesity related inflammatory processes driven by intestinal dysbiosis are not completely understood.
As anticipated, the two main phyla altered in obesity and metabolic syndrome are *Firmicutes* - gram positive bacteria and *Bacteroidetes* – gram negative bacteria. Although obese gut microbiota is characterized by an increase in the percentage of *Firmicutes* (gram - positive bacteria), several reports have shown elevated circulating levels of LPS in both obese mouse models and humans[152]. Cani et al., *in primis*, discovered metabolic endotoxemia, a high fat diet induced elevation of plasma LPS in obesity and its link to metabolic inflammation[97,80].
Recently LPS has been identified as a trigger for insulin resistance in adipose tissue through the induction of low-grade inflammatory processes. Indeed, LPS can be actively transported through trans-cellular pathways along with chylomicrons and then transferred to other lipoproteins by translocases. LPS-rich lipoproteins, in turn, are absorbed by large adipocyte with high metabolic activity and by macrophages in the adipose tissue,

contributing to lipid delivery and storage in adipose tissue, together with induction of tissue inflammation[153].

Association between an increase in circulating LPS levels, induction of subclinical inflammation and insulin resistance has been further demonstrated through the infusion of LPS in control mice on chow diet. LPS infusion resulted in induction of subclinical inflammation, increase adipose mass and development of insulin resistance[152]. Confirming the detrimental role played by gut microbiota derived LPS in the development of obesity and its related metabolic alterations (i.e. insulin resistance).

4.3 Obesity Induced Dysbiosis and alteration of Intestinal Barrier Permeability

The intestinal epithelium represents the first site of interaction between diet, gut microbiota and the host[74], playing a central role in the defense of the host from translocation of bacteria and bacterial antigens (e.g. LPS, peptidoglycans and flagellin) [154].Emerging evidence suggested how intestinal barrier disruption is responsible for the metabolic endotoxemia typical of obesity and type 2 diabetes. Association between obesity and increased intestinal barrier permeability has been observed both in mouse models and in humans[155,75]. Perturbations in paracellular permeability are believed to be related to an alteration in the expression, localization and distribution of tight-junctions proteins linking epithelial cells together. In particular, alterations of zonula-occludens 1 (ZO-1), claudins and occludin, proteins responsible maintenance of intestinal barrier integrity. Mechanisms at the base of alteration of intestinal barrier permeability occurring in obesity are still under investigation. However, the protective effect of SCFAs (i.e. acetate, propionate and butyrate) on the intestinal barrier is well established, and a reduction in the population of bacteria that produces butyrate may contribute to altered intestinal permeability[156]. At the cellular level, SCFAs can have direct or indirect effects on processes such as cell proliferation, differentiation, and gene expression[156]. Therefore, bacterial species feeding on non-digestible fibers and producing these metabolites appear to play a key role in the maintenance of gut health.

Among butyrate-producing bacteria we can find members of Actinobacteria, Bacteroidetes, Fusobacteria, Proteobacteria and Spirochaetes. Moreover, apart from butyrate, the production of other SCFAs such as acetate and lactate during carbohydrate fermantation is mediated by bacteria belonging to the *Actinobacteria* phylum. But also,

the mucin-degrading bacteria *Akkermansia muciniphila* belonging to *Verrucomicrobia* phylum, produces both propionate and acetate[156].

Nevertheless, diets rich in fats and obesity related dietary regimens are characterized by a very low amount of fibers, inducing in turn alterations in gut microbiota composition towards a reduction in bacterial species feeding on fibers and consequently a reduction in SCFAs production.

Indeed, reduced intake of dietary carbohydrates (i.e., plant derived polysaccharides, and resistant starch) was associated with decreases in fecal concentration of butyrate and butyrate-producing bacteria in obese individuals[157]. Furthermore, another study revealed significant reductions in fecal butyrate and total SCFAs when obese subjects had a low-fiber diet. Additionally, low-fiber diets has been shown to enhance pathogen susceptibility by establishing a microbiota feeding on colonic mucus in host[77].Therefore, diets rich in fibers have a beneficial role in obesity management promoting gut bacterial modulation towards SCFAs production and downstream singling pathways.

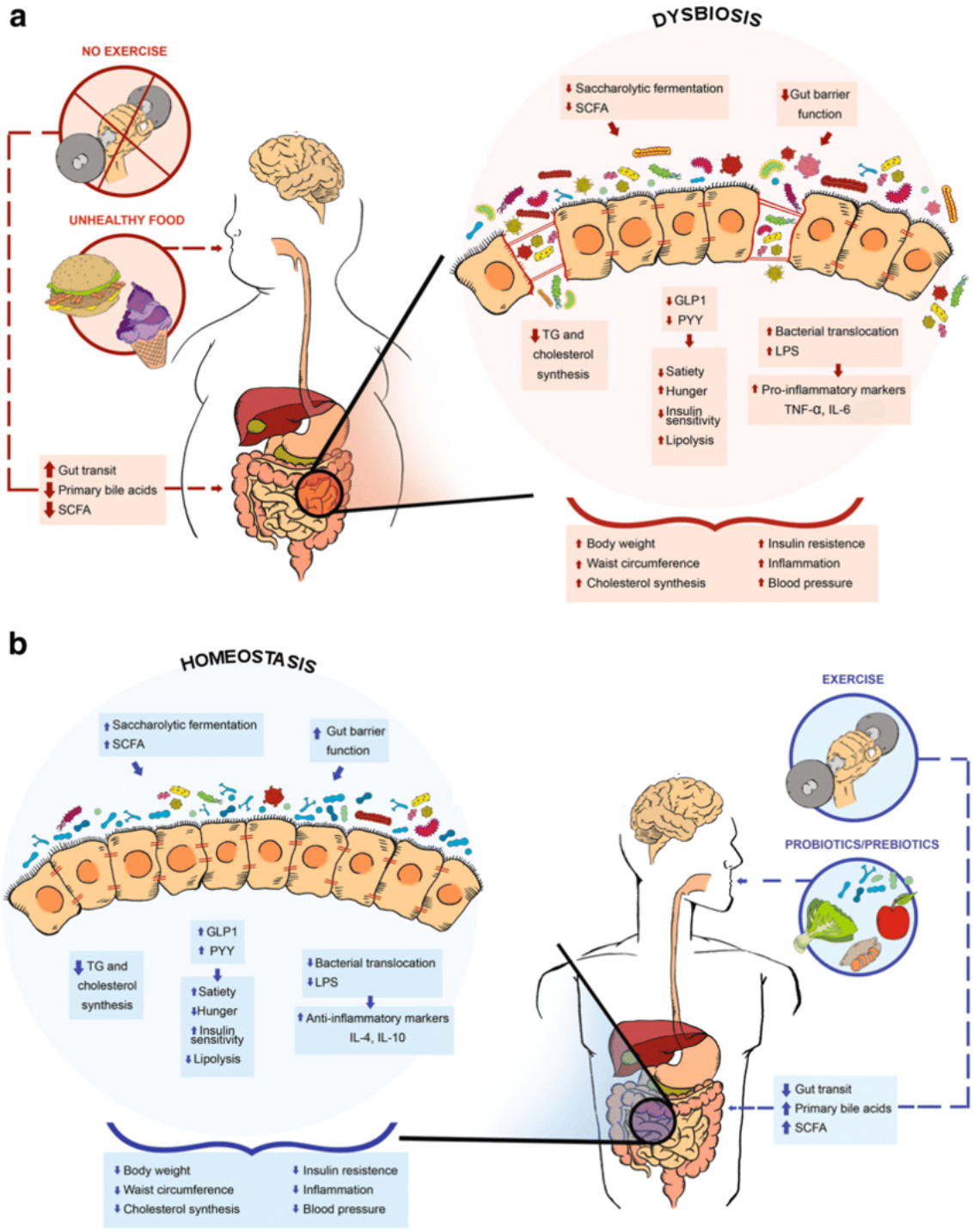

Adapted from Bianchi et al. "*Gut microbiome approaches to treat obesity in humans*" Applied Microbiology and Biotechnology. 103. (2019). 10.1007/s00253-018-9570-8.

Figure 3. Obesity associated alterations of intestinal barrier and gut microbiota.

a. Impact of high-fat and sugar rich diets and the absence of exercise on gut microbiota composition and consequent effects on obesity parameters; **b.** impact of prebiotics, probiotics and physical exercise on gut microbiota modulation and consequent effects on obesity prevention.

5. Superabsorbent Hydrogel

Therapeutic strategies aimed at managing obesity and metabolic syndrome include a change in lifestyle and dietary intervention, pharmacotherapies and bariatric surgery[4].

Dietary intervention is considered the primary strategy to treat obesity and related metabolic disorders, by reducing energy intake and potentially modulating gut microbiota to aid weight loss. However, diet and physical activity interventions often fail to promote sufficient weight loss in patients with morbid obesity, due to the difficulty in promoting long-term adherence to a lifestyle changing process[158]. Pharmacologic therapies on the other hand, are costly and associated with side effects with long term use[159]. Therefore, in this scenario, bariatric surgery remains the most effective treatment for severe obese patients when all other interventions have failed, yet is associated with significant operative risks and complications[160]. Hence, novel, safe and effective therapeutic approaches are required to address the growing obesity epidemic.

Considering the need for an alternative, effective and manageable anti-obesity tool, Gelesis company has designed an ingestible, non-systemic device for the treatment of overweight and obesity, inspired by components and structural features of raw vegetables; Gelesis developed a cellulose-based superabsorbent hydrogel, that can be administered orally and is able to mimic beneficial functions of vegetables within the gastro-intestinal tract. The superabsorbent hydrogel has recently received approval by FDA (Food and Drug Administration) clearance (April,12 2019) [161], under the name of PLENITY^{TM}, as a medical device for weight management in overweight and obese adults with a BMI of 25-40 kg/m^2, when used in association with diet and exercise.

The reason PLENITY^{TM} is considered a medical device and not a drug is related to the fact that hydrogel particles made of cellulose and citric acid expand in the stomach, absorbing water, pass through the digestive tract and are then excreted with bowel movement. Indeed, the hydrogel is not absorbed into the bloodstream during any part of the process. Therefore, the FDA considered hydrogel particles as components of a "machine" rather than a chemical.

The superabsorbent hydrogel is administered in capsules with water before meals. Hydrogel particles, once in the stomach, rapidly absorb water and homogenously mix with ingested food. When hydrated, hydrogel particles, create thousands of small individual three-dimensional gel particles with elasticity of solid ingested food, but devoid of caloric content[162], rather than forming a solid mass.

Hydrogel particles maintain their 3D structure and properties throughout the small intestine; once in the large intestine particles are partially broken down by enteric enzymes, losing their structure along with absorption capacity, releasing water. Released water is reabsorbed and remaining material is eliminated with feces (Figure 4).

Superabsorbent hydrogel administration has been demonstrated to be an effective, safe and well tolerated tool for weight management and the treatment of overweight and obese subjects: in its phase I clinical trial, GLOW (Gelesis Loss Of Weight)[162] the hydrogel, has been found to induce a significant weight loss (≥ 5%) in approximately 6 out of 10 patients, while providing positive effects on glucose homeostasis and insulin resistance. Importantly, no major side effects were observed upon hydrogel treatment, compared to placebo treated group. And no effect on the absorption of vitamins and minerals was observed after 24 weeks of administration[162].

The mechanisms at the base of the superabsorbent hydrogel functionality are still partially unknown; nonetheless, the hydrogel can be undoubtedly a new promising non-systemic strategy for the treatment of overweight and obesity with a high safety and tolerability profile[162].

In this study, we investigated the mechanisms of action of the hydrogel in diet-induced obesity mouse models; this new knowledge will contribute to understand the mechanisms behind hydrogel efficacy in successfully treating obesity and related metabolic alterations.

Adapted from https://www.gelesis.com/technology/

Figure 4. How the super-adsorbent hydrogel acts in the gastro-intestinal tract.

1.Hydrogel filled capsules are administered with water prior to meal (in humans); **2.** Particles released in the stomach expand absorbing water, getting their characteristic 3D structure; **3.** Particles mix homogenously with food increasing volume and elasticity of stomach content: **4.** Particles are cleared with liquified food to the small intestine.**5.** Particles maintain their 3D structure throughout the digestion process. **6.**Particles reach large intestine and are partially degraded; water is released and reabsorbed by body and particle are then eliminated.

AIM OF THE STUDY

The super-adsorbent hydrogel, formulated by Gelesis, has been successfully approved for the treatment of overweight and obesity. However, the mechanisms at the base of its efficacy in body weight management and maintenance of glucose homeostasis in patients are still unclear.

The aim of this work is to perform preclinical studies in diet-induced obesity murine models to investigate the mechanisms through which the hydrogel exerts its therapeutic functions.

We first recapitulated the main beneficial effects of the hydrogel in obese mice upon both prophylactic and therapeutic interventions. Next we focused on the mechanisms of action of the hydrogel in the intestine, a district that has a central role in the development of metabolic disorders and indeed is one of the main targets of the hydrogel.

We hypothesized that the hydrogel, interrelating with the intestinal mucosa, may exert its beneficial functions mainly through two non-mutually exclusive mechanisms of actions:

- Directly, interacting with the intestinal epithelium and reinforcing intestinal barrier function;
- Indirectly, reshaping gut microbiota to modulate intestinal barrier.

MATERIALS AND METHODS

1. Mice experiments

C57BL/6J mice were purchased form Charles River laboratories.

For the treatment of healthy mice with the hydrogel (scheme 1), C57BL6/J male mice at 8 weeks of age were fed with chow diet supplemented with different concentrations of Gel B (2% - 4% - 8%) and the respective control chow diet (4RF21 cod.PF1878; Mucedola Srl) for 4 weeks. After 4 weeks of feeding mice were morning fasted for 6 hours and blood samples were collected from the tail vein to measure glucose and insulin levels (experimental scheme 1).

For the preventive experiments, C57BL6/J male mice at 8 weeks of age were fed with either chow diet, LFD (10% Fat cod.PF1915; Mucedola Srl); HFD (45% Fat cod.PF1916; Mucedola Srl) and HFD supplemented with low or high doses of Gel B (2% - 4%) for short term (1-2-4 weeks – experimental scheme 4) or long term feeding (18 weeks - experimental scheme 2).

For the therapeutic setting, C57BL6/J male mice at 8 weeks of age were fed with either chow diet (Mucedola Srl) or HFD (45% Fat cod.PF1916; Mucedola Srl) for 12 weeks. After this period HFD fed mice were randomly divided in 4 experimental groups and either fed with HFD (45% Fat cod.PF1916; Mucedola Srl) or HFD supplemented with low or high doses of Gel B (2% - 4%) (experimental scheme 3).

Throughout the experiment mice were weighted and food and water intake was monitored. Mice were sacrificed at different time-points. Blood was collected through cardiac puncture to obtain sera, while internal organs, small and large intestine were collected from each mouse. Internal organs and different intestine segments were fixed in PFA 4% (paraformaldehyde 4%) and PLP Buffer (Paraformaldehyde, L-Lysine pH 7.4 and $NaIO_4$), liver and intestine samples were also collected in TRIzol Reagent for RNA extraction (Invitrogen cat.15596026). In all experiments, age-and gender-matched C57BL/6J mice were used. Diet administration started around 8-9 weeks of age for all the experiments.

All mice were maintained on a 12 hours light-dark cycle, under specific pathogen-free conditions. Experiments were performed in accordance with the guidelines established in the Principles of Laboratory Animal Care (directive 86/609/EEC) and approved by the Italian Ministry of Health. Mice were not randomized. Investigators were not blinded during experimental mice allocation and outcome assessment.

2. Rodent Diets

Mice were fed with both unrefined (chow) and adjusted-calories purified diet during the experimental procedures. Both unrefined and purified diets were supplemented with different hydrogel Gel B doses, substituting partially or entirely their cellulose component: since the hydrogel is made up of carboxymethyl cellulose and like cellulose (a natural polysaccharide present in rodent diets) it does not have any caloric contribution, we decided to replace cellulose with the hydrogel, such that the caloric content of the diets was unmodified.

As control diets we both used standard chow unrefined diet and a purified Low Fat Diet (LFD), meaning that in this diet 10% of energy comes from fat , with the majority of caloric contribution derived from carbohydrates. LFD was used mainly as a control for metabolic parameters and microbiota alterations induced by HFD. Differently from chow unrefined diet, both LFD and HFD contain low amount of fibers which are mainly responsible for gut microbiota health. Contrarily chow standard diets are very rich in fibers of different origin.

To induce obesity and metabolic disorders we used a HFD 45 % fat, in which the caloric contribution is mainly due to animal origin fat (lard). The three different diets have a different caloric intake contribution as depicted in the following pie charts, with HFD having the highest caloric content per gram of food (4,6 Kcal/gr), followed by LFD (3,6-3,8 Kcal/gr) and chow diet (3,15 Kcal/gr) as shown in Figure 5.

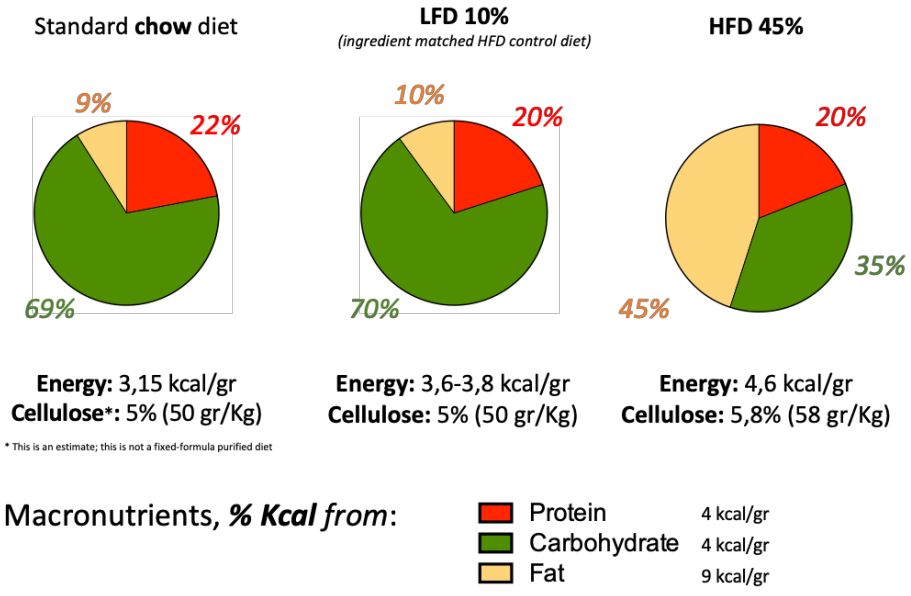

Figure 5. Macronutrient composition (% kcal) and caloric content (kcal/gr) of chow diet, LFD and HFD.

Hydrogel-Gel B was added at different concentrations in both chow and HF diets. Gel B was added in the form of a powder during diet manufacturing avoiding addition of water during the preparation procedure, in order to prevent hydrogel hydration and consequent swelling.

3. Hydrogel – Gel B

The hydrogel Gel B is an oral, non-systemic superabsorbent hydrogel made by the cross-linking of two naturally derived building blocks: carboxymethylcellulose sodium salt (CMC), obtained from the processing of plant cellulose and largely used as a thickening agent in the food industry, and citric acid (CA), a natural component of citrus fruits.
The hydrogel is created through cross-linking of cellulose by CA as previously detailed in the literature[163]. Cross-linking procedure is based on a heat activated esterification reaction occurring between the carboxylic groups of CA and the hydroxyl groups of cellulose. Combination of these two ingredients create a three-dimensional matrix that once inside the stomach adsorbs water, homogenously mixing with ingested food and gastric content. Hydrogel is highly sensitive to ionic strength and pH variations. In particular, hydrogel swelling is higher at a pH higher than the pK_a of the ionizable groups (i.e. at acidic pH, like in the stomach).
Differently from other hydrogels, rather than forming a unique mass once hydrated, the hydrogel forms small individual gel particles with an average dimension of about 2 mm, suitable to pass through pylorus and enter duodenum, minimizing the risk of obstruction in any part of the GI tract. This multiple 3D individual structures confer to the hydrogel elastic properties similar to those of solid plant-based foods with no caloric contribution. Hydrogel particles, once in the stomach, expand absorbing water and acquire a 3D structure, that is maintained throughout small intestine during the digestion process. When in the large intestine, hydrogel particles are partially degraded and eliminated. Differently from humans, in which hydrogel was administered as a powder in capsules prior to meals, hydrogel administration in mice was achieved by mixing the powder with the food recipe.

4. FITC-Dextran permeability assay

Mice were subjected to FITC-Dextran permeability assay. Animals were morning starved for 4 hours and orally administered through gavage with ~400 mg/Kg FITC-Dextran (4 kDa; Sigma Srl); blood was collected from the tail vain after 4 hours and the concentration

of FITC-Dextran in plasma samples was measured as fluorescence intensity (Clariostar Plus Microplate Reader; BMG Labtech).

5. Glucose Tolerance Test and Insulin Tolerance Test

Mice were subjected to Glucose Tolerance Test (GTT) and Insulin Tolerance Test (ITT) after different time points of feeding. Mice were morning fasted for 6 hours; basal glycemia was measured collecting blood from the tail vain using an hand-held whole-blood glucose monitor. Subsequently a bolus of glucose (GTT; 2gr/kg mouse) or insulin (ITT; 0,2UI/kg mouse) was intraperitoneally injected; blood glucose levels were then recorded every 30 minutes for 2 hours in both tests.

6. Analysis of serum parameters

Insulin and GLP-1 levels were measured by ELISA kits (Mouse Ultrasensitive Insulin ELISA, Mercodia AB and Mouse Glucagon Like Peptide 1 ELISA Kit, MyBiosource), following manufacturer's instructions. Glucose was measured on blood samples using a hand-held whole-blood glucose monitor from Roche (Accu-Chek Aviva, Roche). LPS was measured by the Limulus Amebocyte Lysate assay (Pierce), serum alanine aminotransferase (ALT) was measured using a kit (MAK052, Sigma-Aldrich, St. Louis, MO) both according to the manufacturer's instructions.

7. Immunofluorescence and confocal microscopy

Intestinal samples were fixed overnight in paraformaldehyde, L-Lysine pH 7.4 and NaIO4 (PLP buffer). They were then washed, dehydrated in 20% sucrose for at least 4 hours and included in OCT compound (Sakura). 10 μm cryosections were rehydrated, blocked with 0.1M Tris-HCl pH 7.4, 2% FBS, 0.3% Triton X-100 and stained with the following antibodies: anti-mouse CD34 (clone RAM34, eBioscience) and anti-mouse ZO-1 (clone ZO1-1A12, Invitrogen). Slices were then incubated with the appropriate fluorophore-conjugated secondary antibody. Before imaging, nuclei were counterstained with 4',6-diamidin-2-fenilindolo (DAPI) and slides were mounted in VECTASHIELD® Mounting Media (Cat.H-1000). Coverslips were permanently sealed around the perimeter with nail polish.

Slides were stored at +4°C in the dark till acquisition by confocal microscopy performed on a Leica SP8, using oil immersion objectives with x40 or x63 magnification. Fiji software package was used for image analysis.

8. ZO-1 immunofluorescence quantification

Intestinal epithelial ZO-1 was quantified using Fiji image software performing a mask on CD34 channel, to exclude endothelial ZO-1 expression. Integrated density values as the product of the area and mean intensity (intensity of fluorescence) were plotted as fold change of chow/HFD values.

9. Histological Staining

Oil red O (ORO) (Sigma) was performed on PLP buffer fixed OCT embedded frozen liver sections according to manufacturer protocol.
Sirius red (Sigma) was performed on 4 μm formalin-fixed paraffin embedded mouse liver tissue sections according to manufacturer protocol.
Brightfield images were acquired with virtual slide microscope VS120 (Olympus) using dry objective with x20 magnification. Fiji (ImageJ) software was used for image analysis.

10. Adipocyte area quantification

Adipose tissue sections (PFA fixed, paraffin embedded) were stained with Hematoxylin and Eosin and images were acquired with widefield microscope BX51 (Zaiss) using 10X objective. Adipocytes area was calculated with Imaje J software and Adiposoft plugin[164]. One field for each mouse EAT was analyzed; each field comprises an average of 70-100 adipocytes. A cut-off of 100 pixel for the equivalent diameter was set to exclude partial adipocytes from the analyses.

11. Oil Red O quantification

Oil Red O staining scoring was performed on individual mice giving a blind score from 0 to 4; where 0 represented absence of liver triglycerides and 4 represented a strong accumulation of liver triglycerides in Oil Red O stained liver sections. Scoring was

performed by two independent observers. Each square in the graph represents an individual mouse; empty – white squares represent missing animals.

12. Real-time PCR

Total RNA was extracted from ileum samples by using the DirectZol kit with on-column DNAse I treatment (Zymo Research R2071). cDNA was retrotranscribed starting from 0,5-1 µg of total RNA (Improm-II, Promega). Real time-PCR was performed on QuantStudio7 (AB, ThermoFisher), by using SybrGreen Master Mix (AB) and Quantitect oligos (Quiagen). Quantitation was done according to $2^{-\Delta\Delta Ct}$ method[165].

13. Gut microbiota analysis

DNA Extraction, Library Preparation and Sequencing

DNA was extracted and quantified, and library preparation was performed with Illumina's NexteraXT protocol. Whole metagenome sequencing was performed to a target depth of 10 million reads per sample on Illumina's NextSeq platform.

Taxonomic Classification

Sequence reads were assigned a species-level taxonomic classification using a reference taxonomic database.

Preprocessing and quality filtering of sequencing data

Sequencing reads were processed to remove sequencing adapters and filtered to remove low-quality reads, as well as contaminant reads from ribosomal or host DNA.

Functional Classification

The quality controlled metagenomes were annotated with organism-specific gene family and metabolic pathway abundances.

Beta diversity analysis

Bray-Curtis dissimilarity was used to determine the variance between all sample pairs, and the mean dissimilarity between individuals in each group.

Principal Coordinates analysis

The Bray-Curtis dissimilarity was used to generate principal coordinates (PCoA) plots.

DNA extraction, library preparation and sequencing of gut microbiota samples was performed by DNA Genoteck and Geno Finds genomic services.

14. Statistical analysis

Statistical analysis was performed using GraphPad Prism software. Values were compared using either a Student's t-test for single variable or one-way ANOVA and two-way ANOVA Tukey's multiple comparison test depending on the distribution of the data. Results were represented as Mean ± SEM. *$p<0.05$, **$p<0.01$, ***$p<0.001$.

RESULTS

1. Administration of high doses of hydrogel modulates body weight and glycemia in standard diet fed mice

It has been widely reported that alteration of the intestinal function can contribute to the pathogenesis of obesity, Type 2 Diabetes (T2D) and the metabolic syndrome in general[166].Thus, the gastrointestinal (GI) tract can represent a potential target for the prevention and the treatment of both intestinal and systemic GI-related disorders[167]. The hydrogel Gel B was designed to swell in the stomach and travel along the intestine maintaining its 3D structure, potentially targeting the whole GI tract, thereby representing a potential way for intervention. Previous clinical trials in humans (FLOW and GLOW studies[162]) pointed out two primary effects of hydrogel treatment: the induction of body weight loss and the amelioration of impaired fasting blood glucose levels in obese patients. However, the mechanisms at the base of these phenomena are still unclear. Hence, we set up an *in vivo* murine model to investigate these mechanisms, studying the potential involvement of different systems and organs in an integrated way.

At first, we wanted to identify the most suitable dose to be used in mice to recapitulate effects obtained in humans, without inducing side effects. For this purpose, we tested the effect of different doses of the hydrogel Gel B in healthy animals.

Mice were fed with a standard chow diet and with diets supplemented with different doses of hydrogel Gel B for a period of 4 weeks, as indicated in the following experimental scheme (Experimental scheme 1). Body weight, food and water intake, stool consistency and general health status of the animals were daily monitored throughout the experiment.

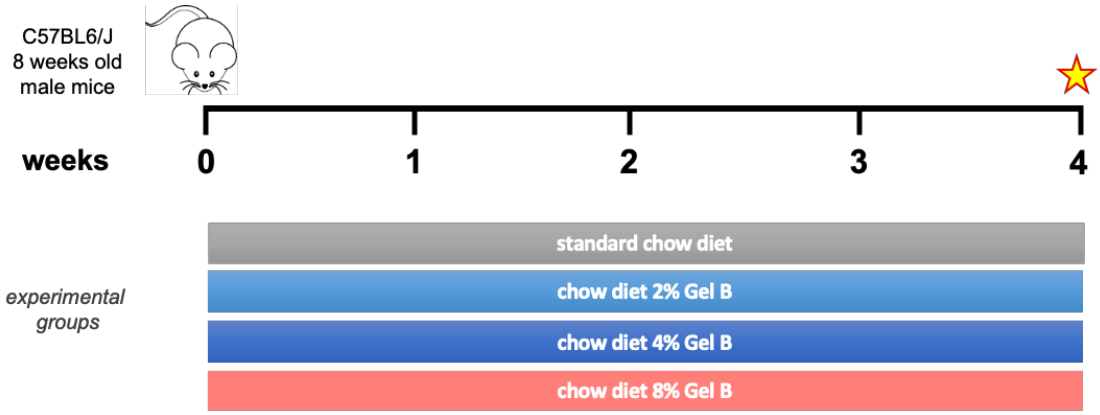

Experimental Scheme 1. Administration of hydrogel (Gel B) in healthy mice.

C57BL6/J male mice at 8 weeks of age were fed for 4 weeks with: standard chow diet (gray), chow diet supplemented with 2% hydrogel Gel B (light blue), chow diet supplemented with 4% hydrogel Gel B (blue) and chow diet supplemented with 8% hydrogel Gel B (pink). Body weight together with food and water intake were recorded throughout the experiment. At the end of the for 4 weeks of feeding (star) mice were sacrificed and several parameters were analyzed.

Mice fed with a standard chow diet supplemented with Gel B (2%, 4% and 8%) showed a dose-response reduction in body weight, with a significant decrease in those fed with the diet supplemented with the highest dose tested (Figure 6a; b). No differences in water and food intake were observed (Figure 6c), indicating that body weight loss in these animals was not paralleled by a decrease in appetite, in response to an increased gastric content volume due to hydrogel swelling in the stomach. No signs of diarrhea were observed, demonstrating that weight loss was not related to an improper intestinal transit or fluid loss either.

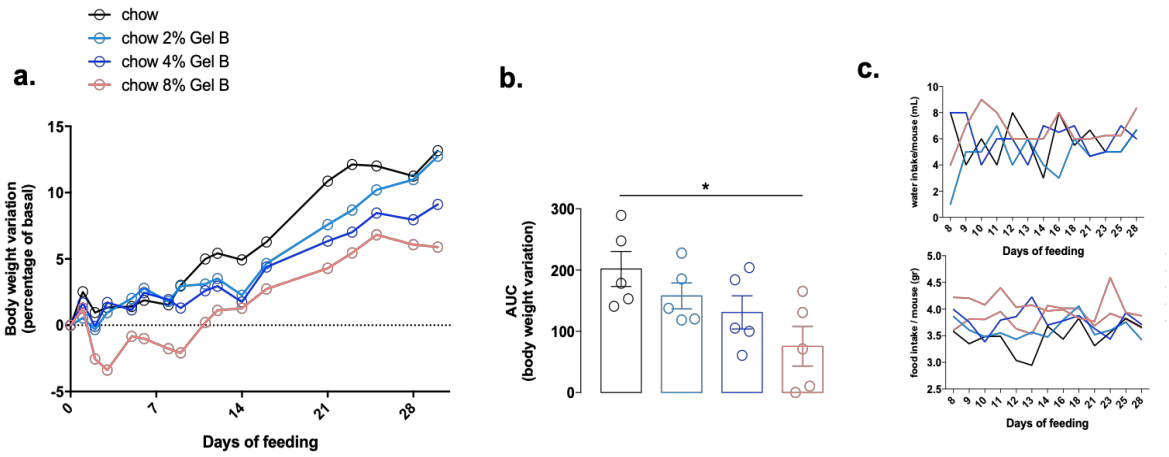

Figure 6. Administration of standard diet supplemented with increasing doses of hydrogel induces significant reduction in body weight in heathy mice, without changes in food and water intake.

Body weight together with food and water intake were monitored throughout 4 weeks of feeding **a.** body weight variation (expressed as percentage of basal); **b.** Area Under the Curve (AUC) of body weight variation curve (* p<0,5 one-way ANOVA Tukey post-test, line at mean with SEM); **c.** water intake (top panel) and food intake (lower panel) calculated for each mouse as average of 5 mice per cage.

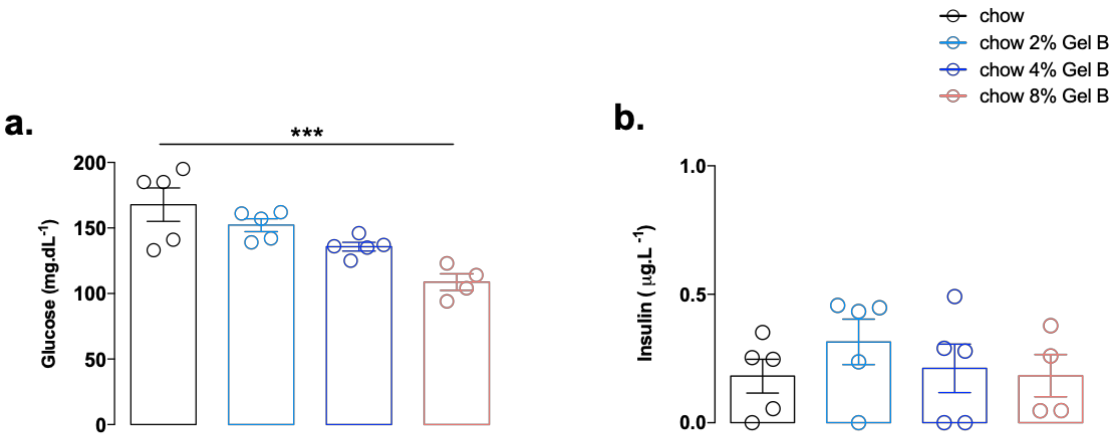

Figure 7. Administration of standard diet supplemented with high doses of hydrogel induces a significant reduction in fasting blood glucose levels without changes in insulin homeostasis.

Circulating glucose and insulin levels (**a, b** respectively) after 4 weeks of feeding with hydrogel supplemented chow diet. Mice were morning fasted for 6 hours before glucose and insulin measurements (*p<0,05, **p<0,01; ***p<0,001 one-way ANOVA Tukey post-test, line at mean with SEM; 5 mice per experimental group).

Besides, a significant reduction of fasting blood glucose concentration (although in the physiological healthy range) was observed with the highest concentration (chow 8% Gel B), without changes in blood insulin levels (Figure 7 a, b); this pointed out the ability of hydrogel Gel B to modulate blood glucose levels without interfering with insulin homeostasis.

Taken together, these data indicate that low-medium doses of hydrogel Gel B (i.e. 2% and 4%) do not elicit strong modifications in body weight and glycemia in physiological conditions. On the other hand, high doses (chow 8% Gel B) of the hydrogel induced a notable reduction in body weight and lowered blood glucose levels.

The fact that the hydrogel exerted these effects in healthy mice highlights an intrinsic ability of Gel B to control body weight gain and glycemia, anticipating what could be the *therapeutic* effect of the hydrogel in obese patients. Moreover, based on these data we choose the 2% and 4% hydrogel concentrations for further studies, performed in a diet-induced obesity mouse model.

2. Hydrogel dietary supplementation prevents alterations induced by long term high fat diet feeding

As body weight reduction and improvement in glucose metabolism were observed in overweight and obese patients, after 24 weeks of hydrogel administration[162], we set up a mouse model of diet-induced obesity to mimic these alterations and study hydrogel mechanism of action. Of note, among patients, pre-diabetic and drug-naïve type 2 diabetic individuals showed a six times higher chance of achieving more than 10% weight loss[162] after hydrogel administration. For this purpose, we induced obesity and mild metabolic alterations in animals by feeding mice with a High Fat Diet (HFD). In particular, 45% fat HFD (i.e. 45% of the kcal come from lard) was used to better mimic, in mice, the dietary regime of overweight and obese individuals.

Hydrogel was administered through the HFD, without changing the calorie content (see material and methods), by supplementing it with two doses of hydrogel (2% and 4% Gel B). Selection of these doses was based on previous preclinical data (experimental scheme 1). Indeed, both doses had a low impact on basal physiological conditions and at the same time resemble doses administered in human patients.

At first, we wanted to assess hydrogel ability in preventing the development of diet-induced obesity and correlated metabolic alterations.

We fed mice for 18 weeks with either HFD (45% fat) or HFD supplemented with low hydrogel dose (HFD 2% Gel B) and high hydrogel dose (HFD 4% Gel B); a purified Low Fat Diet (LFD, 10% fat) was used as control diet, according to the experimental design shown in Experimental scheme 2.

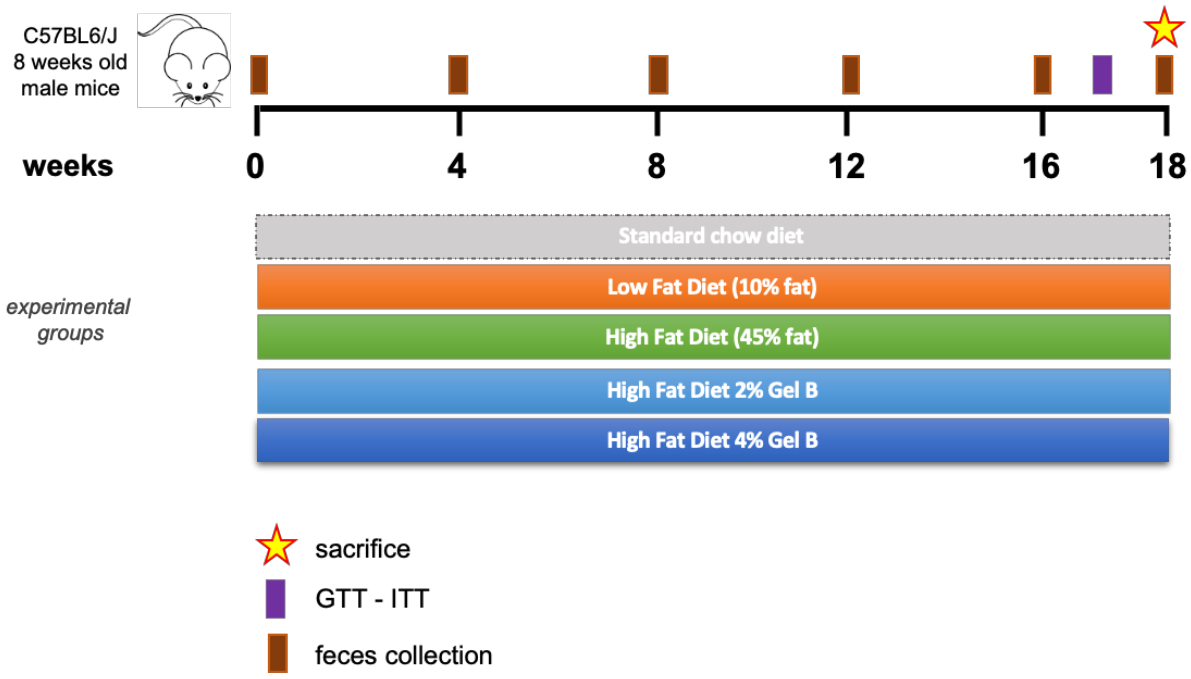

Experimental Scheme 2. Preventive hydrogel administration in a model of long term high fat diet feeding.

C57BL6/J male mice at 8 weeks of age were fed for 18 weeks with: Low Fat Diet (LFD 10% fat) in orange, High Fat Diet (HFD 45% fat) in green, HFD supplemented with 2% hydrogel Gel B in light blue and HFD supplemented with 4% hydrogel Gel B in blue; standard diet fed, aged match, mice were used as a further control group for some parameters. Body weight, food and water intake were measured throughout the experiment. Fecal samples were collected from individual mice at the beginning of the experiment, every 4 weeks through the experiment and at sacrifice. Glucose Tolerance Test (GTT) and Insulin Tolerance Test (ITT) were performed after 17 weeks of feeding. Mice were sacrificed after 18 weeks of feeding. At the moment of sacrifice, EAT was collected and weighted, intestine length was measured and organs were collected for further analysis (i.e. histology, IF, inflammatory response)

After 18 weeks, mice fed with HFD 2% and 4% Gel B displayed a significant reduction in body weight compared to those fed with HFD (Figure 8a, b), with no differences in water and food intake among the groups (Figure 9a,b). Moreover, the trend of weight curves relative to treated mice were more similar to that of control mice (Figure 8a, b), suggesting that both doses of Gel B succeeded in preventing weight gain induced by HFD.

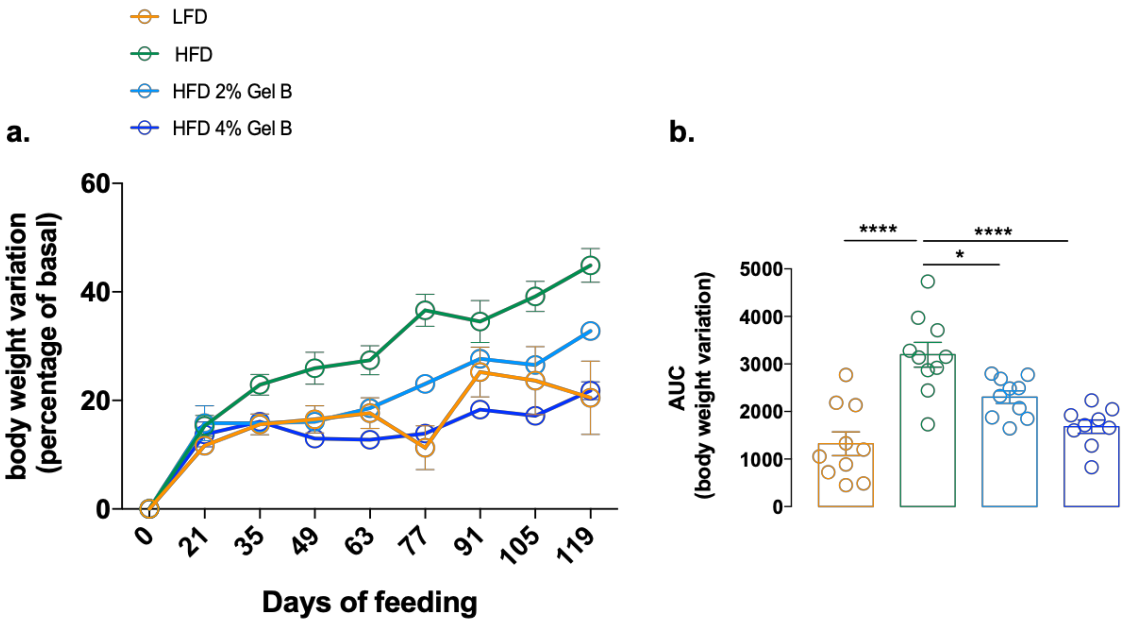

Figure 8. Hydrogel supplemented high fat diet administration prevents body weight gain over 18 weeks of feeding.

Body weight was monitored throughout 18 weeks of hydrogel supplemented HFD administration. **a.** body weight variation (expressed in percentage of basal); **b.** Area Under the Curve (AUC) of body weight variation curve (* p<0,5; **p<0,01; ***p<0,001 one-way ANOVA Tukey post-test, line at mean with SEM; 5-10 mice per group).

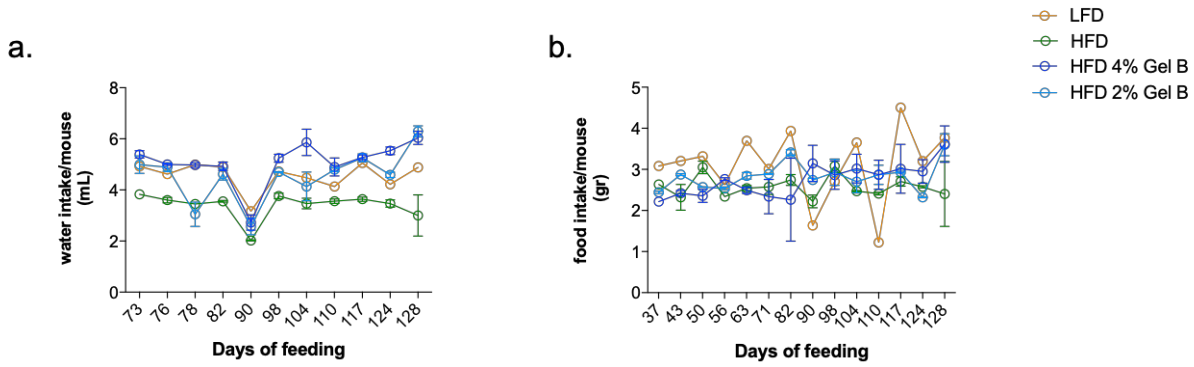

Figure 9.Hydrogel diet supplementation did not induce changes in food and water intake over 18 weeks of feeding.

a. water and **b.** food intake throughout 18 weeks of feeding with hydrogel supplemented HFD (line at mean with SEM; 5-10 mice per group)

In a state of caloric excess induced by HFD feeding, white adipose tissue (WAT) plays a critical role in storing the surplus energy and accumulating triglycerides, which in turn lead to an increase in adipocytes number and size, resulting in the expansion of subcutaneous adipose visceral depots[168]. In mice, the effect of long term HFD mainly occurs on WAT visceral pads, known as Epididymal Adipose Tissue (EAT)[169]. In our experimental model, mice fed a HFD showed a significant increase of EAT weight, that was completely prevented in mice treated with Gel B at both doses (Figure 10a). This was likely due to the blockade of adipocytes hypertrophy induced by HFD feeding, as shown by a reduced adipocyte area in fat pads tissue sections (stained with H&E) of mice treated with the Gel compared to that of HFD fed mice (Figure 10b, c). Therefore, hydrogel administration was able to fully prevent WAT remodeling induced by HFD, in parallel with weight management.

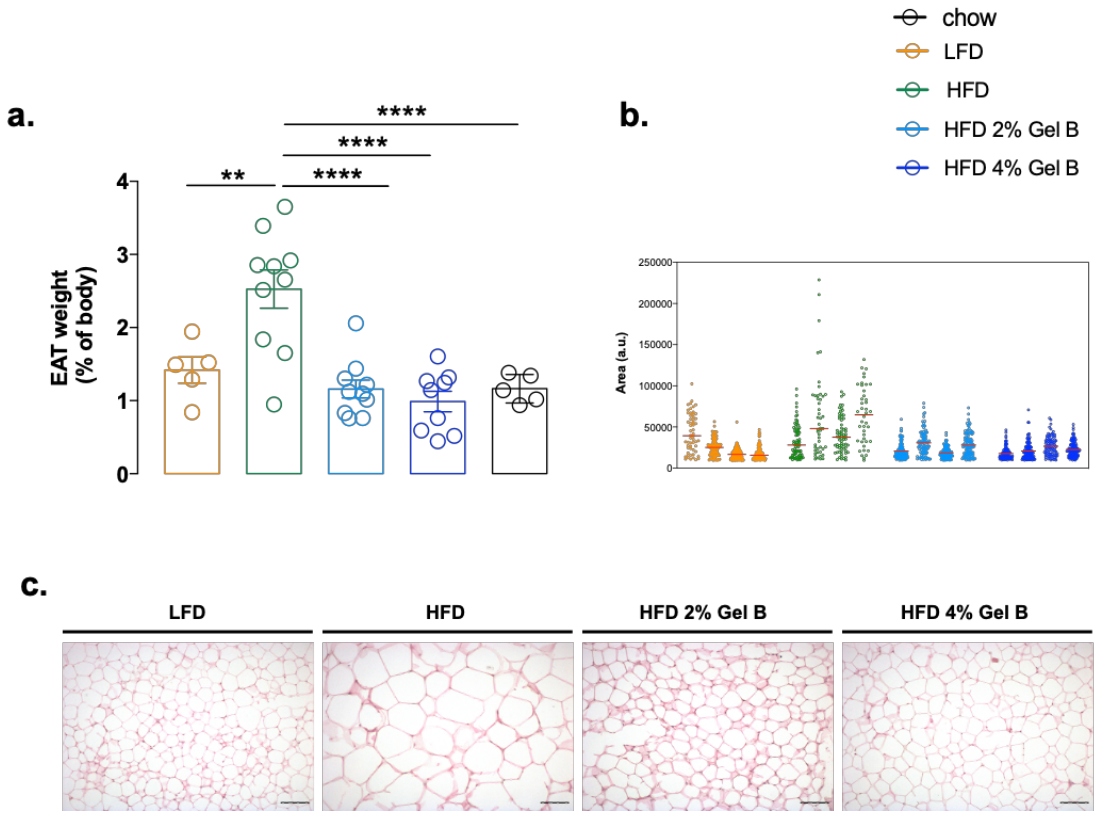

Figure 10.Hydrogel supplemented high fat diet administration prevents white adipose tissue deposition and adipocyte hypertrophy over 18 weeks of feeding.

a. Epididymal Adipose Tissue (EAT) weight expressed as percentage of body weight after 18 weeks of feeding (* p<0,5; **p<0,01; ***p<0,001 one-way ANOVA Tukey post-test, line at mean with SEM; 5-10 mice per group). **b.** Epididymal adipocyte area distribution, with statistically significant difference (***p<0,001 LFD vs HFD ; ***p<0,001 HFD vs HFD 2% Gel B; ***p<0,001 HFD vs HFD 4% Gel B one-way ANOVA Tukey post-test, red line at median; 75-100 cells per field per mouse); **c.** Hematoxylin & Eosin staining of EAT formalin fixed paraffin embedded sections (scale bar 100 µm).

In addition to body weight gain and visceral fat enlargement, HFD is known to induce reduction in small intestine length and ileum circumference. Intestinal atrophy and shortening are believed to happen through the induction of low-grade inflammation generated by consumption of diets rich in fats[170,171]. We hence assessed if hydrogel supplementation was able to prevent intestinal alterations prompted by long-term HFD nourishment.

After 18 weeks of feeding, mice fed with either LFD or HFD showed a significant reduction in small intestine and colon length compared to standard diet (chow) fed mice (Figure 11). Conversely, hydrogel diet supplementation was able to maintain intestine length, actually protecting animals from intestine shortening and keeping intestine length similar to that of age matched chow diet fed mice.

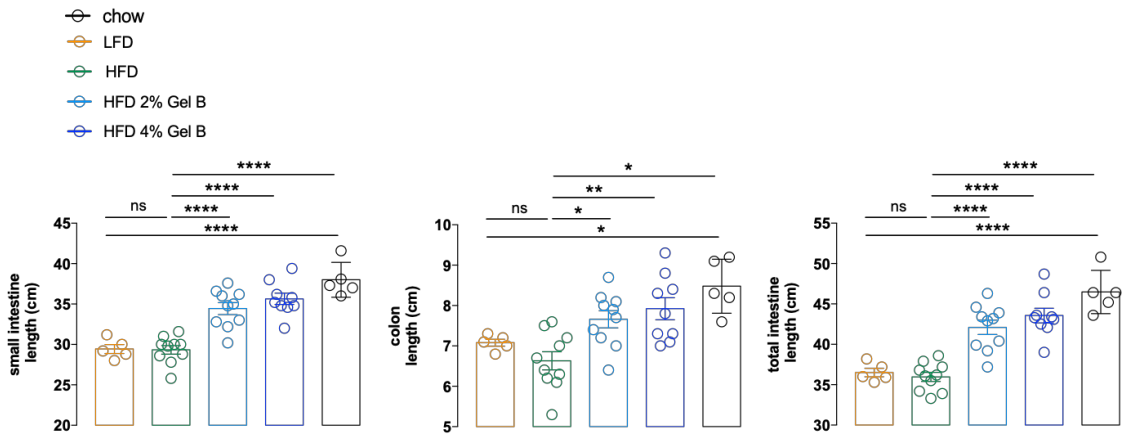

Figure 11.Hydrogel diet supplementation prevents intestinal shortening associated to long term high fat diet feeding.

After 18 weeks of feeding mice were sacrificed and intestine length was measured. From left to right graphs are depicting: small intestine length, colon length and total intestine length. (* p<0,5; **p<0,01; ***p<0,001 one-way ANOVA Tukey post-test, line at mean with SEM; 5-10 mice per group).

As intestinal alterations related to HFD feeding are mainly due to low-grade inflammatory processes[172], we wanted to evaluate the expression of inflammatory genes in the gut of our mice. Several studies report that HFD promotes inflammation in the distal small bowel[173], while data related to the colon are less consistent[89]; we hence evaluated ileal expression of pro-inflammatory cytokines *TNF-α, IL-1β, INF-γ* and of anti-inflammatory cytokine *IL-10*.

Mice fed with hydrogel supplemented HFD showed a reduction in *IL-1β* expression paralleled by a slight increase in *IL-10,* respect to LFD and HFD groups; conversely, no differences in the expression of pro-inflammatory cytokines *TNF-α* and *INF-γ* were detected among groups (Figure 12).

We hence concluded that the type of HFD that we used in our experimental setting (45% fat) is not inducing a strong inflammatory response at the intestinal level, suggesting that the intestinal shortening (Figure 12) likely depends on other factors, like a change in the gut microbiota or the transit and stiffness of the GI lumen content[174] . Overall, hydrogel administration was able to prevent alterations related to HFD feeding, like body weight gain, adipose tissue deposition and remodeling, together with intestinal shortening.

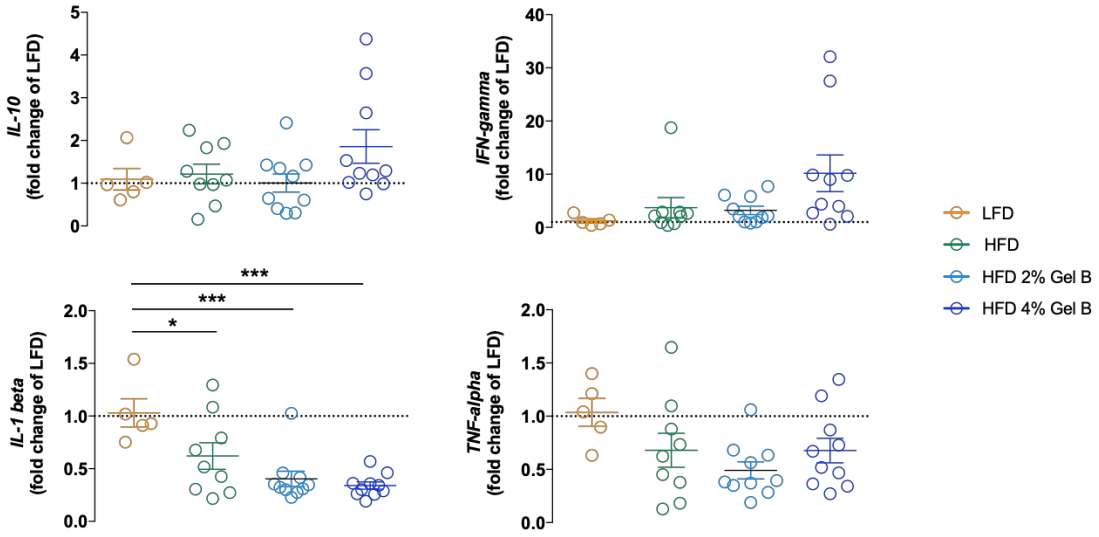

Figure 12. Expression of intestinal pro and anti-inflammatory cytokines after 18 weeks of feeding with hydrogel supplemented HFD.

Relative gene expression levels of pro-inflammatory cytokines TNF-α, IL-1β, INF-γ and of anti-inflammatory cytokine IL-10, expressed as fold change of LFD fed group(* p<0,5; **p<0,01; ***p<0,001 one-way ANOVA Tukey post-test, line at mean with SEM; 5-10 mice per group).

Along with effects on body composition (i.e. adiposity) and low grade inflammatory processes, long-term HFD is known to induce typical metabolic alterations in glucose homeostasis and insulin sensitivity[175,176] that can consequently lead to the development of T2DM (Type 2 Diabetes) and NAFLD.

In order to assess the effect of the hydrogel on glycemic control, we measured several metabolic parameters, namely fasting blood glucose, fasting blood insulin levels and responses to glucose (Glucose Tolerance Test, GTT) and insulin (Insulin Tolerance Test, ITT) challenges, which are typically altered after long term HFD feeding.

As expected, mice fed with HFD for 18 weeks displayed altered response to both ITT and GTT tests (Figure 13), elevated levels of fasting blood insulin compared to controls (LFD), paralleled by a poor HOMA-IR index (i.e. Homeostatic Model Assessment of Insulin Resistance) (Figure 14).

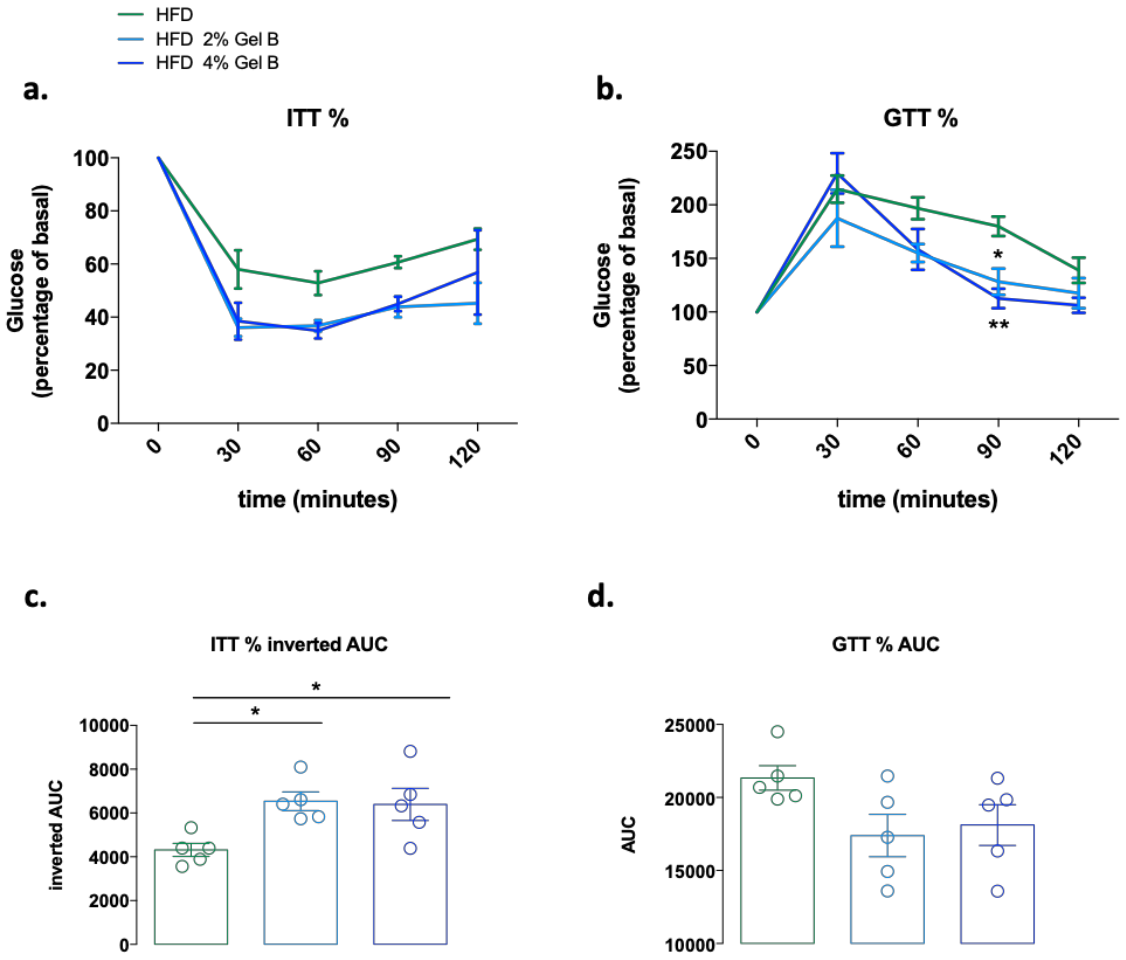

Figure 13. Hydrogel diet supplementation ameliorates response to ITT and GTT after long term high fat diet feeding.

a. and **b.** Intra-peritoneal ITT and intra-peritoneal GTT expressed as percentage of basal performed after 17 weeks of feeding following 6 hours of morning fasting; **c**. inverted AUC of ITT expressed as percentage of basal; **d**. AUC of GTT expressed as percentage of basal (* p<0,5; **p<0,01; ***p<0,001 one-way and two-way ANOVA Tukey post-test, line at mean with SEM; 5 mice per group).

Interestingly, mice fed with HFD 2% Gel B and HFD 4% Gel B showed a better response to both insulin and glucose load in ITT and GTT tests (Figure 13 a,c and b,d respectively), lower fasting blood insulin levels (Figure 14b), improved insulin sensitivity and glycemic control (Figure 14a), mirrored by lower HOMA-IR index (Figure 14c) and higher GLP-1 serum levels (Figure 14d), an intestinal hormone with potent insulinotropic effect[177,178]. Overall, these data support hydrogel ability to prevent insulin resistance development and metabolic impairment due to HFD feeding.

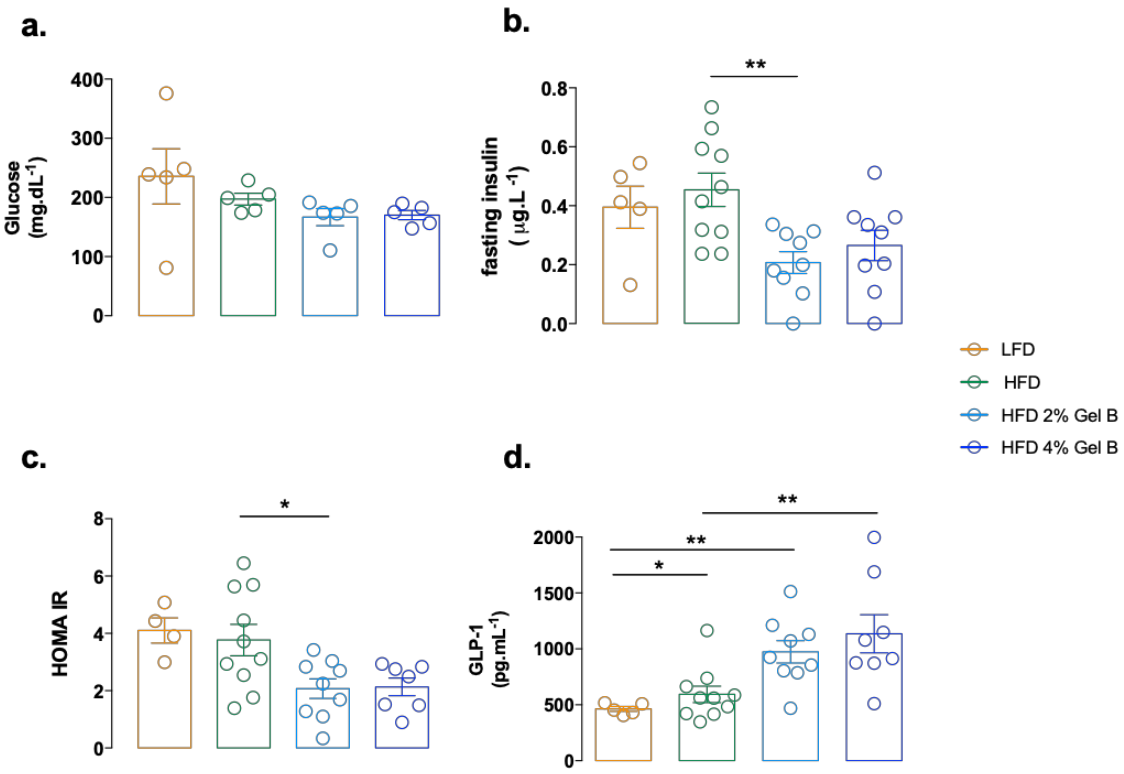

Figure 14. Hydrogel diet supplementation prevents HFD associated metabolic alterations.

a. fasting blood glucose levels after 18 weeks of feeding; **b.** fasting circulating insulin levels after 18 weeks of feeding; **c.** HOMA-IR **(**Homeostatic Model Assessment of Insulin Resistance) values; **d.** circulating GLP-1 levels after 18 weeks of feeding (* p<0,5; **p<0,01; ***p<0,001 one-way ANOVA Tukey post-test, line at mean with SEM; 5-10 mice per group).

Obesity and metabolic alterations have been associated with an increased risk of non-alcoholic fatty liver disease (NAFLD)[179]. A closed relationship between NAFLD and metabolic syndrome has been highlighted, linking liver fat accumulation, visceral overweight, dyslipidemia and hyperinsulinemia, resulting in the generally accepted concept that NAFLD is the hepatic manifestation of the metabolic syndrome[180,181].

It has also been reported that long term HFD feeding induces hepatic steatosis in mice (i.e. triglyceride accumulation in the liver), a hallmark of NAFLD, often associated with obesity and type 2 diabetes[182,183]; accordingly, our mouse model was suitable to study the effect of hydrogel administration on hepatic steatosis.

To assess whether hydrogel administration was able to also prevent hepatic steatosis progression, inhibiting lipid accumulation in the liver, we performed histological analysis on liver sections from mice fed for 18 weeks: Hematoxylin and Eosin (H&E) staining allowed us to analyze liver parenchyma architecture and damage (Figure 15), and Oil Red O staining (Figure 16) was used to visualize triglyceride accumulation in hepatocytes, a marker of steatosis.

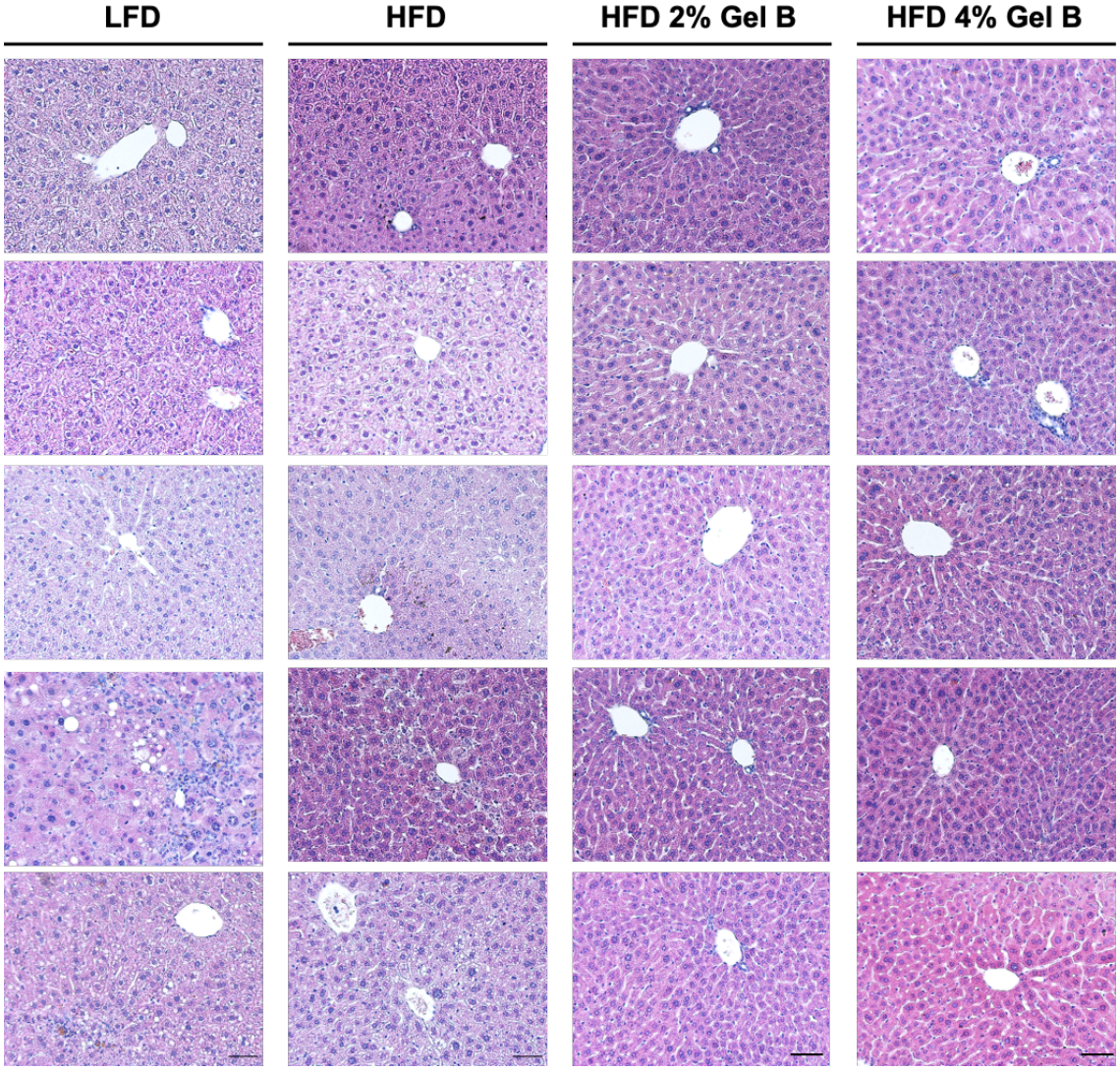

Figure 15.Histological analysis of liver sections after 18 weeks high fat diet feeding.

H&E staining of formalin fixed paraffin embedded liver sections of mice fed for 18 weeks with LFD, HFD, HFD 2% Gel B and HFD 4% Gel B (in column images of 5 representative mice per group), scale bar 100 µm.

Both LFD and HFD fed mice showed intracytoplasmic lipid accumulation in the form of triglycerides within hepatocytes and the presence of droplets of macro-vesicular fat filling the cytoplasm in the liver (Figure 15 and 16), characteristic alterations of NAFLD steatosis[184]. Lipid deposition (i.e. triglyceride accumulation), visualized through Oil red O staining, was efficiently prevented in mice fed with HFD supplemented with hydrogel Gel B (Figure 15 and 16) and complete lipid clearance in the liver was achieved with the highest dose of the hydrogel (HFD 4% Gel B), as also indicated by the Oil red O scoring (Figure 16b).

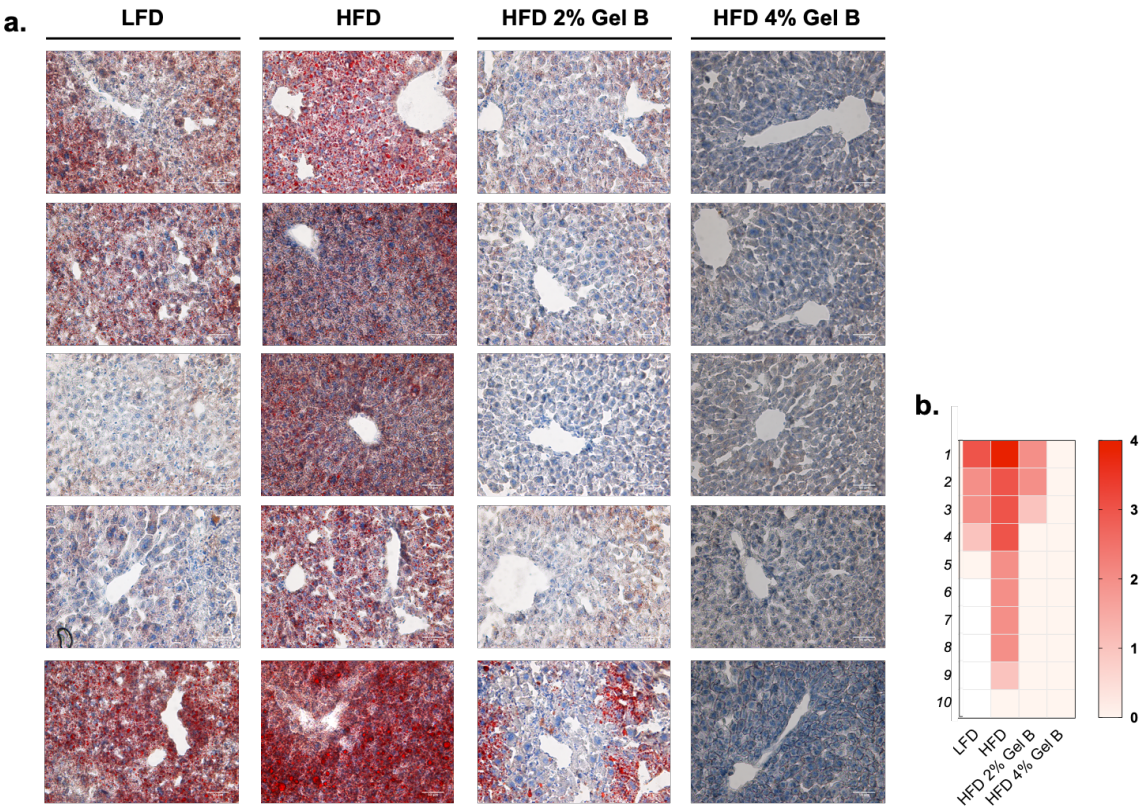

Figure 16. Hydrogel diet supplementation prevents accumulation of triglycerides in the liver after 18 weeks of feeding.

a. Oil Red O staining of PLP fixed OCT embedded liver samples, after 18 weeks of feeding with LFD, HFD, HFD 2% Gel B and HFD 4% Gel B. In red Oil Red O staining for liver triglyceride, in blue hematoxylin counterstaining; scale bar 50 µm (5 representative animals per group). **b.** Oil Red O staining scoring. Score from 0 (no triglyceride - beige) to 4 (high accumulation of triglyceride - red) was given. Each square in the graph represents a mouse; empty (white) squares represent missing mice (5 mice LFD fed group, 10 mice HFD fed group, 10 mice HFD 2% Gel B fed group and 10 mice HFD 4% Gel B fed group).

Liver sections were also stained with Sirius Red to look for the presence of collagen fibers (a marker of liver fibrosis) (Figure 17); however, no signs of liver fibrosis were observed in LFD and HFD fed mice at this stage, or in hydrogel supplemented HFD fed experimental groups.

In conclusion, hydrogel administration was able to prevent body weight gain, adipose tissue deposition and adipocyte hypertrophy, intestinal shortening, metabolic alterations (i.e. response to glucose and insulin challenges, hyperglycemia, hyperinsulinemia) together with liver steatosis development in mice fed with HFD for 18 weeks.

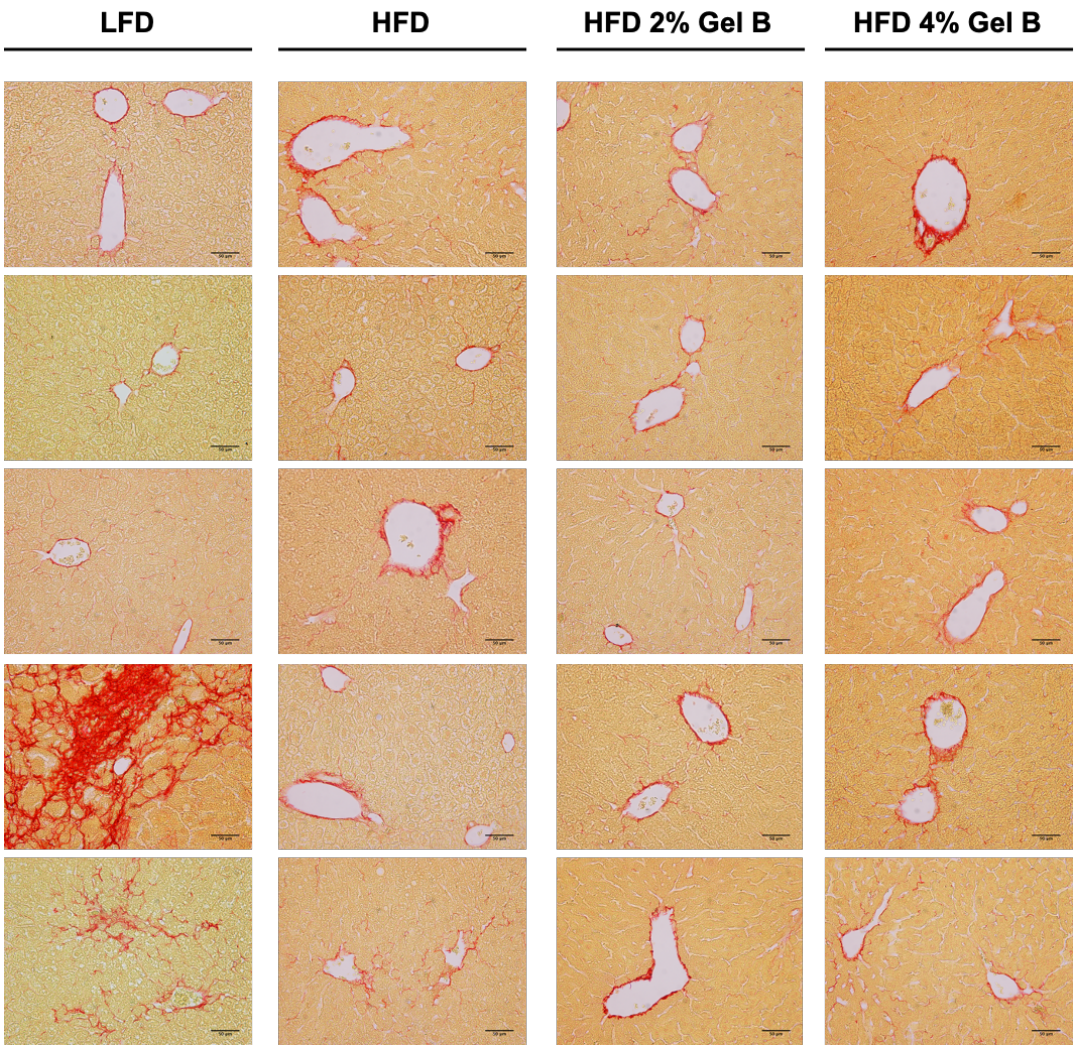

Figure 17. Long term feeding with high fat diet does not induce liver fibrosis.

Sirius Red staining (in red) for collagen fibers of formalin fixed paraffin embedded liver sections of mice fed for 18 weeks with LFD, HFD, HFD 2% Gel B and HFD 4% Gel B (in column images of 5 representative mice per group); scale bar 50 µm.

3. Hydrogel dietary supplementation as a therapeutic tool for long term high fat diet feeding

Previous data fully demonstrated the efficacy of Gel B (at both doses tested) in preventing alterations induced by HFD in mice, namely weight gain, alteration of glycemic control, intestine length and hepatic steatosis. We next wanted to evaluate the therapeutic potential of hydrogel Gel B in the context of a metabolic disorder. In other words, we made use of our HFD model to assess the ability of the hydrogel to treat or prevent the progression of typical alterations of metabolic syndrome related to high caloric diet consumption. The hydrogel, in fact, was initially designed and recently approved by FDA (April 12, 2019)[161] and EMA (June,2020) under the name of PLENITY™ as an aid for weight management in overweight and obese adults with Body Mass Index (BMI) of 25 - 40 kg/m^2, when used in conjunction with diet and exercise.

To this end, we first induced metabolic alterations in mice, feeding C57BL6/J *wild type* male mice for 12 weeks with HFD (45 % fat) – *induction phase*. At the end of the induction phase, mice were randomly divided in three experimental groups: HFD (45% fat) fed mice, HFD 2% Gel B and HFD 4% Gel B and fed them for further 4 and 12 weeks - *therapeutic phase* - with these different diets. The experimental design is depicted in Experimental scheme 3.

We mainly focused on three time points: a) 12 weeks HFD, which coincides with the end of obesity induction phase and represents the starting point for Gel B treatment; b) 4 weeks of Gel B administration, which coincides with 16 weeks of HFD feeding and 4 weeks of Gel B treatment for the groups HFD 2% Gel B and HFD 4% Gel B; c) 12 weeks of Gel B administration, which coincides with 24 weeks of HFD feeding and 12 weeks of Gel B treatment for the groups HFD 2% Gel B and HFD 4% Gel B.

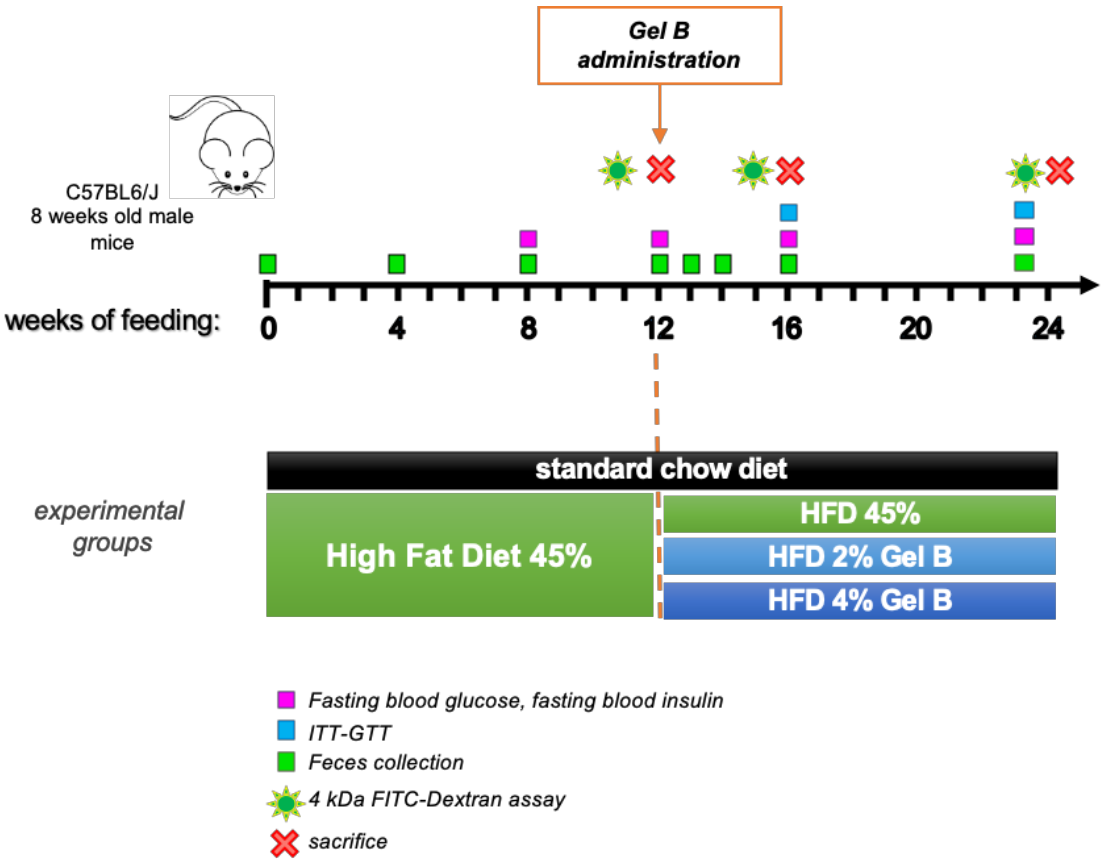

Experimental Scheme 3. Therapeutic hydrogel administration in a model of long term high fat diet feeding.

C57BL6/J male mice at 8 weeks of age were fed for 12 weeks with: chow diet in black and HFD in green. After 12 weeks 5 mice per group were sacrificed. Mice initially fed with HFD were randomly divided in 3 experimental groups: HFD in green, HFD 2% hydrogel Gel B in light blue and HFD 4% hydrogel Gel B in blue. Body weight and food intake were measured throughout the experiment. Fecal samples were collected at the beginning of the experiment, at several time-points throughout the experiment (green squares) and at sacrifice. Fasting blood glucose and insulin levels were measured after 8 and 12 weeks of feeding with HFD and after 4 and 12 weeks of feeding with hydrogel supplemented diets (pink squares). Glucose tolerance test (GTT) and Insulin Tolerance Test (ITT) were performed after 4 and 12 weeks of feeding with hydrogel supplemented diet (light blue squares). FITC-Dextran intestinal permeability assays were performed after 12 weeks of feeding with HFD and after 4 and 12 weeks of feeding with hydrogel supplemented diets (described in paragraph 5). Mice were sacrificed after 12 weeks of feeding with HFD and after 4 and 12 weeks of feeding with hydrogel supplemented diets and several parameters were analyzed.

After 12 weeks of HFD, mice showed a significant increase in body weight compared to those fed a standard chow diet, as shown in Figure 18; at this time-point some mice (5 per group) from chow and HFD experimental groups were sacrificed and metabolic and histological parameters were evaluated. Remaining mice fed with HFD, HFD 2% Gel B and HFD 4% Gel B were monitored throughout the experiment to assess hydrogel therapeutic potential.

After 4 weeks of feeding with hydrogel supplemented diets, mice showed a dose-dependent decrease in body weight compared to those fed with HFD (Figure 18a,b); body weight variation was kept constant until 12 weeks of hydrogel treatment (both doses) at a level comparable to that of age-matched chow control mice (Figure 18a,c). Mice from each experimental group were sacrificed after 4 weeks and 12 weeks of Gel B administration, in order to evaluate the effect of the treatment, in a way similar to the preventive experiment (previous data).

We hence investigated whether hydrogel administration was able to revert WAT enlargement induced by HFD feeding. Indeed, hydrogel administration resulted in a strong reduction of white adipose tissue deposition, reflected by a reduction in EAT weight, already after 4 weeks of feeding; this reduction was even stronger after 12 weeks of treatment (Figure 19a). Reduction of EAT weight was accompanied by a remarkable decrease in adipocyte size (hypertrophy) in hydrogel treated mice: adipocyte area evaluation in H&E histological sections showed a mild reduction of adipocyte size after 4 weeks, which turned to be statistically significant after 12 weeks of Gel B treatment, compared to HFD fed mice (Figure 19d). We confirmed that hydrogel administration was able to revert white adipose tissue remodeling and enlargement, likely contributing to body weight decrease.

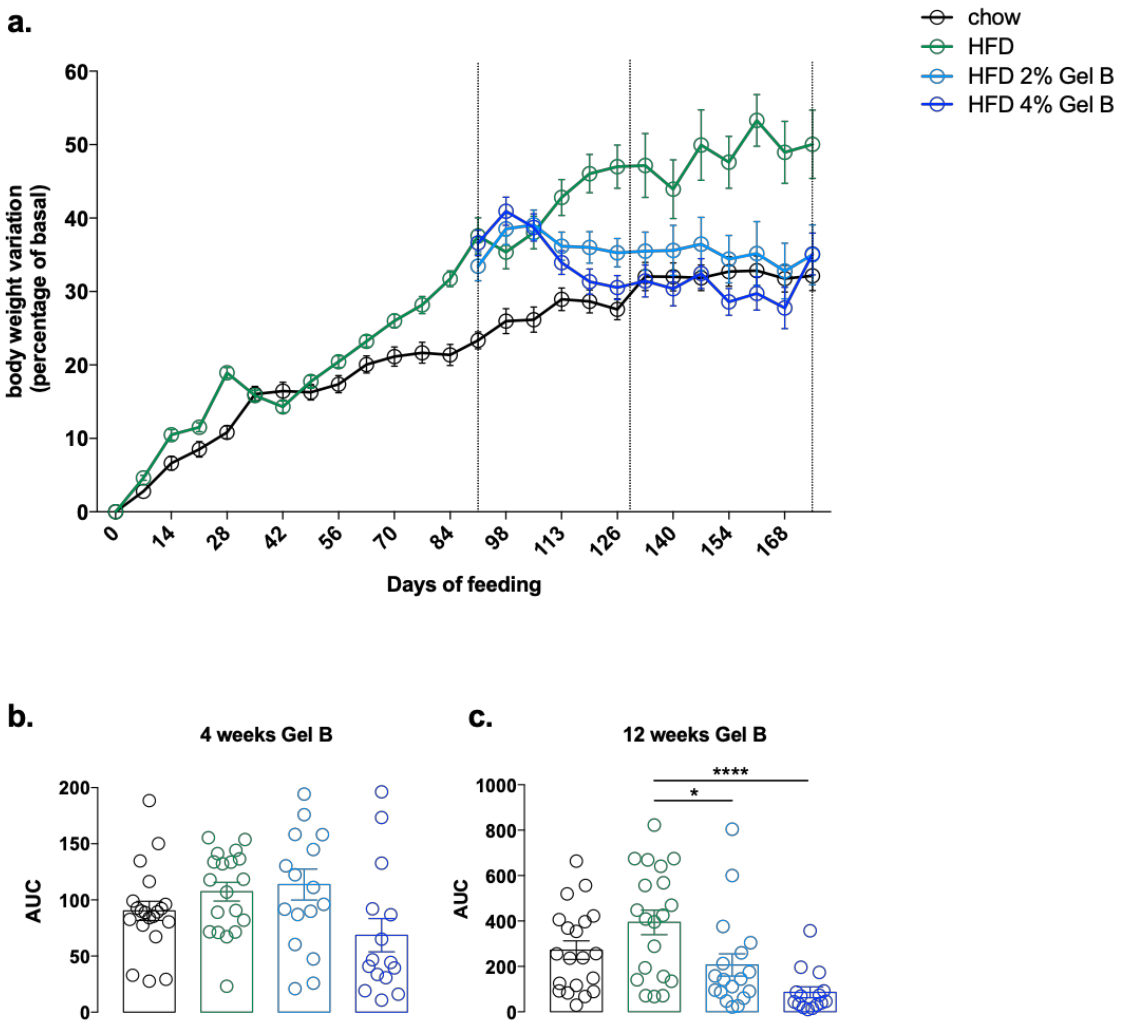

Figure 18. Therapeutic hydrogel administration induces body weight loss after long term high fat diet feeding.

Body weight was monitored throughout 24 weeks of feeding. **a.** Body weight variation, expressed in percentage of basal. Statistical significant difference: at day 91 (12 weeks HFD) *** p<0,001 chow vs of HFD, at day 129 (4 weeks of hydrogel treatment) *** p<0,001 chow vs of HFD and HFD vs HFD 4% Gel B, at day 172 (12 weeks of hydrogel treatment) *** p<0,001 chow vs of HFD and HFD vs HFD 4% Gel B; **b.** Area Under the Curve (AUC) of body weight variation curve after 4 weeks of feeding with hydrogel supplemented diets; **c.** Area Under the Curve (AUC) of body weight variation curve after 12 weeks of feeding with hydrogel supplemented diets (* p<0,5; **p<0,01; ***p<0,001 one-way and two-way ANOVA Tukey post-test, line at mean with SEM).

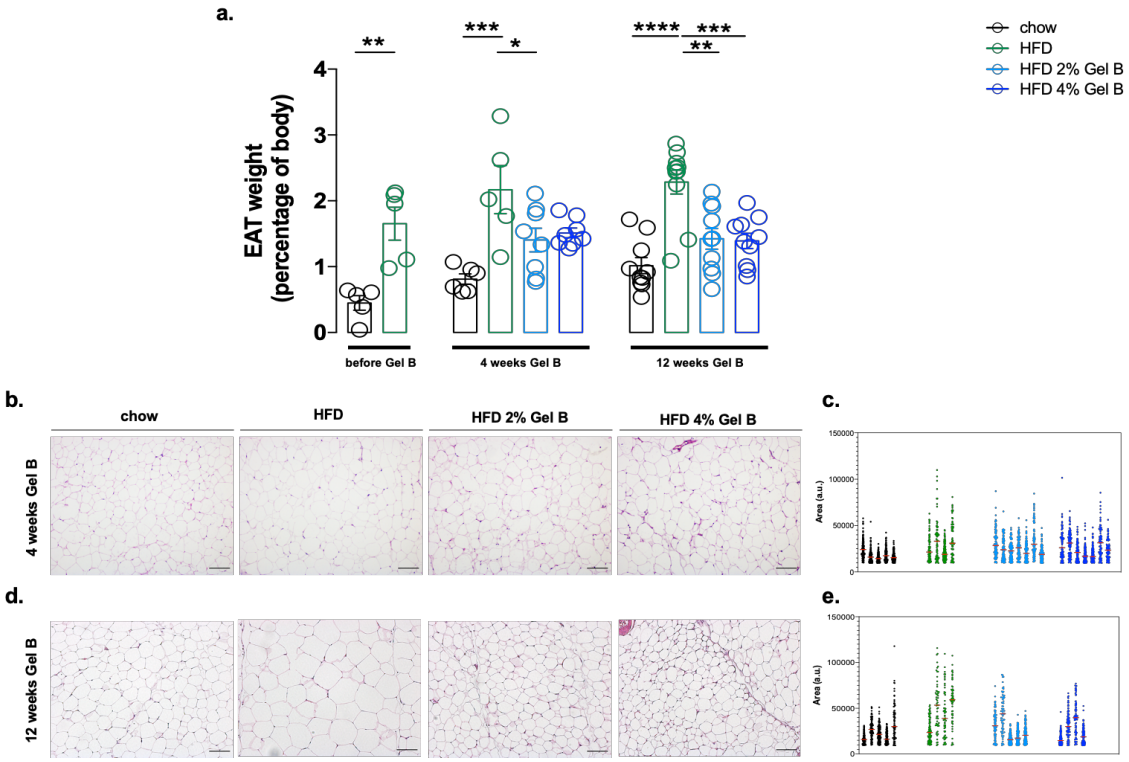

Figure 19. Therapeutic hydrogel administration reduces adiposity and adipocyte hypertrophy in long term high fat diet feeding.

a. Epididymal Adipose Tissue (EAT) weight expressed as percentage of body weight after 12 weeks of HFD feeding (before Gel B) and after 4 and 12 weeks of hydrogel supplemented diet feeding (* p<0,5; **p<0,01; ***p<0,001 one-way ANOVA Tukey post-test, line at mean with SEM; 5-8 mice per group). **b.** Hematoxylin & Eosin staining of formalin fixed paraffin embedded sections of epididymal adipose tissue after 4 weeks of hydrogel supplemented diet administration(scale bar 100 µm).**c.** EAT adipocytes area, after 4 weeks of hydrogel supplemented diet administration, with significant difference (****p<0,0001 LFD vs HFD ; one-way ANOVA Tukey post-test, distribution with red line at median); **d.** Hematoxylin & Eosin staining of formalin fixed paraffin embedded sections of epididymal adipose tissue after 12 weeks of hydrogel supplemented diet administration(scale bar 100 µm); **e.** Epididymal white adipose tissue adipocytes area distribution, after 12 weeks of hydrogel supplemented diet administration, with significant difference (****p<0,0001 LFD vs HFD ; ****p<0,0001 HFD vs HFD 2% Gel B; ****p<0,0001 HFD vs HFD 4% Gel B one-way ANOVA Tukey post-test, distribution with red line at median).

Concerning the intestinal length, we wondered whether hydrogel therapeutic administration was able to restore intestinal shortening induced by long-term HFD feeding.

Mice fed with HFD for 12 weeks showed a marked reduction of intestinal length, driven by small intestine (statistically significant) and colon (not significant but still evident) shortening, with a general reduction of the total intestine length (Figure 20). Hydrogel therapeutic administration resulted in a rescue of small intestine, colon and total intestine length already after 4 weeks of treatment, followed by the complete restoration of intestine length after 12 weeks of hydrogel administration, to levels equal to those of chow diet fed mice (Figure 20).

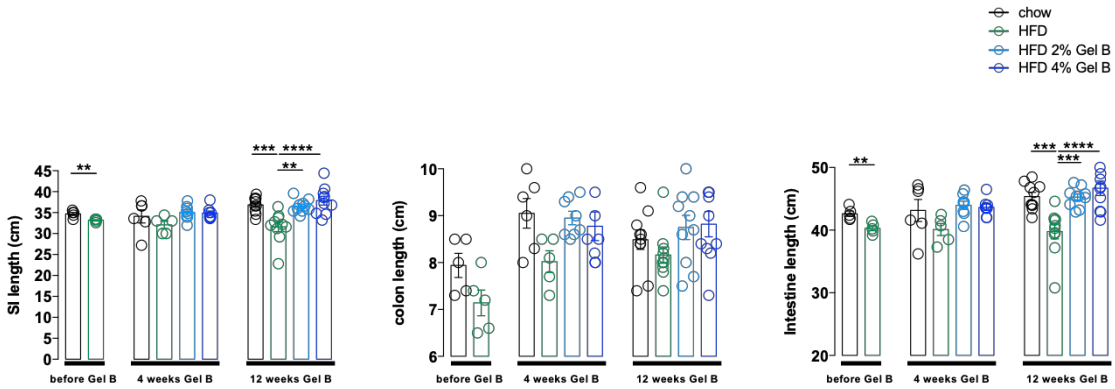

Figure 20. Therapeutic hydrogel administration reverts intestine shortening induced by long term high fat diet feeding.

Mice were sacrificed 12 weeks after HFD feeding (before Gel B) and after 4 and 12 weeks of hydrogel supplemented HFD feeding and intestine length was measured. From left to right graphs are depicting: small intestine length, colon length and total intestine length. (* p<0,5; **p<0,01; ***p<0,001 t-test and one-way ANOVA Tukey post-test, line at mean with SEM; 5-8 mice per group).

Having demonstrated that the therapeutic administration of the hydrogel in HFD fed mice was able to rescue EAT enlargement and intestine length, we wanted to assess whether therapeutic hydrogel administration was also able to counteract metabolic alterations induced by long term HFD feeding; to this end, we measured fasting blood glucose, fasting blood insulin levels and response to glucose (Glucose Tolerance Test, GTT) and insulin (Insulin Tolerance Test, ITT) challenges at the main time points we focused on.

HFD mice showed higher fasting blood glucose levels and higher fasting insulin levels than chow fed control mice, resulting in impaired HOMA-IR index (Figure 21a,b,c), at least after 8 weeks and 16 weeks of HFD feeding. This indicates that impairment of

fasting blood glucose control in these mice is taking place, even if with oscillations over time (i.e. 12 and 24 weeks of HFD) (Figure 21a,b,c).

Interestingly, 4 weeks after Gel B treatment, hydrogel supplementation significantly ameliorated these parameters, lowering both fasting blood glucose and insulin levels, thereby improving HOMA-IR (Figure 21a,b,c). However, 12 weeks after hydrogel therapeutic treatment, fasting blood glucose and insulin levels in HFD mice (24 weeks HFD feeding) were such that we were not able to detect differences among groups (Figure 21a,b,c). We thought that age-related confounding effects came into play, masking differences in very sensitive metabolic parameters among groups. Even if we lost the statistical significance after 12 weeks of Gel B treatment, still we can argue that fasting blood glucose and insulin and the HOMA-IR index in HFD 4% Gel B are closer to those of chow control mice, suggesting a slight amelioration of these parameters going on in treated mice respect to HFD fed mice.

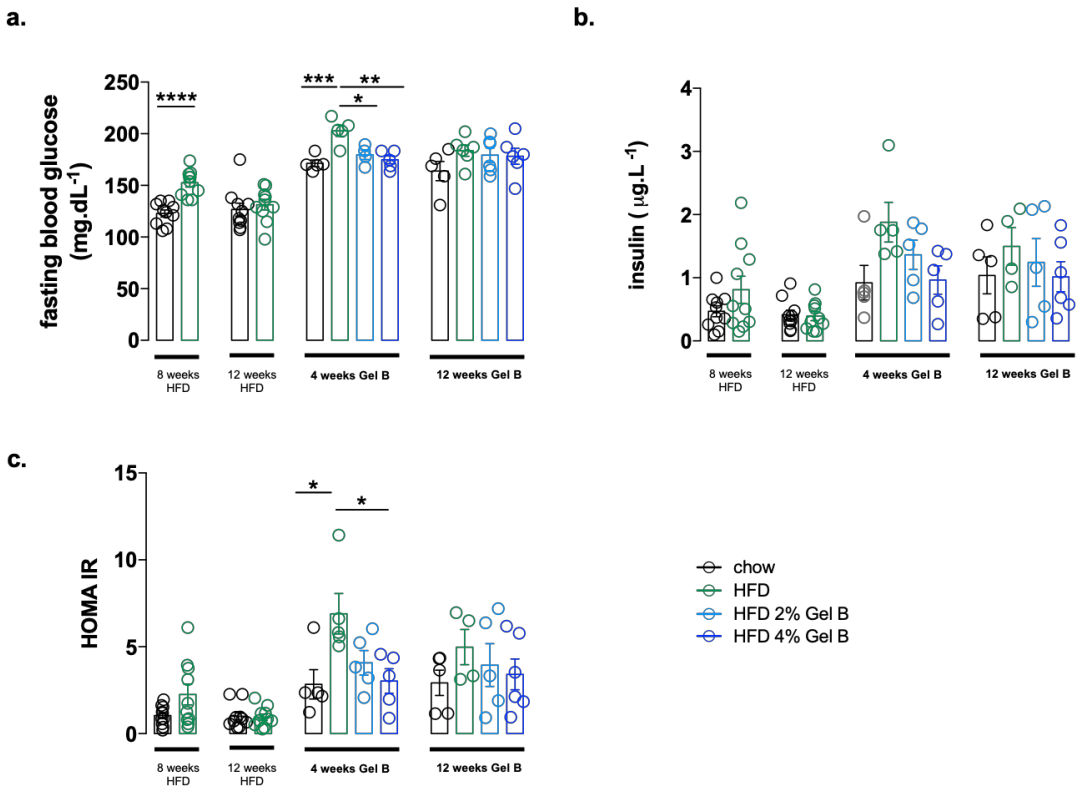

Figure 21.Therapeutic hydrogel administration improves glucose levels after long term high fat diet feeding.

Fasting glucose and fasting insulin were measured after 8 and 12 weeks of HFD feeding (before Gel B administration) and after 4 and 12 weeks of feeding with hydrogel supplemented diets. **a.** blood glucose levels measured after 6 hours of morning fasting**; b.** blood insulin levels measured after 6 hours of morning fasting; **c.** HOMA-IR **(**Homeostatic Model Assessment of Insulin Resistance) values; (* p<0,5; **p<0,01; ***p<0,001 one-way ANOVA Tukey post-test, line at mean with SEM; 5-10 mice per group).

In light of these data, we investigated the response of mice of the different groups to glucose and insulin challenges after therapeutic hydrogel administrations (Figure 22). We performed ITT and GTT test both after 4 and 12 weeks of hydrogel treatment. In the previously shown preventive experiment, we observed an impairment of glucose metabolic response to insulin challenge in HFD fed mice (18 weeks of feeding), that was prevented with hydrogel diet supplementation. Here, after 4 weeks of hydrogel administration (corresponding to 16 weeks of HFD feeding), we could not detect any relevant impairment of the metabolic response in HFD mice *versus* chow diet fed mice or Gel B treated mice, neither in the ITT or in the GTT test (Figure 22a,b,c). Notably, we found remarkable differences in the ITT test performed after 12 weeks of hydrogel supplemented diet feeding (24 weeks HFD feeding) (Figure 22 d,e,f): in particular, we witnessed an impaired response of HFD fed mice to insulin challenge, with a significant improvement in ITT response of HFD 4% Gel B fed mice, to levels comparable to those of the chow diet animals (Figure 22d).Taken together these data support that the therapeutic administration of Gel B in long term HFD was able to blunt the progression of some of HFD induced metabolic alterations, in particular acting on glucose homeostasis and probably counteracting insulin resistance development.

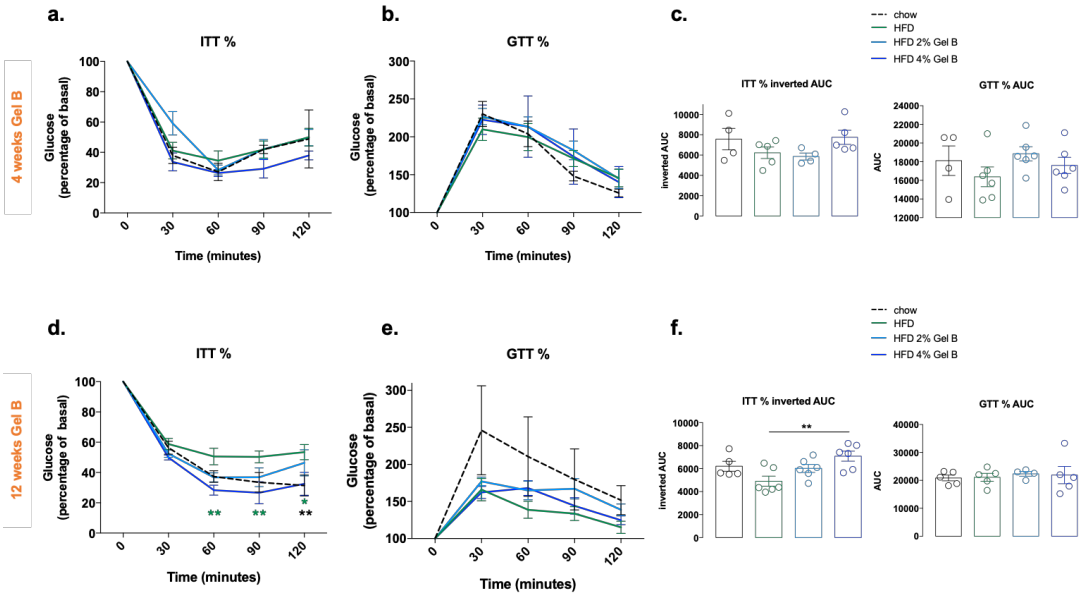

Figure 22. Therapeutic hydrogel administration improves response to insulin challenges after long term high fat diet feeding.

a.and **b.** Intra-peritoneal ITT and intra-peritoneal GTT expressed as percentage of basal performed after 4 weeks of feeding with hydrogel supplemented diets, following 6 hours of morning fasting; **c**. inverted AUC of ITT expressed as percentage of basal (left) and AUC of GTT expressed as percentage of basal; **d.** and **e.** Intra-peritoneal ITT and intra-peritoneal GTT expressed as percentage of basal performed after 12 weeks of feeding with hydrogel supplemented diets, following 6 hours of morning fasting. * in green indicating statistical difference between HFD 4% Gel B and HFD group, *in black indicating statistical difference between chow and HFD **f**. inverted AUC of ITT expressed as percentage of basal (left), and AUC of GTT expressed as percentage of basal (right); (* p<0,5; **p<0,01; ***p<0,001 one-way and two-way ANOVA Tukey post-test, line at mean with SEM).

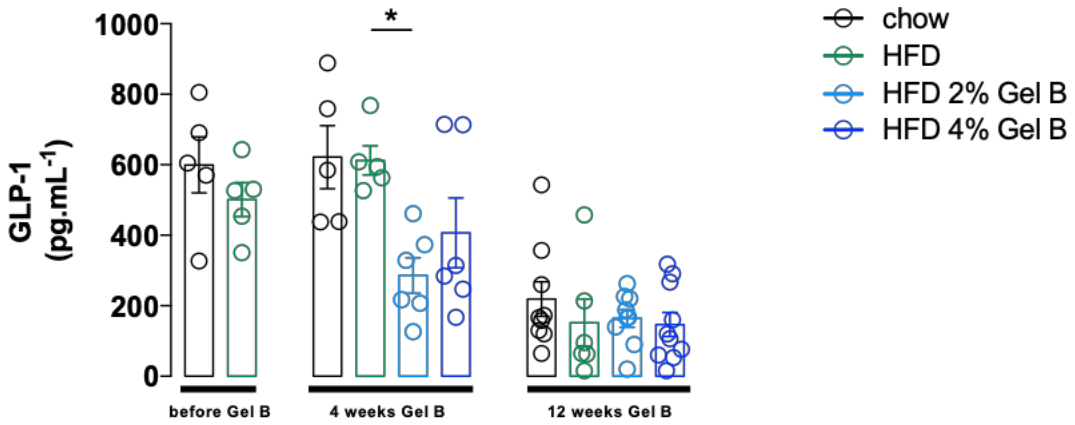

Figure 23. Effects of therapeutic hydrogel administration on GLP-1 after long term high fat diet feeding.

Circulating GLP-1 levels after 18 weeks of feeding (* p<0,5; **p<0,01; ***p<0,001 one-way ANOVA Tukey post-test, line at mean with SEM; 5-10 mice per group).

Since in the preventive setting (Experimental scheme 2) we observed an increase in circulating GLP-1 levels upon hydrogel diet supplementation, we wanted to assess weather therapeutic hydrogel administration was also able to influence GLP-1 circulating levels.

No increase in circulating GLP-1 levels were observed either after 4 or 12 weeks of feeding with hydrogel supplemented diets (Figure 23). Differently from what we detected in the preventive setting, 4 weeks of therapeutic hydrogel supplemented feeding reduced circulating GLP-1 levels in comparison to both chow diet and HFD fed mice. Furthermore, after 12 weeks of feeding we detected similar circulating GLP-1 levels among all the experimental groups. According to the literature, the effects of HFD feeding on circulating GLP-1 levels in mice are still controversial: there are reports claiming that HFD induces an increase in GLP-1 secretion[185] and others are in favor of a reduction in GLP-1 secretion upon HFD feeding (as in human metabolic syndrome)[186]. Clearly, the interpretation of GLP-1 circulating level in the context of HFD models requires further investigation.In conclusion, therapeutic administration of Gel B in long term HFD reduced body weight and adipose tissue deposition, restored intestine length and partially improved metabolic parameters, recapitulating the effects observed in the long term preventive setting, except for GLP-1 induction.

Finally, we sought to evaluate the ability of the hydrogel to revert or at least block the progression of liver steatosis induced by long term HFD feeding.

We performed histological analysis (H&E staining) (Figure 24) and Oil Red O staining (Figure 25) on liver sections from mice fed for 12 weeks with HFD (before Gel B treatment) and from mice treated for 4 and 12 weeks with hydrogel supplemented diets.

The observation of histological samples from 12 weeks HFD fed mice didn't highlight major alterations in the liver parenchyma compared to standard chow fed mice (Figure 24 top panel). In H&E stained liver sections from mice fed for 4 weeks with hydrogel supplemented diet (16 weeks HFD), HFD fed mice showed mild intracytoplasmic lipid accumulation within hepatocytes and the presence of some droplets of macro-vesicular fat filling the cytoplasm of hepatocytes (Figure 24 middle), that was partially restored in hydrogel supplemented diet fed groups.

A milder but similar pattern was observed after 12 weeks of feeding with hydrogel supplemented diet (Figure 24 lower panel).

Lipid deposition (i.e. triglyceride accumulation) was observed through Oil red O staining (Figure 25). After 12 weeks of feeding with HFD we detected an accumulation of liver triglycerides (Figure 25a top panel) in the HFD fed group compared to chow diet fed mice (quantitation in Figure 25b).

Following 4 weeks of hydrogel administration, no differences in liver triglyceride accumulation among HFD and hydrogel supplemented HFD groups were observed (Figure 25a middle panel and Figure 20b). Interestingly, after 12 weeks of hydrogel treatment, HFD 4% Gel B fed mice displayed a less intense ORO staining compared to HFD and HFD 2% Gel B fed groups. Since HFD fed animals showed a worsening of liver fat accumulation and score, we concluded that in HFD 4% Gel B fed mice a slowdown (or even a slight reduction) in hepatic lipid accumulation took place (Figure 25a lower and 25b). No significant effects on liver steatosis were associated to 2% Gel B dose after 12 weeks of treatment.

Overall, reduction in body weight and visceral adipose tissue deposition induced by long term therapeutic hydrogel administration were accompanied by an arrest in liver triglyceride accumulation, rather than a complete elimination of hepatic steatosis. We hence speculated that longer intervals of hydrogel administration could have had a better impact on liver healing and that liver fat clearance presumably is partly independent from body weight and marginal white adipose tissue reduction.

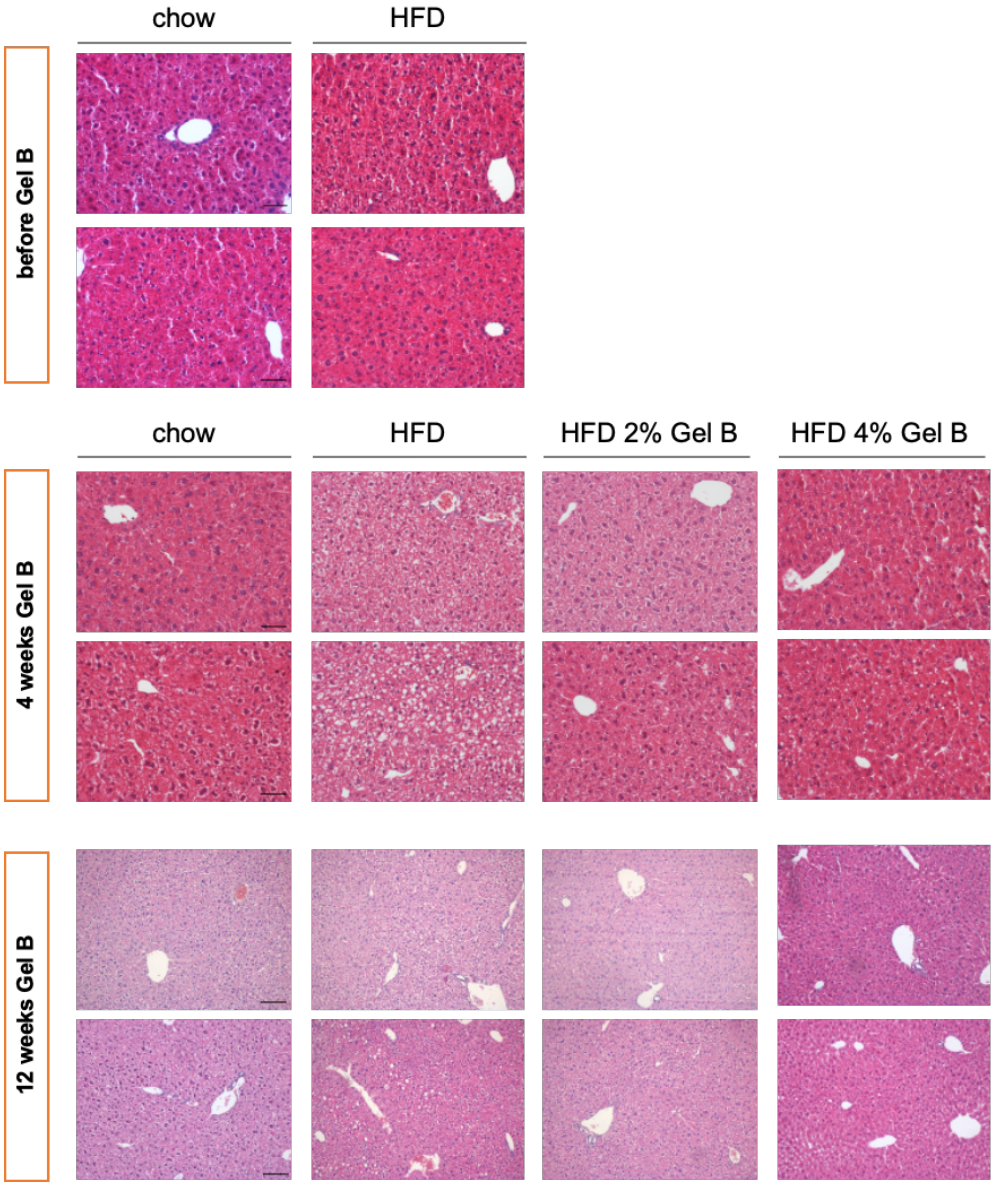

Figure 24. Histological analysis of liver sections before and after therapeutic hydrogel administration.

H&E staining of formalin fixed paraffin embedded liver sections of mice fed for 12 weeks with chow and HFD (before Gel B) and for 4 and 12 weeks with chow, HFD, HFD 2% Gel B and HFD 4% Gel B (in column images of 2 representative mice per group per time point), scale bar 100 µm.

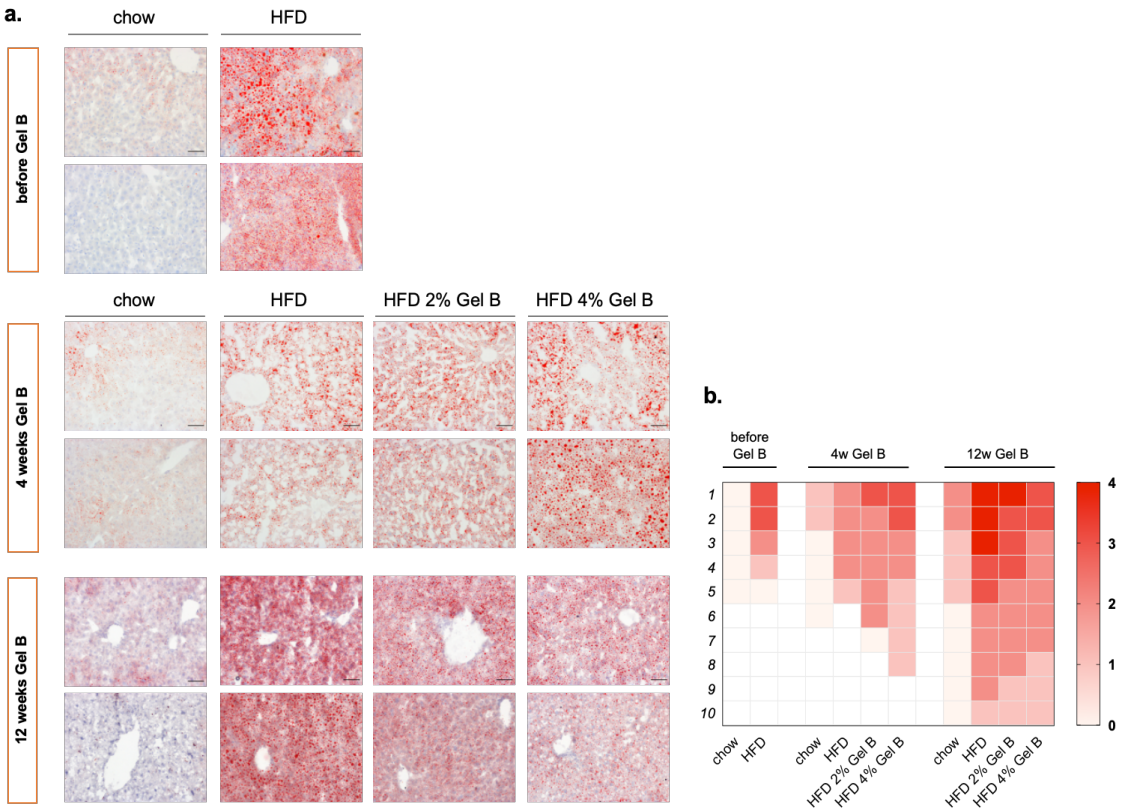

Figure 25. Therapeutic hydrogel administration effect on liver triglyceride accumulation after long term HFD feeding

a. Oil Red O staining of PLP fixed OCT embedded liver samples, after 12 weeks of feeding with chow diet and HFD (top panel), after 4 and 12 weeks of feeding with chow diet, HFD, HFD 2% Gel B and HFD 4% Gel B (top and middle panel respectively). In red Oil Red O staining for liver triglyceride, in blue hematoxylin counterstaining, scale bar 50 µm (in column 2 representative animals per group per time point); **b.** Oil Red O staining scoring. Score from 0 (no triglyceride - beige) to 4 (high accumulation of triglyceride - red) was given. Each square in the graph represents a mouse; empty (white) squares represent missing mice.

4. Hydrogel dietary supplementation prevents early manifestations of high fat diet feeding through reduction of intestinal permeability

In recent years several reports have shown an association between altered intestinal microbiota, impaired intestinal permeability, low-grade inflammation and the onset of metabolic disorders[187,188,189].

Increased gut permeability is commonly believed to have a major role in HFD-induced obesity, resulting in translocation of bacteria and or microbial products (i.e. LPS) through the mucus layer and intestinal epithelial barrier (tight junctions, TJ)[80,190] into the bloodstream. Bacteria and bacterial molecules can then reach distant organs, where they interact with host immune cells inducing low-grade inflammatory processes, hallmarks of metabolic disorders like obesity and insulin resistance[191,150] and NAFLD[192]

Recent work in our laboratory demonstrated that disruption of intestinal epithelial barrier is an early event in the development of HFD-induced metabolic syndrome[193], occurring already after 1 week of feeding.

For this reason and in light of the results previously described, we decided to focus our attention on initial alterations induced by HFD-feeding, in particular on early changes in intestinal permeability.

We made use of preventive hydrogel administration to assess if Gel B was able to prevent impairment of intestinal TJ and gut permeability, after relatively short-term HFD feeding (i.e. 2-4 weeks). To this end, we fed mice for a period of 4 weeks with HFD or HFD 2% Gel B and HFD 4% Gel B; we hence assessed intestinal barrier impairment after 1, 2, 3 and 4 weeks of treatment, as well as hepatic triglyceride accumulation after 2 and 4 weeks. The experimental design is summarized in Experimental scheme 4.

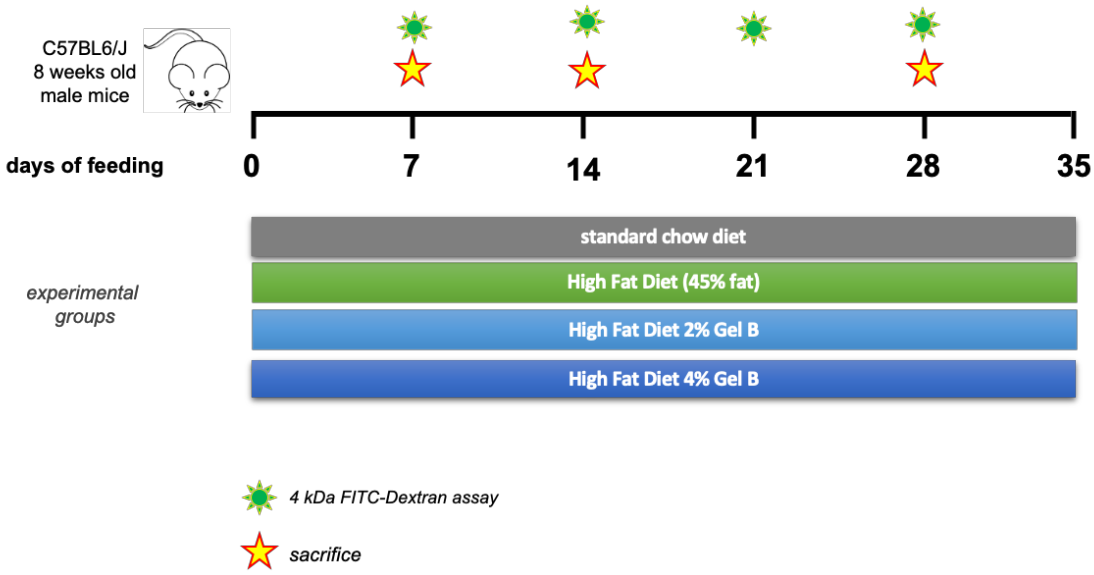

Experimental scheme 4. Short term preventive feeding with hydrogel supplemented high fat diet.

C57BL6/J male mice at 8 weeks of age were fed for 35 days with: chow diet in black, HFD in green, HFD supplemented with 2% Gel B in light blue and HFD supplemented with 4% Gel B. After 1-2-3 and 4 weeks of feeding with the different diets, intestinal permeability was functionally evaluated performing 4kDa FITC-Dextran permeability assay. After 1-2 and 4 weeks 5 mice per group were sacrificed, to evaluate intestinal length and tight junction expression, adipose tissue deposition and liver triglyceride accumulation.

Mice fed with HFD showed an increase in body and adipose tissue weight, compared to standard diet fed mice, already after 4 weeks of feeding. Both alterations were efficiently prevented by hydrogel supplementation (Figure 26a, b and c). Accordingly, hydrogel administration prevented intestine shortening due to HFD (Figure 27), in particular at the small intestine level (where the hydrogel is completely hydrated with intact 3D structure). We then analyzed lipid accumulation in the liver after both 2 and 4 weeks of feeding (Figure 28a and b): we found that an interval of 4 weeks of HFD-feeding was sufficient to induce triglyceride accumulation in the liver, as indicated by Oil red O staining (Figure 28); this could represent early step of steatosis development. Nicely, mice fed with HFD 2% and 4% Gel B were protected from hepatic lipid accumulation (Figure 28b). These data clearly show that body weight gain, EAT enlargement, intestine shortening and liver triglyceride accumulation induced by HFD in mice occurred rather early, and that the preventive administration of Gel B is efficiently able to block the development of such alterations.

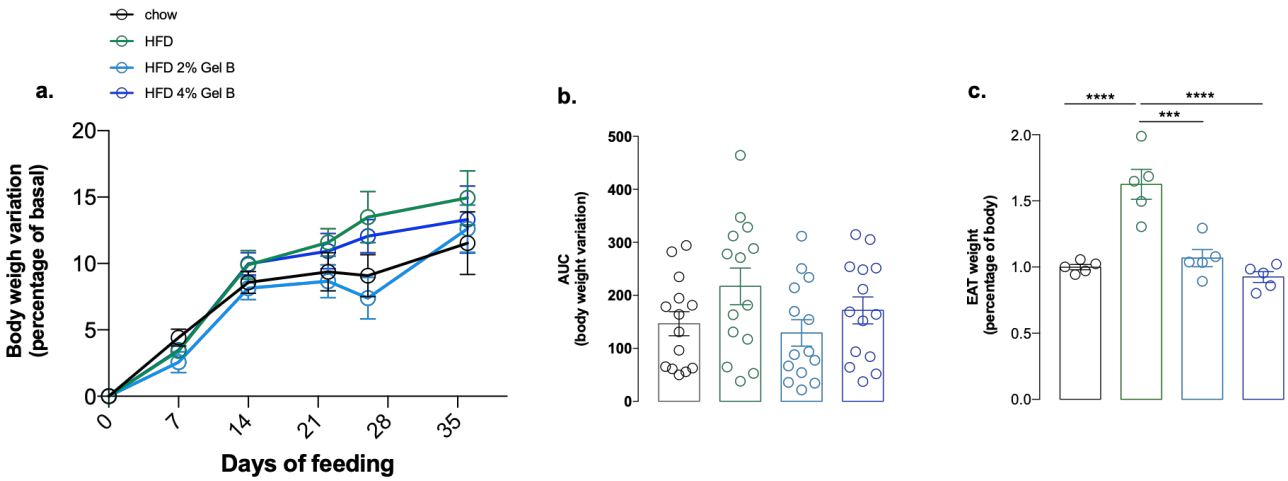

Figure 26. Short term preventive feeding with hydrogel supplemented diet prevents body weight gain and white adipose tissue deposition induced by HFD feeding.

a. Body weight variation expressed in percentage of basal; **b.** Area Under the Curve (AUC) of body weight variation; c. Epididymal Adipose Tissue (EAT) weight expressed in percentage of body weight, at sacrifice after 4 weeks of feeding (* p<0,5; **p<0,01; ***p<0,001 one-way ANOVA Tukey post-test, line at mean with SEM; 5-15 mice per group).

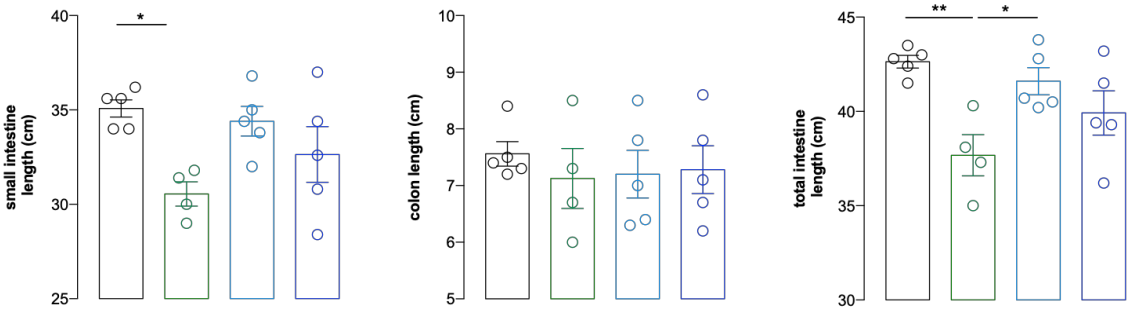

Figure 27. Short term feeding with hydrogel supplemented diet prevents intestine shortening induced by HFD feeding.

Intestine length measured at sacrifice after 4 weeks of preventive feeding with HFD supplemented diets. From left to right: small intestine length, colon length and total intestine length. (* p<0,5; **p<0,01; ***p<0,001 one-way ANOVA Tukey post-test, line at mean with SEM; 4-5 mice per group).

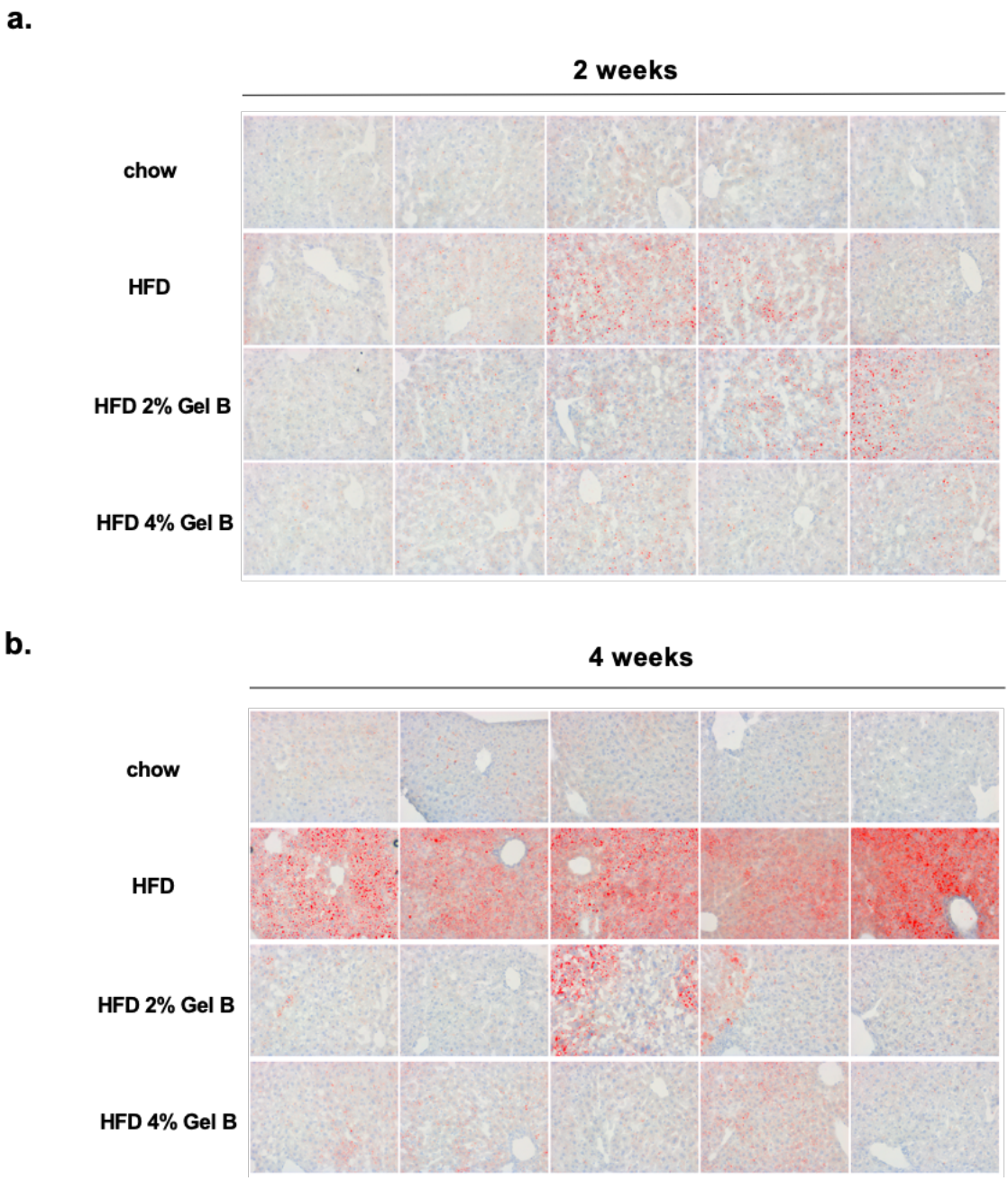

Figure 28. Short term feeding with hydrogel supplemented diet prevents liver triglyceride accumulation induced by HFD feeding.

Oil Red O staining of PLP fixed OCT embedded liver samples **a.** after 2 weeks of feeding with hydrogel supplemented diet and **b.** after 2 weeks of feeding with hydrogel supplemented diet. In line images from 5 individual mice per group.

With this in mind, we hypothesized that also alterations in intestinal barrier permeability (often reported in long term HFD-feeding or in genetic, i.e. ob/ob mice, or pharmacologically induced models of metabolic disorders [194]) could be detectable together with early intestine alterations in short term HFD feeding. Indeed, here we provide evidence that functional alterations of intestinal permeability occur as early as after 2 weeks of feeding with HFD; these data are consistent with other reports showing that HFD feeding induces small intestine and colon atrophy and impairment of immune system after 3 weeks of feeding[195], together with alterations of intestinal barrier permeability and gut microbiota after 4 weeks of HFD administration[196].

To assess impairment of gut permeability in the HFD model, we made use of 4 kDa FITC-dextran assay (Figure 29a; see also material and methods). Significant increase in gut permeability, indicated by higher diffusion of 4 kDa FITC-Dextran into the bloodstream from the gut, was observed after 2 weeks in mice fed a HFD (Figure 29c); increased permeability persisted over time and was maintained almost equally after 3 and 4 weeks of feeding (Figure 29 d and e). Hydrogel diet supplementation guaranteed protection from HFD-induced permeability impairment (both Gel B doses worked), preventing 4 kDa FITC-Dextran translocation from gut lumen to the bloodstream, similarly to mice fed with standard chow diet (Figure 29 c, d and e).

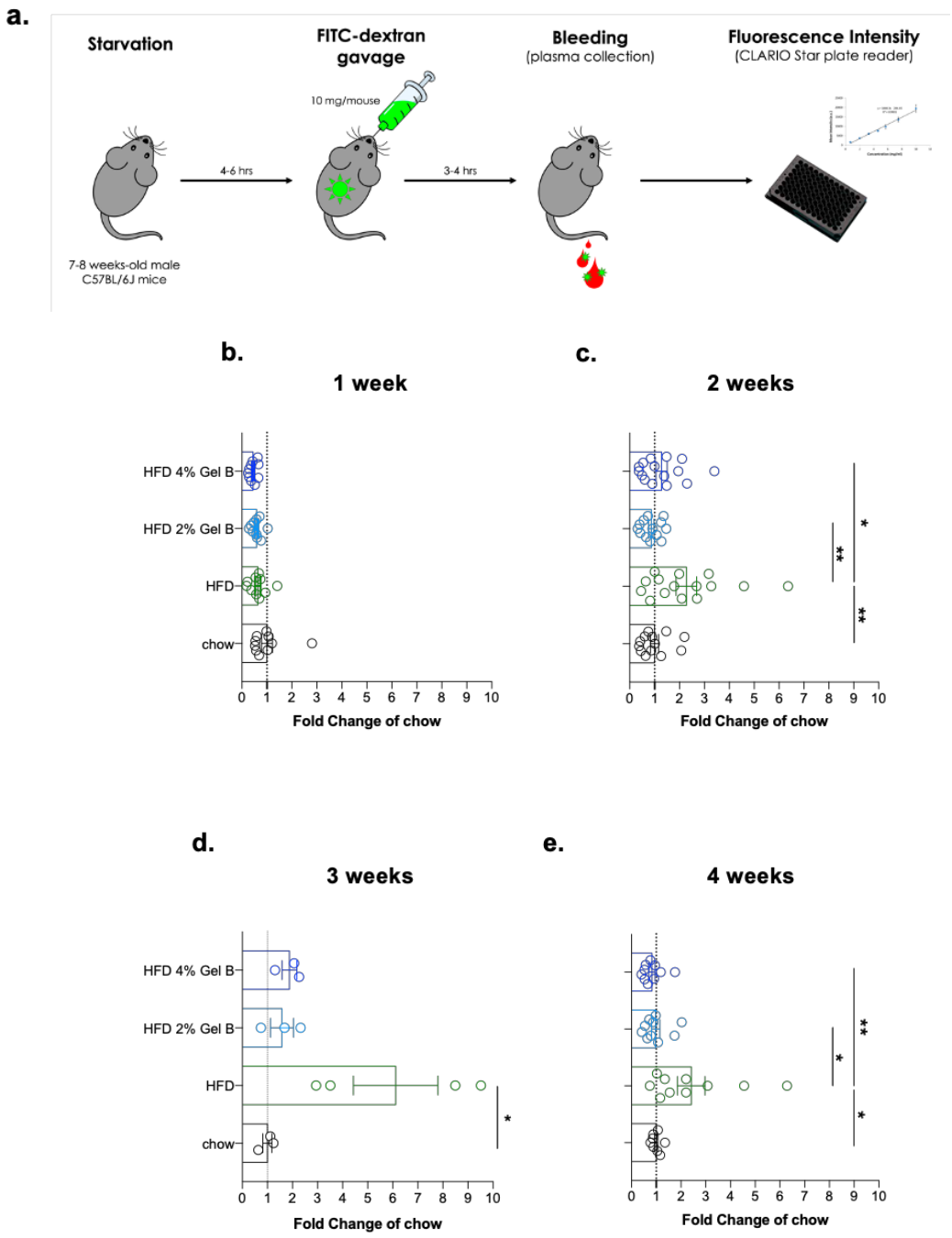

Figure 29. Short term feeding with hydrogel supplemented diet prevents alteration of intestinal permeability induced by HFD feeding.

a. Experimental scheme of 4kDa FITC-Dextran permeability assay. After 4-6 hours of morning fasting mice were gavaged with 10 mg of 4kDa FITC-Dextran, after 4 hours blood was collected from the tail vain and plasma FITC-Dextran was measured using CLARIO Star plate reader; **b, c, d, e.** FITC-Dextran permeability levels after 1 week (**b**), 2 weeks (**c**), 3 weeks (**d**) and 4 weeks (**e**) of feeding, expressed as fold change of chow; (* p<0,5; **p<0,01; ***p<0,001 one-way ANOVA Tukey post-test, line at mean with SEM; 5-15 mice per group).

The impairment in gut permeability in HFD mice and the functional rescue obtained through Gel B administration let us to hypothesize that these phenomena involved the function of tight junctions. TJ are the primary determinant of paracellular permeability[197], playing a critical role in the pathogenesis of intestinal and systemic diseases. Many TJ proteins bind to the N-terminal half region of ZO proteins. For this reason, we focused on ZO proteins expression, in particular on ZO-1. ZO-1 is localized at the nascent cell-cell contacts and it has been proposed that ZO proteins may mediate the early assembly of TJ proteins into cell-cell contacts[68]. Hence, we analyzed alterations of ZO-1 expressions induced by HFD through immunofluorescence. We detected a partial alteration of ZO-1 expression at ileum level already after 1 week of feeding with HFD, that was completely prevented in mice fed with hydrogel supplemented diets at both doses (Figure 30a, b). We even observed an increase in ZO-1 expression as compared to chow fed mice, even though not statistically significant (Figure 30a, b) Of note, 1 week time-point is not associated with functional permeability impairment yet (Figure 29b), suggesting that ZO-1 levels alteration could precede functional impairment of the intestinal epithelium permeability. After 2 weeks of feeding with HFD, alteration in ZO-1 protein level persisted, becoming even more evident and paralleling functional permeability alteration; similarly, at this time-point hydrogel diet supplementation was able to prevent HFD-induced ZO-1 depletion at TJ (Figure 30c, d), in agreement with dextran permeability (Figure 30c). Consistently, after 4 weeks of feeding, hydrogel administration was able to prevent HFD-induced ileum ZO-1 downregulation (Figure 30e,f) as well as the impairment of functional permeability (Figure 29e).

Taken together, these data demonstrate hydrogel ability in preserving intestinal epithelial barrier integrity through stabilization of tight junction (ZO-1) and maintenance of correct intestinal barrier permeability during short-term HFD feeding.

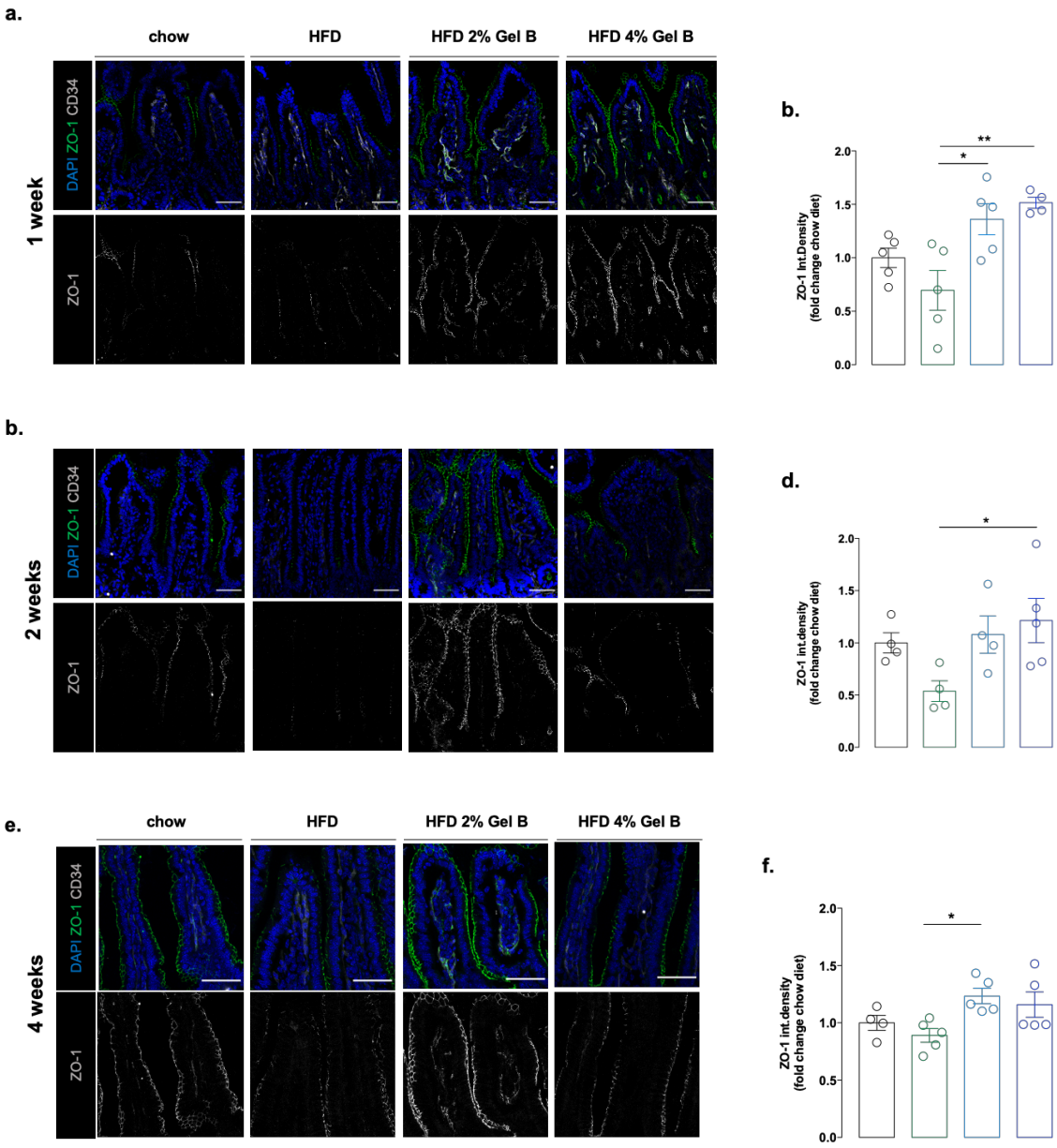

Figure 30. Short term feeding with hydrogel supplemented diet prevents alteration of tight junction protein ZO-1 induced by HFD feeding.

Mice were sacrificed after 1, 2 and 4 weeks of feeding. **a. c**. and **d.** Ileum tissue sections of mice fed for 1 week, 2 weeks and 4 weeks respectively. Tissue sections were stained for ZO-1, tight junction component (in green), CD34, marker of intestinal endothelium (in gray) and DAPI, marker for nuclei (in blue). In each panel, first line is depicting an image of the three merged channels. Second line of images is depicting images of ZO-1 channel alone (in gray). Representative images of a single mouse out of five per group. Scale bar 50 µm; **b**. **d**. and **f**. Quantification of ZO-1 integrated density expressed as fold change of chow diet, performed using Fiji image software (* p<0,5; **p<0,01; ***p<0,001 one-way ANOVA Tukey post-test, line at mean with SEM; 5 mice per group).

Based on these data, we then wanted to assess whether hydrogel administration could have a direct effect on the intestinal barrier, independently on HFD induced alterations.

For this purpose, we studied the effect of hydrogel administration on the intestinal barrier of healthy mice. We analyzed ZO-1 protein through immunofluorescence staining in both ileum and colon sections of mice fed for 4 weeks with hydrogel supplemented chow diet, carrying increasing doses of Gel B for 4 weeks (Experimental scheme 1).

Hydrogel supplementation boosted ZO-1 protein signal in mice fed with the highest concentration of Gel B (chow 8% Gel B), while physiological ZO-1 levels were not affected in mice fed with low and intermediate concentrations of Gel B (2% and 4% Gel B), both at the ileum and colon levels (Figure 31a,b,c).

Of note, higher level of tight junction protein ZO-1 was detected in mice fed with chow diet supplemented with 8% Gel B where we also observed a significant reduction in body weight and fasting glycemia.

Together these data denote the intrinsic ability of the hydrogel to target the intestine, acting on barrier tightness through a direct or an indirect (i.e. microbiota mediated) action on epithelial tight junction proteins, both in healthy (at very high dosage) and pathological conditions.

We reasonably argued that the hydrogel, by targeting the intestine, could in turn be able to prevent systemic manifestation induced by HFD-feeding.

Together these data demonstrate that hydrogel diet supplementation is able to prevent high fat diet induced alterations of intestinal barrier, improving epithelial tight junctions and functional permeability.

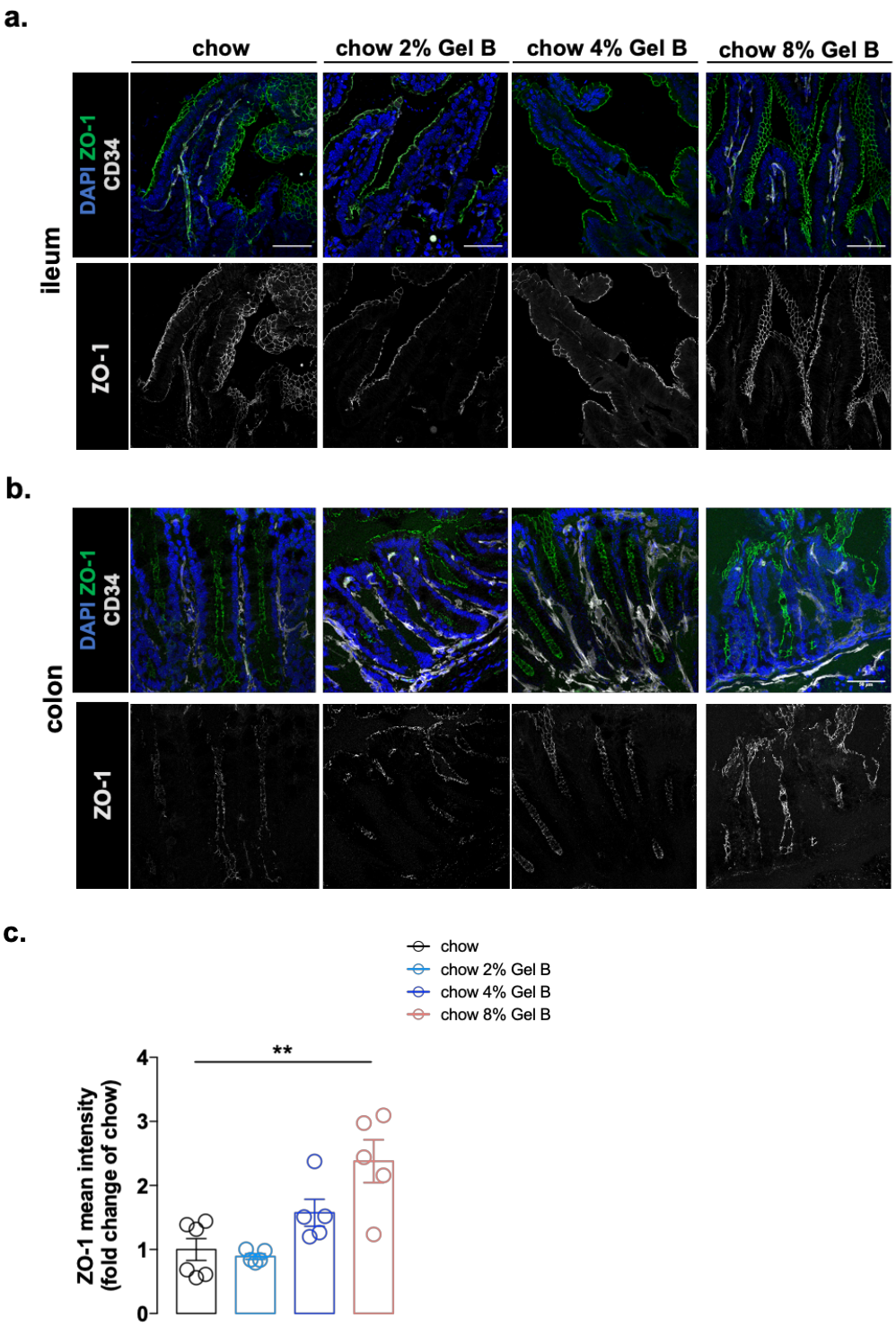

Figure 31. High hydrogel dosages improve intestinal epithelial ZO-1 expression in standard diet fed mice.

a.Ileum tissue sections and **b.** colon tissue sections stained for ZO-1, tight junction component (in green) and CD34, marker of intestinal endothelium (in gray) and DAPI, marker of nuclei (in blue). First line depicting merged channels images. Second line depicting ZO-1 channel images (in gray). For each group one representative image out of 5 mice per group. Scale bar 50 µm; **c**. Quantification of colon ZO-1 mean intensity expressed in fold change of HFD (* p<0,5; **p<0,01; ***p<0,001 one-way ANOVA Tukey post-test, line at mean with SEM).

5. Hydrogel dietary supplementation prevents intestinal barrier impairment induced by long term high fat diet feeding

We showed that HFD-induced intestinal barrier alterations occur rather early in the progression toward metabolic disorders; in parallel, we demonstrated that hydrogel HFD supplementation was able to successfully prevent these modifications, namely increased intestinal permeability which correlated with alteration in ZO-1 protein levels. We next wanted to assess the status of intestinal epithelial barrier after long term HFD-feeding and concomitant (preventive) hydrogel administration.

We analyzed ZO-1 tight junction protein level in mice fed for 18 weeks with HFD and HFD 2% and 4% Gel B (that is the very same preventive experiment summarized in Experimental scheme 2.

Mice fed with both LFD and HFD displayed a marked reduction of TJ protein ZO-1, being the protein almost at undetectable levels (Figure 32a, b). Per contra, preventive administration of hydrogel supplemented HFD was able to preserve epithelial ZO-1 level after 18 weeks of feeding (Figure 32a, b).

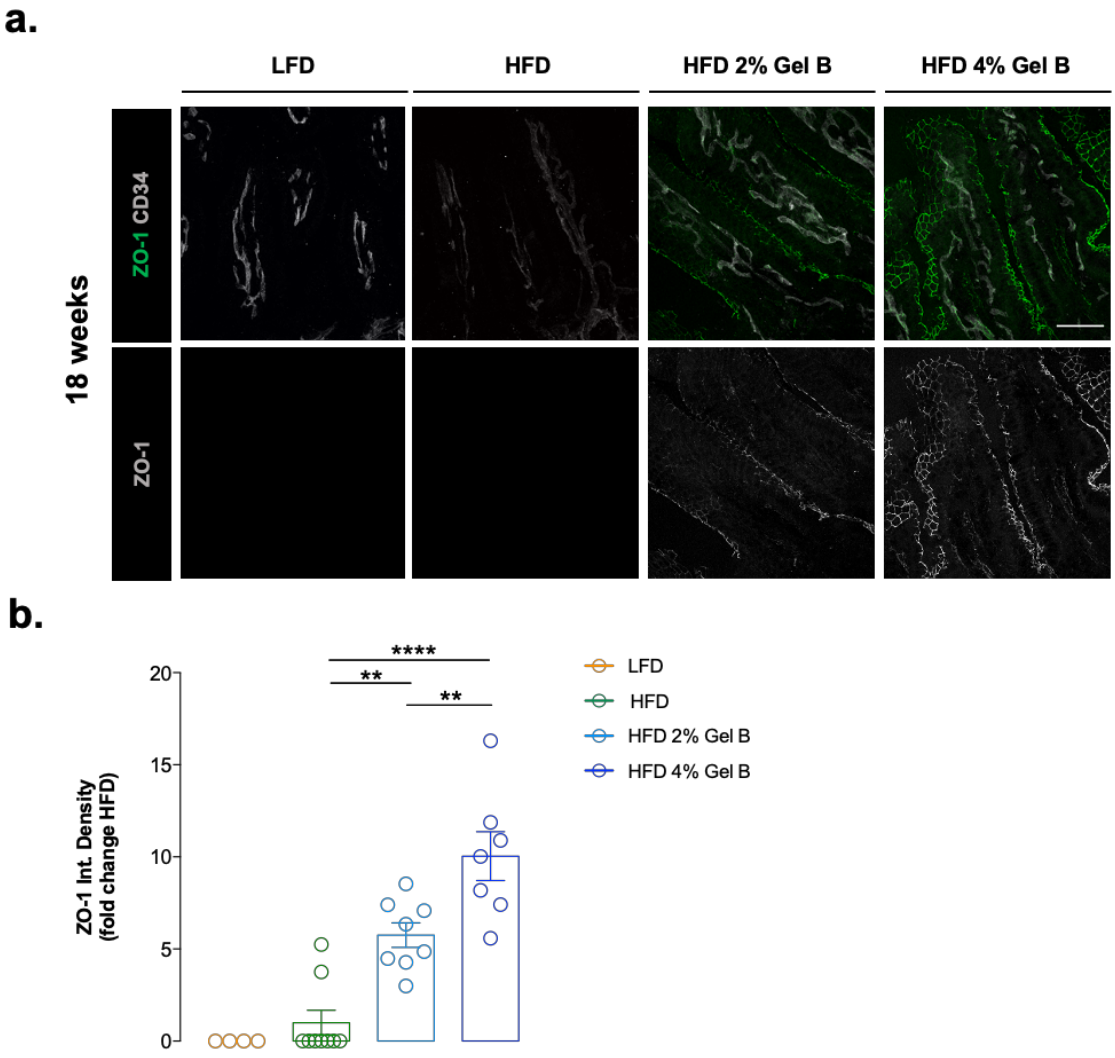

Figure 32. Hydrogel diet supplementation prevents intestinal epithelial ZO-1 downregulation induced by 18 weeks of high fat diet feeding.

Mice were fed for 18 weeks with LFD, HFD, HFD 2% Gel B and HFD 4% Gel B. **a.** Ileum tissue sections stained for ZO-1, tight junction component (in green) and CD34, marker of intestinal endothelium (in gray). First line is depicting the two merged channels. Second line of images is depicting ZO-1 channel alone (in gray). For each group one representative image out of 5-10 mice per group. Scale bar 50 µm; **b**. Quantification of ZO-1 integrated density expressed in fold change of HFD (values equal to zero are indicating images were ZO-1 signal was not detectable for image quantification).

We then analyzed expression level of TJ genes: *ZO-1 (TJP-1), Occludin, Claudin-1* and *Claudin-2* after 18 weeks of feeding (Figure 33). Probably, as a mean to counteract the downregulation of ZO-1 at protein level, ZO-1 gene expression levels were increased in LFD and HFD compared to standard chow diet fed mice, while partially restored to standard diet levels in mice fed with hydrogel supplemented diet (Figure 33a). Occludin is the first TJ-specific integral membrane protein identified, and is believed to be a regulator of paracellular permeability[48]. Occludin expression is markedly decreased in intestinal permeability disorders (i.e UC, Crohn's disease and celiac disease) suggesting that low *occludin* expression may promote increase in intestinal permeability[198]. However, no significant difference was observed in the *occludin* gene expression level among mice fed with chow, LFD and HFD, while a slight reduction was detected in mice fed with hydrogel supplemented HFD compared to HFD fed mice (Figure 33b).

We then analyzed gene expression of *claudin-1* and *claudin-2*. General functions of claudins are: formation of barrier or channel/pore, regulation of cellular polarity and boundary establishment to limit inter-mixing of lateral and apical membrane proteins[68]. Claudins prevent the passage of solutes and water as well as penetration of luminal toxins and antigens. Although more studies are necessary to determine the exact functions of claudins in TJs, animal studies have shown the importance of claudins in regulating the integrity of gut burrier and its correlated disorders. Claudin-1 expression is known to be increased in the areas of active inflammation[199]. Claudin-1-deficient mice exhibited abnormal TJ barrier formation, which induced cancer development and metastasis. Of interest, a correlation between increased claudin-1 expression and neoplastic transformation was also noted in colitis-associated cancer[86]. In our experimental setting mice fed a HFD showed an increase in claudin-1 ileal gene expression, that was not as pronounced in mice fed with a hydrogel supplemented diet (which was actually closer to chow mice level) (Figure 33c).

Claudin-2 is a pore-forming claudin responsible for paracellular Na^+ permeability and trans-mucosal resistance. Upregulation of Claudin-2 in disease tissues can potentially affect the structure and function of tight junctions, resulting in barrier dysfunction[200]. A slight reduction in the gene expression of *claudin-2*, even if not statistically significant was observed in mice fed with hydrogel supplemented HFD compared to HFD alone (Figure 33d).

Through the analysis of TJ gene expression, we detected mild alterations in the expression levels of ZO-1, Occludin, Claudin-1 and Claudin-2 due to HFD; moreover, these variation in gene expression point toward compensatory mechanisms aimed at replenishing putatively disrupted TJ levels and consequent increased gut permeability. This would be in agreement with the fact that Gel B administration partly prevents those gene expression alterations and gut permeability.

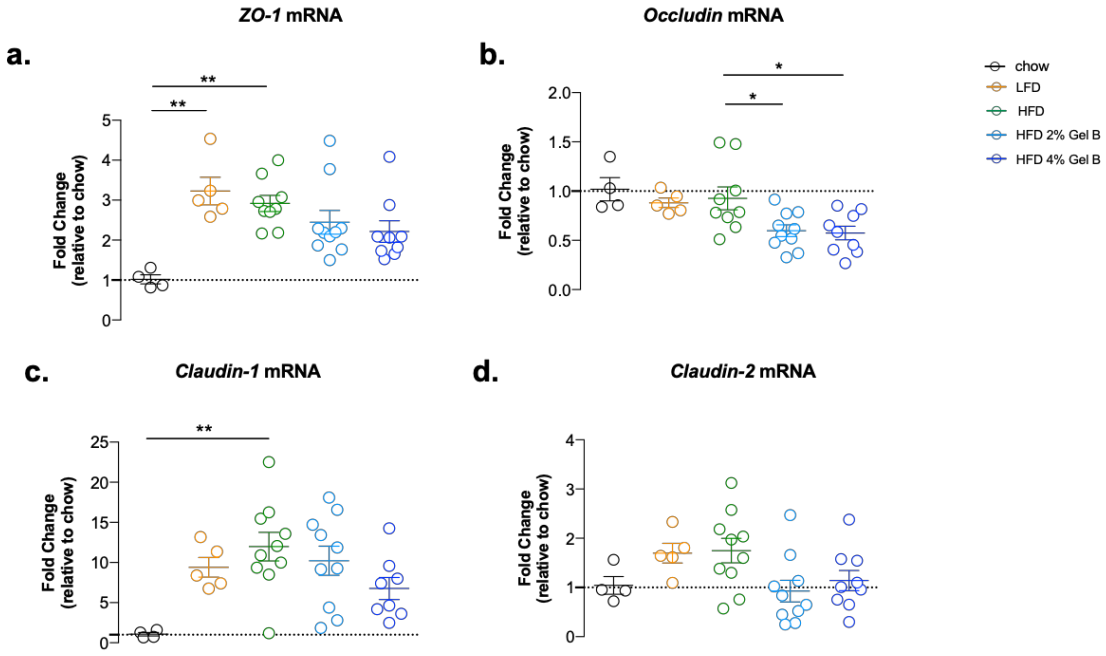

Figure 33. Intestinal tight junction gene expression after 18 weeks of feeding.

Relative gene expression levels of intestinal tight junction ZO-1 (**a.**), Occludin (**b.**), Claudin-1 (**c.**), Claudin-2 (**d.**); * p<0,5; **p<0,01; ***p<0,001 one-way ANOVA Tukey post-test, line at mean with SEM.

6. Therapeutic hydrogel administration reverts intestinal barrier impairment and induced by long term high fat diet feeding

The therapeutic administration of Gel B was able to restore many of the alterations induced by the HFD, with milder effects concerning liver steatosis. Still, we think that an effect on intestinal permeability in a therapeutic setting could represent an important achievement, strengthening the rationale of using the hydrogel to target the intestine, as a therapeutic intervention for GI-tract related diseases. Hence, we wanted to assess the status of intestinal epithelial barrier in mice therapeutically treated with hydrogel supplemented HFD (in the experiment summarized in Experimental scheme 3).

As expected, mice fed with HFD display a reduction in ZO-1 protein level, at both the time points we analyzed after hydrogel treatment, namely 4 weeks (Figure 34a, c) and 12 weeks (Figure 34b, d) of Gel B treatment. Surprisingly, in HFD 2% Gel B and HFD 4% Gel B treated mice, ZO-1 protein level was higher than that in HFD mice and basically comparable to ZO-1 level of control chow mice, at both 4 weeks (Figure 31a, c) and 12 weeks (Figure 31b, d) of Gel B treatment.

This demonstrate that therapeutic hydrogel administration was able to preserve intestinal tight junction protein ZO-1 upon progressive alterations induced by long term HFD feeding.

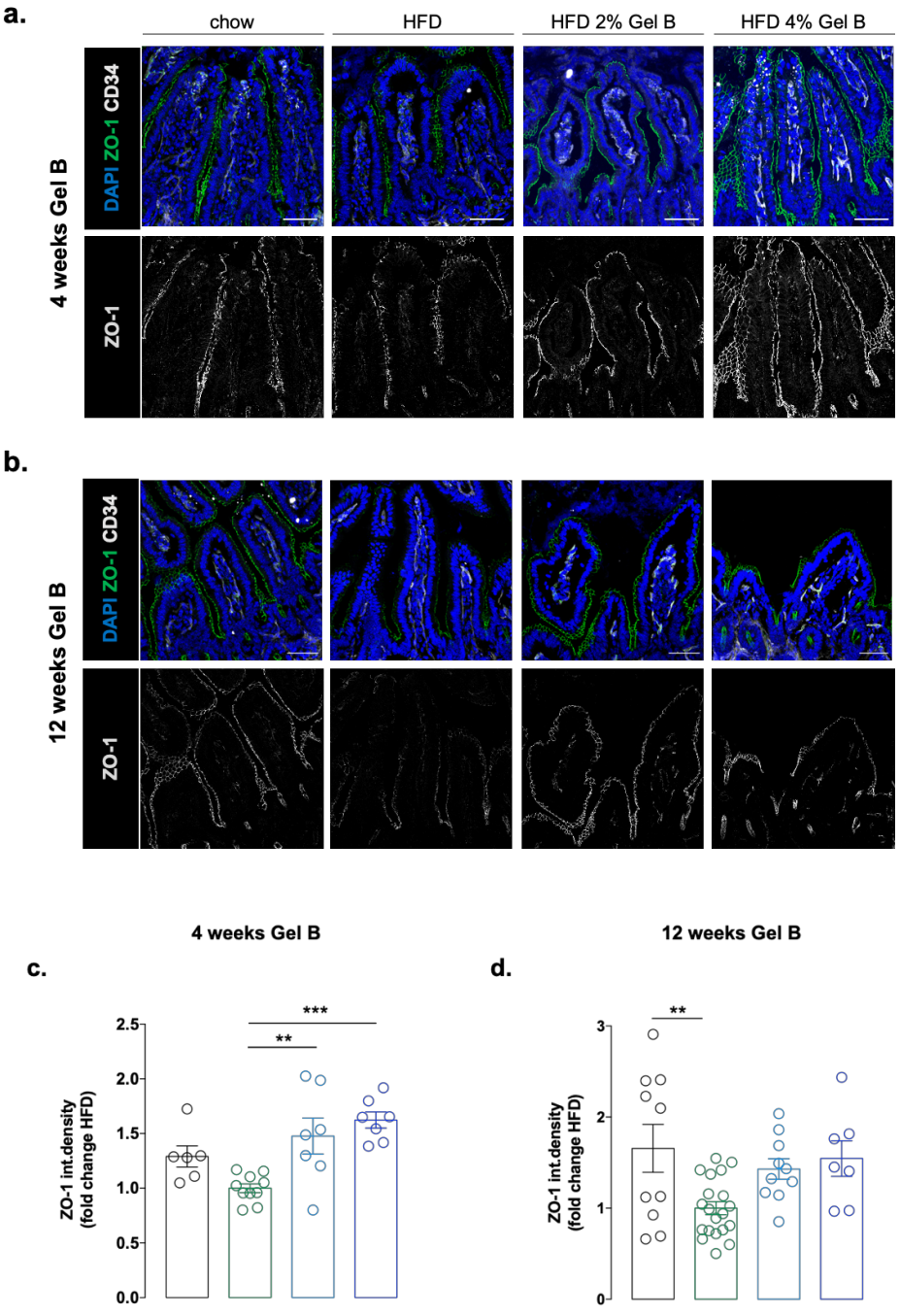

Figure 34. Therapeutic hydrogel administration restored intestinal epithelial tight junction protein ZO-1 expression.

Ileum tissue sections stained for ZO-1, tight junction component (in green) and CD34, marker of intestinal endothelium (in gray) and DAPI, marker of nuclei (in blue) **a.** after 4 weeks of feeding with Gel B supplemented diet (16 weeks HFD) and **b**. after 12 weeks of feeding with Gel B supplemented diet (24 weeks HFD). First line depicting merged channels images. Second line depicting ZO-1 channel images (in gray). For each group one representative image out of 5-10 mice per group. Scale bar 50 µm. **c** and **d**. Quantification of colon ZO-1 integrated intensity expressed in fold change of HFD after 4 and 12 weeks of hydrogel supplemented diet feeding respectively (* p<0,5; **p<0,01; ***p<0,001 one-way ANOVA Tukey post-test, line at mean with SEM).

We also analyzed the expression level of TJ genes: *ZO-1 (TJP-1), Occludin, Claudin-1* and *Claudin-2* after therapeutic administration of Gel B (Figure 35). As previously observed in the preventive setting, also in the therapeutic experiment ZO-1 gene expression level was slightly increased after long term HFD feeding, compared to standard chow diet fed mice, both at 4 weeks and 12 weeks of treatment (for the HFD mice these corresponded to 16 weeks and 24 weeks of HFD respectively). However, we could not detect any significant difference in ZO-1 expression level among groups once mice were treated either for 4 weeks or for 12 weeks with the hydrogel, except in the case of HFD 4% Gel B treated mice (12 weeks of treatment): on the contrary, in these mice ZO-1 gene expression was slightly downregulated respect to control chow mice (Figure 35a).

Similarly to ZO-1 gene expression level, we observed a slight increase in *occludin* gene expression level in HFD fed mice (only 4 weeks after hydrogel treatment) that was blunted by hydrogel diet supplementation; moreover, HFD 4% Gel B showed a downregulation of *occludin* gene expression when compared to HFD or chow mice (Figure 35b).

Concerning *claudin-1* and *claudin-2* gene expression levels, we did not find relevant difference among groups, in most of the time points we analyzed (Figure 35c, d), with the exception of *claudin-1* gene expression level after 12 weeks of hydrogel administration (Figure 35d): *claudin-1* gene was upregulated in HFD fed mice compared to chow diet fed mice, while HFD 4% Gel B treatment reverted *claudin-1* gene expression to level comparable to that of control chow mice (Figure 35c).

No significant alterations in *claudin-2* gene expression were observed among the groups at any of the analyzed time-points (Figure 35d).

In conclusion, concerning TJ gene expression we recapitulated what we already found in the preventive experiment. Going further, we could speculate that HFD 4% Gel B in some way (e.g. through microbiota modulation) efficiently preserve ZO-1 protein level at the junctions – and perhaps other TJ proteins - such that upregulation at the gene level during HFD feeding is not required; nevertheless, how ZO-1 protein is modulated in the presence of Gel B requires further investigation.

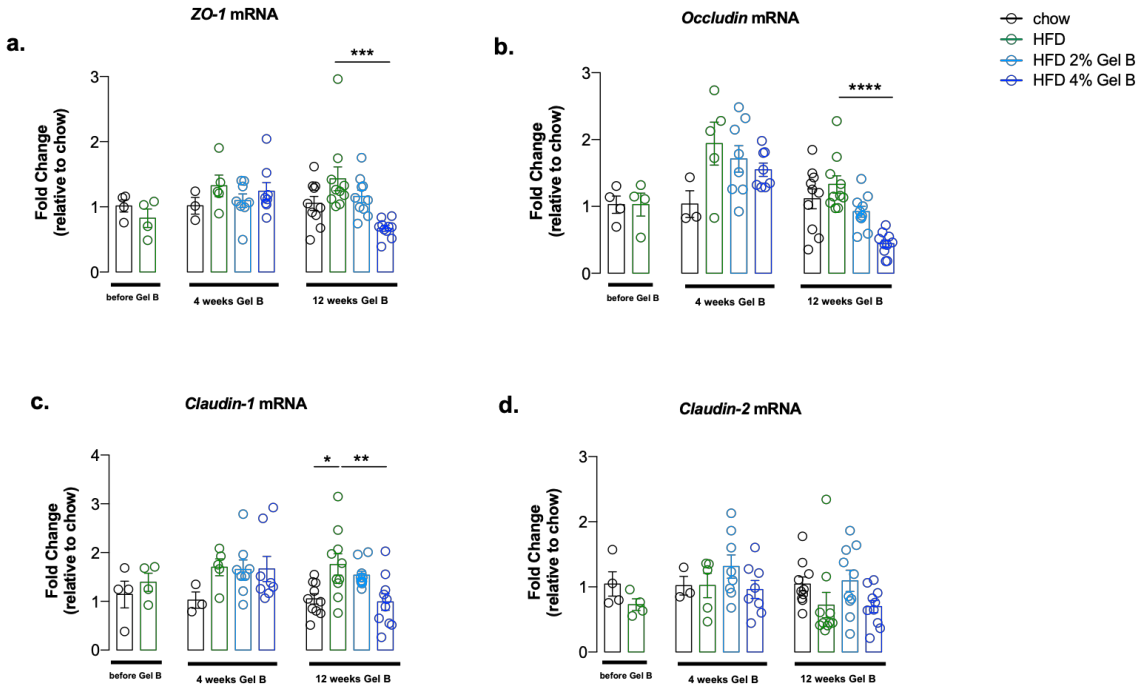

Figure 35. Intestinal tight junction gene expression after therapeutic hydrogel supplemented diet administration.

Relative gene expression levels of intestinal tight junction ZO-1 (**a.**), Occludin (**b.**), Claudin-1 (**c.**), Claudin-2 (**d.**); * p<0,5; **p<0,01; ***p<0,001 one-way ANOVA Tukey post-test, line at mean with SEM.

Next, to determine whether improvement in intestinal epithelial ZO-1 expression after therapeutic hydrogel administration was also associated to a functional amelioration of intestinal permeability, we performed 4 kDa FITC-Dextran permeability assays after 12 weeks of HFD feeding (before hydrogel treatment) and after 4 weeks and 12 weeks of hydrogel treatment (Figure 36).

As expected, after 12 weeks of HFD mice showed an augmented translocation of 4kDa FITC-dextran from the intestinal lumen to blood circulation, compared to standard diet fed mice, indicating that alteration of intestinal epithelial permeability occurred in these mice (Figure 36a). After 4 weeks of therapeutic hydrogel administration HFD 2% and 4% Gel B mice showed a slight amelioration in intestinal permeability compared to HFD-fed mice (Figure 36b), which was stronger after 12 weeks of therapeutic hydrogel administration, at which permeability to 4 kDa FITC-dextran was blocked by both doses of the hydrogel (Figure 36c). However, chow fed mice, at these time points, showed levels of intestinal 4 kDa FITC-dextran permeability comparable to those of HFD fed mice; we hypothesized that this phenomenon could be dued to the occurrence of aging-related intestinal barrier alterations.

Overall, these data show that the hydrogel is able to target intestinal epithelial barrier, improving tight junctions and intestinal permeability altered by HFD feeding. We concluded that the hydrogel acts directly or indirectly (through the microbiota) on the intestine, both preventing and treating intestinal epithelial barrier alterations induced by an unhealthy dietary regimen rich in fats.

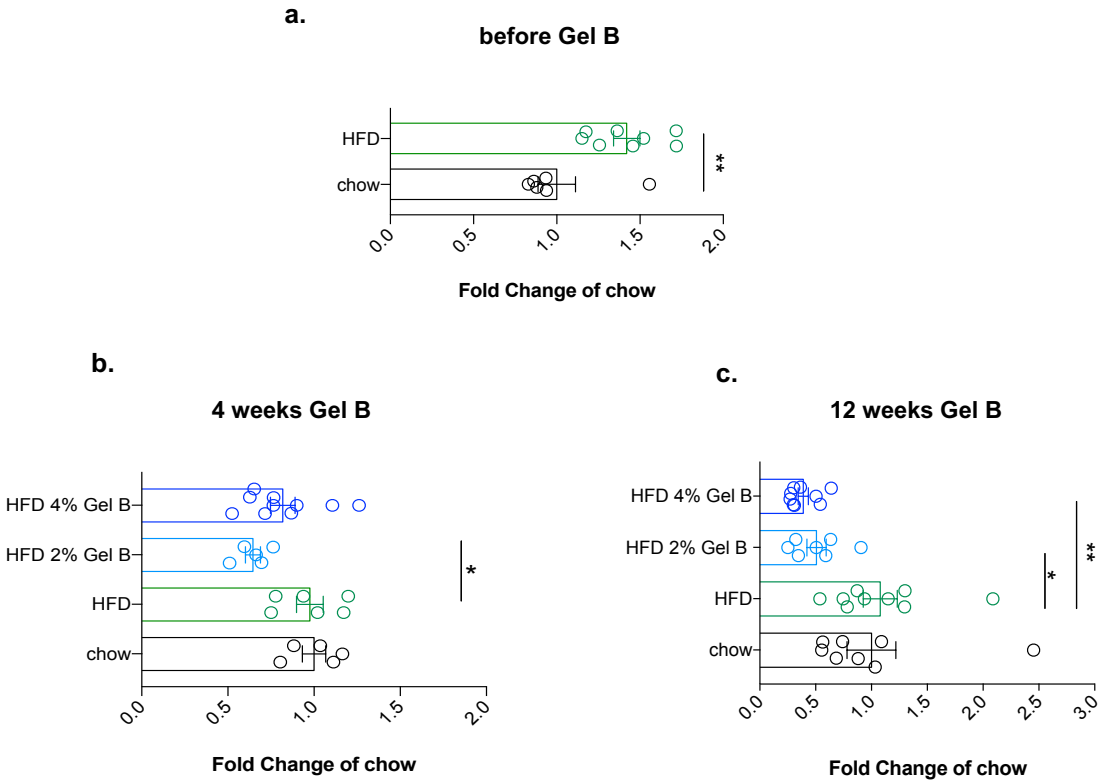

Figure 36. Therapeutic hydrogel administration improves intestinal barrier permeability.

After 4-6 hours of morning fasting mice were gavaged with 10 mg of 4kDa FITC-Dextran, after 4 hours blood was collected from the tail vain and plasma FITC-Dextran was measured using CLARIO Star plate reader; **a.** 4kDa FITC-Dextran permeability levels after 12 weeks of HFD-feeding (before Gel B administration) expressed in fold change of chow; **c.** 4kDa FITC-Dextran permeability levels after 4 weeks of feeding with hydrogel supplemented-HFD expressed in fold change of chow; **d.** 4kDa FITC-Dextran permeability levels after 12 weeks of feeding with hydrogel supplemented-HFD expressed in fold change of chow (* p<0,5; **p<0,01; ***p<0,001 one-way ANOVA Tukey post-test, line at mean with SEM).

7. Hydrogel dietary supplementation prevents and improves HFD – induced metabolic endotoxemia

As previously mentioned, HFD-induced metabolic alterations are believed to be associated with low-grade inflammation that in turn contributes to the onset of metabolic disease[201]. Bacterial product translocation from gut lumen to blood circulation (generally referred to as endotoxemia) are considered the culprits of this low-grade inflammation. Recently, gut microbiota-derived lipopolysaccharide (LPS) has been identified as a factor involved in the onset and progression of inflammation associated to metabolic diseases[80,97]. On the other hand, it has been reported the occurrence of LPS tolerance in both obese and T2 diabetic humans[202] and rats[203]. This phenomenon is promoted by adiponectine, whose levels are reduced in obesity, which in turn boosts the pro-inflammatory responses due to obesity-associated endotoxemia[204]
As impaired gut permeability must be involved in the translocation of microbial molecules, we wanted at first to assess if endotoxemia was induced after short-term HFD feeding and whether hydrogel diet supplementation was able to prevent LPS translocation, likely through the improvement of intestinal permeability.
We measured circulating LPS levels after 2 and 4 weeks of feeding with HFD: an increase in circulating LPS levels was detectable already after 2 weeks of feeding with HFD (Figure 37a), as well as after 4 weeks (Figure 37b). Nevertheless, hydrogel diet supplementation was able to prevent LPS translocation induced by HFD both after 2 and 4 weeks of feeding (Figure 37a,b).
Prevention of LPS translocation was accompanied by improvement of intestinal barrier permeability and expression of tight junction protein ZO-1 at both time-points (as previously shown), underling a direct effect of the hydrogel on intestinal barrier tightening.

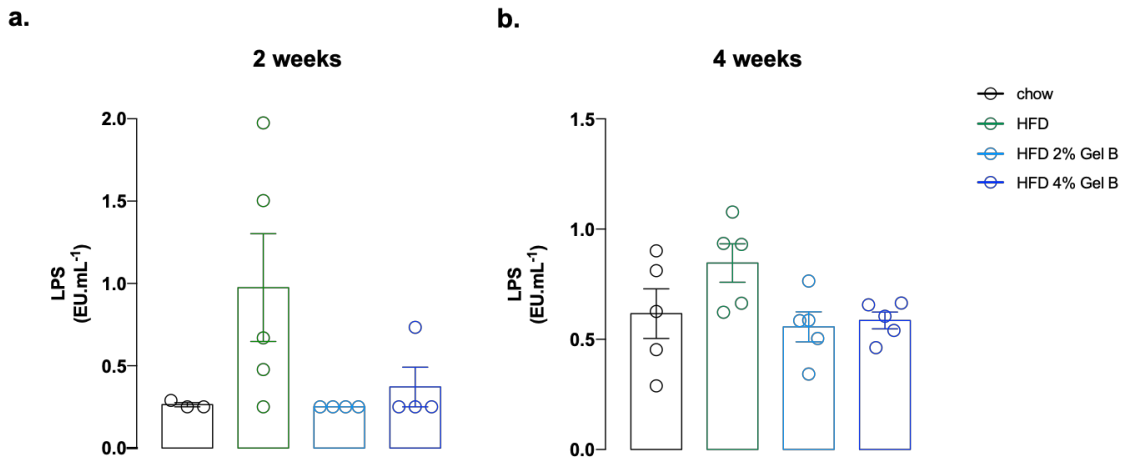

Figure 37. Short term feeding with hydrogel supplemented diet prevents lipopolysaccharide (LPS) translocation in blood circulation.

a. circulating LPS levels measured after 2 weeks of feeding. **b.** circulating LPS levels measured after 4 weeks of feeding line at mean with SEM; 4-5 mice per group).

Since the hydrogel was able to efficiently prevent the onset of metabolic endotoxemia after short term HFD, likely through an improvement in gut barrier tightness and permeability, we were interested in recapitulating the effect of hydrogel supplementation on endotoxemia after long term HFD-feeding.

We first wanted to assess the existence of a link between intestinal barrier perturbations, LPS translocation and the development of obesity-related metabolic alterations in our preventive murine model shown in Experimental scheme 2.

Mice fed a HFD for 18 weeks showed higher levels of serum LPS, indicative of metabolic endotoxemia. Interestingly, hydrogel supplementation fully protected animals from LPS translocation. Indeed, mice fed a hydrogel supplemented diet showed circulating LPS levels comparable to those of aged-matched mice fed with standard chow diet (Figure 38).

Therefore, preventive hydrogel supplementation during long term HFD-feeding was able to block the occurrence of metabolic endotoxemia through preservation of intestinal barrier integrity and permeability.

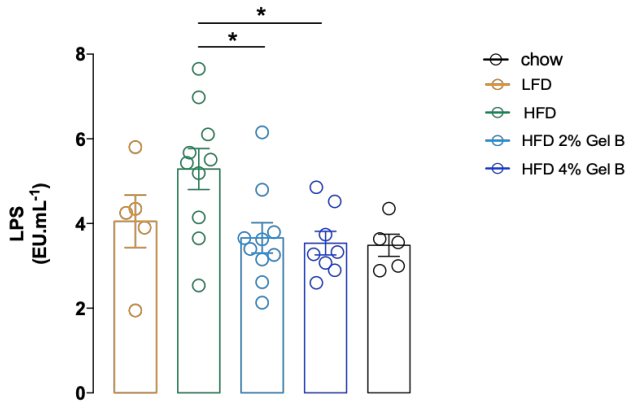

Figure 38. Hydrogel diet supplementation prevents endotoxemia induced by 18 weeks of high fat diet feeding.

Circulating LPS levels measured after 18 weeks of feeding with LFD, HFD, HFD 2% Gel B and HFD 4% Gel B compared to standard chow diet (* p<0,5; **p<0,01; ***p<0,001 one-way ANOVA Tukey post-test, line at mean with SEM).

The effect of the hydrogel on LPS translocation was rather strong and led us to hypothesize that the same could have happened in the therapeutic experiment. We hence measured serum LPS levels in mice before and after 12 weeks of hydrogel therapeutic administration (Experimental scheme 3).

Mice fed with HFD displayed an increase in serum LPS already after 12 weeks of HFD feeding; this trend was maintained till 24 weeks of feeding when compared to control (chow fed) mice. After 12 weeks of hydrogel treatment both HFD 2% Gel B and HFD 4% Gel B treated mice displayed a reduction in circulating LPS levels and consequent endotoxemia when compared to chow diet and HFD fed mice (Figure 39). In particular hydrogel supplementation at both concentrations, was able to maintain circulating LPS concentration stable in time, to levels comparable to those of mice fed for 12 weeks with HFD (before Gel B). Indeed, mice fed with both chow and HFD showed an increase in serum LPS after additional 12 weeks of feeding.

Taken together, the data suggest that the action of the hydrogel on intestinal permeability is key for counteracting HFD-induced LPS translocation, a hallmark of metabolic endotoxemia. This could be one of the mechanisms through which the hydrogel is able to prevent major metabolic alterations linked to endotoxemia and consequent low-grade inflammation.

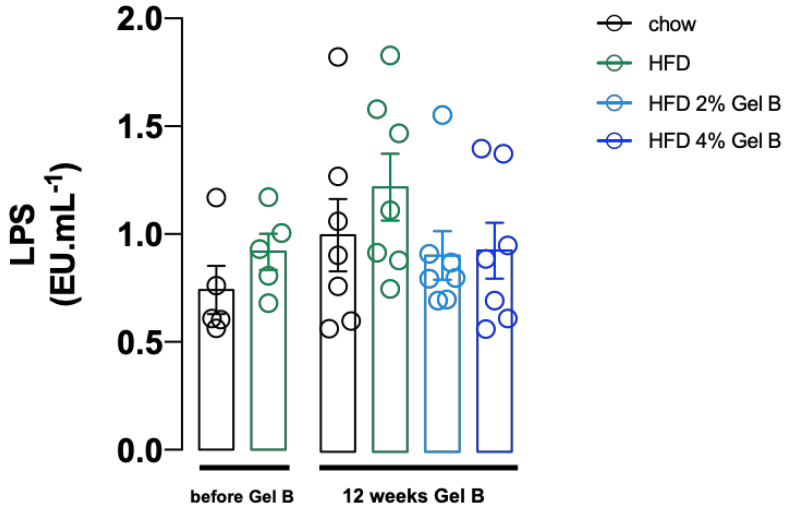

Figure 39. Effects of therapeutic hydrogel administration on endotoxemia.

Circulating LPS levels measured respectively before Gel B administration (12 weeks HFD) and after 12 weeks of therapeutic Gel B administration (line at mean with SEM, 5-8 mice per group).

8. Hydrogel diet supplementation modifies gut microbiota composition and partially prevents HFD induced dysbiosis

Alterations in gut microbiota, increased intestinal permeability and endotoxemia are believed to play a role in the development of a chronic low-grade inflammatory state that in turn contributes to the development of obesity and associated chronic metabolic diseases[205,206,207,208]. In recent years, accumulating evidence suggest that HFD-induced metabolic disorders are associated with dysbiosis and modifications of gut microbiota composition[209]. However, mechanisms by which microbiota promotes metabolic alterations are still not well understood. To date, leading theories about the mechanisms include changes in signaling molecules released by bacteria in contact with local tissue or distant organs[206] and increased energy harvesting by obesity associated gut microbiota[210]. Nevertheless, altered intestinal barrier and subsequent translocation of bacteria or bacterial products from altered intestinal microbiota is now regarded as an important mechanism associated with obesity[211,189]. Indeed, we have shown that modifications of intestinal permeability are mainly due to HFD-induced microbiota dysbiosis[193].

In order to study dysbiosis associated with the HFD (namely, the microbiota composition in HFD 45% fed mice) and to assess if the hydrogel was able to reshape the microbiota turning it into a "protective" one in the context of HFD, we performed the analysis of fecal samples harvested from the experiment described in experimental scheme 2 (i.e. the preventive experiment). More specifically, we analyzed fecal samples from individual mice fed for 18 weeks with LFD, HFD and HFD 2% Gel B and HFD 4% Gel B. Fecal samples were collected at basal and terminal time-points, and every four weeks throughout the experiment (Experimental scheme 2). Bacterial DNA was extracted and sequenced on Illumina's Next Seq platform to perform microbiota analysis.

Principal Coordinate Analysis (PCoA) of Bray Curtis dissimilarity (beta-diversity) highlighted a shift in gut microbiota composition between mice fed with and without hydrogel supplemented diets, independently from the type of diet (Figure 40).

The Shannon index highlights a decreased heterogeneicity of community composition within individual samples (alpha-diversity) (Figure 41). This indicates that the hydrogel *per se* stabilizes gut microbiota diversity.

Firmicutes and *Bacteroidetes* are two major microbial phyla, dominant in the gut, and their ratio (F/B ratio) has been extensively correlated with obesity and other metabolic or systemic diseases[212].

The microbiota associated to obesity is characterized by a reduced presence of taxa belonging to the Bacteroidetes *phylum* and a proportional increase in members of the Firmicutes *phylum*, revealing an association with a higher presence of enzymes for complex carbohydrate degradation and fermentation [129].

Evaluation of the mean relative abundance of *phyla* per group revealed an alteration of Firmicutes/Bacteroidetes ratio with a significant increase of the *Firmicutes* and decrease of the *Bacteroidetes* in mice fed with either LFD or HFD, already after one month of feeding. Hydrogel supplementation bluntsed alterations of this ratio (Figure 42), suggesting that it can prevent HFD-induced dysbiosis.

Moreover, mice fed with LFD and HFD, but not hydrogel treated mice, displayed an increase in *Actinobacteria*, which are known to be associated with obesity[213]. Furthermore mice fed with hydrogel supplemented HFD show an increase in *Alistipes a* species associated to a better success in weight loss in obese humans[214], together with an increase in *Verrucomicrobia* (Figure 42), in particular *Akkermansia genera* (Figure 43). *Akkermansia* is a member of the *Verrucomicrobia* known to be inversely associated to obesity, diabetes and low-grade inflammation in humans[215].

Overall, these data show that the hydrogel administration can modulate the gut microbiota, preventing those microbiota alterations and dysbiosis typical of HFD and western dietary habits.

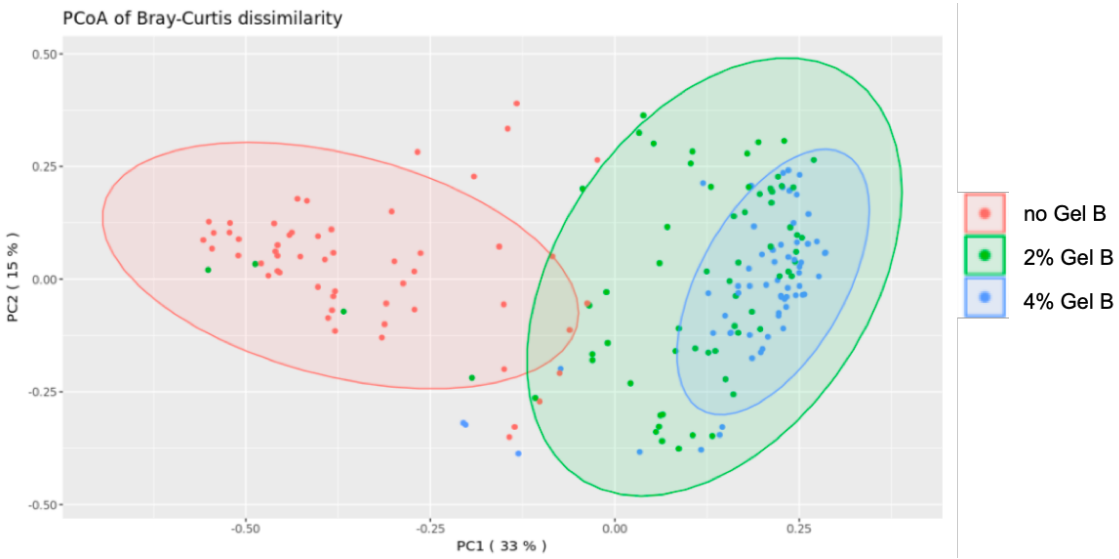

Figure 40. Hydrogel diet supplementation modifies gut microbiota composition.

Principal Coordinates Analysis (PCoA) of Bray-Curtis dissimilarity for all fecal samples highlighting hydrogel diet supplementation; no Gel B in red, 2% Gel B in green and 4% Gel B in blue.

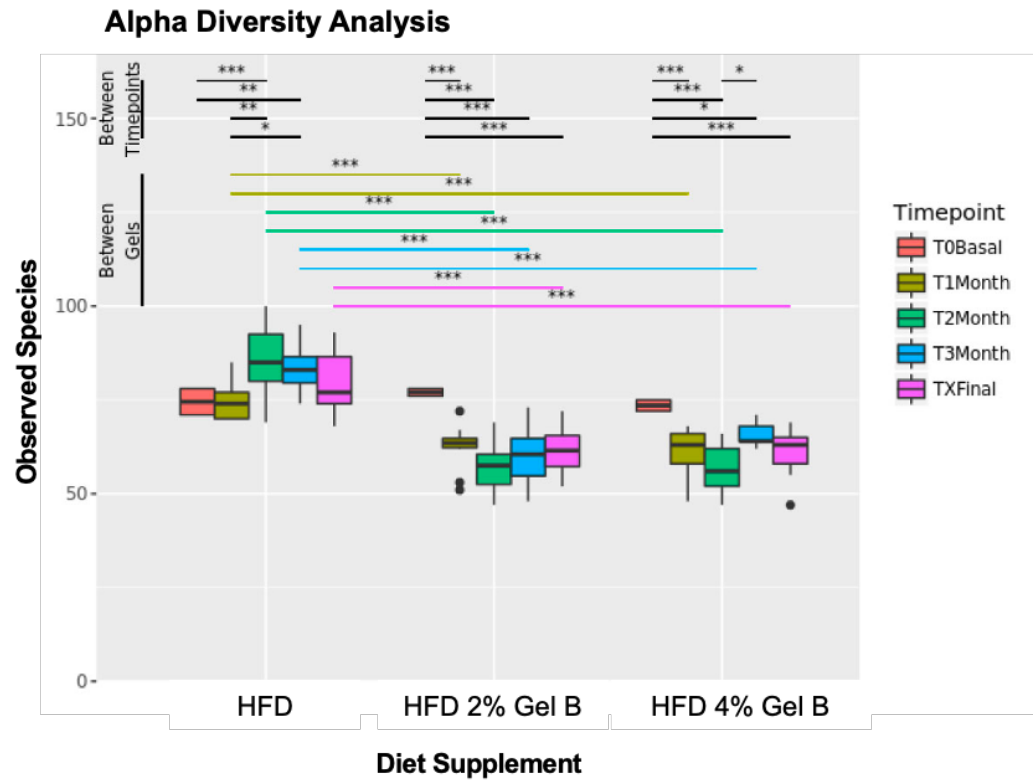

Figure 41. Hydrogel diet supplementation stabilizes gut microbiota diversity.

Alpha diversity analysis, as a measure of community composition within individual samples; observed species plotted by sample with outliers marked as individual points. Estimated marginal means was used to determine significant differences between diets and between time-points.

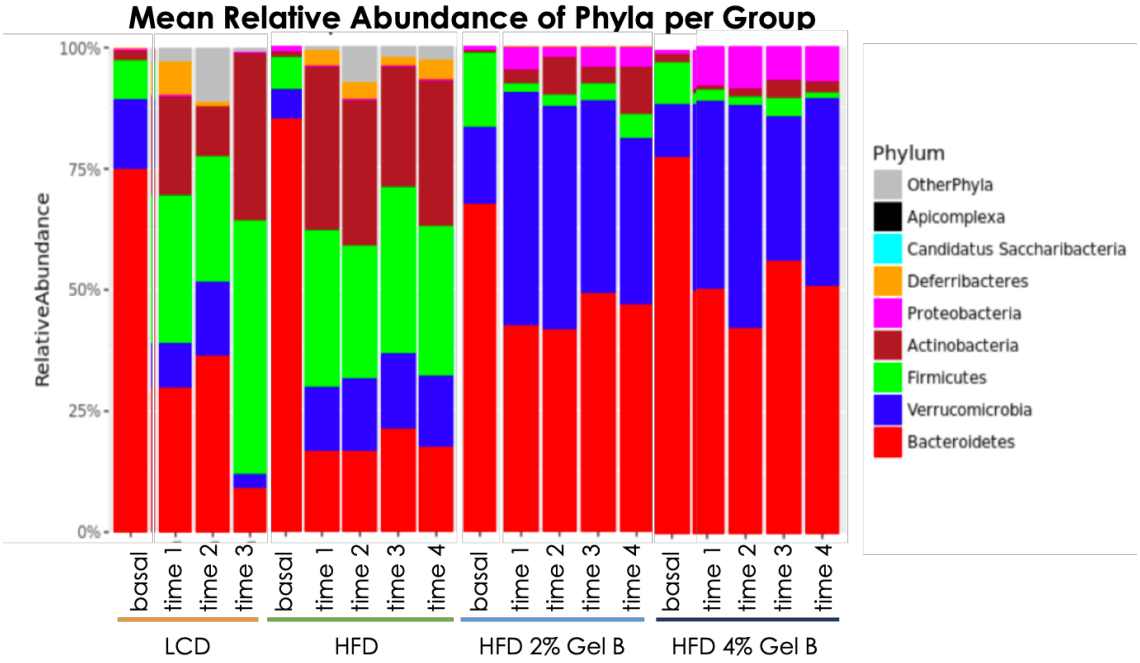

Figure 42. Mean relative abundance of phyla per group in mice fed with hydrogel supplemented diet.

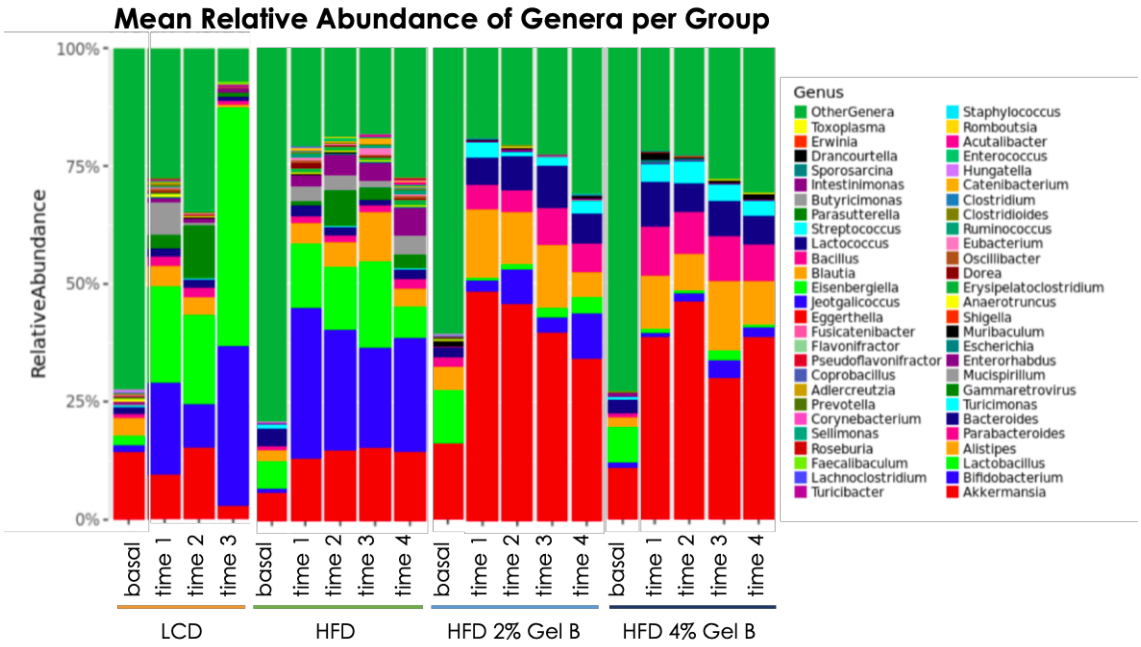

Figure 43. Mean relative abundance of genera per group in mice fed with hydrogel supplemented diet.

DISCUSSION

In the last two decades, several reports have shown a correlation between intestinal permeability impairment and the development of obesity[216,80,207], T2D[205,217]and NAFLD[75,84]. Moreover, it has been recently reported that gut barrier disruption, induced by gut microbiota dysbiosis, is a prerequisite for NAFLD development[193]. However, the association between metabolic disorders and malfunctioning of the intestinal barrier is poorly understood[218]. Alterations of intestinal microbiota, intestinal epithelial barrier, and consequent translocation of bacteria and bacterial endotoxins have been strictly correlated to the onset of obesity and its associated metabolic disorders. This highlights the central role of the intestine in the development of metabolic diseases[80,197,152]. Even though the precise mechanisms t the base of intestinal barrier dysfunction accompanying these disorders remain unknown, there is enough evidence for considering the intestine an attractive target for the treatment and prevention of obesity and its associated co-morbidities.

The superabsorbent hydrogel, produced by Gelesis and used in this work, was designed to hydrate in the stomach and to exert its function throughout the gastro-intestinal tract. Phase I clinical trials demonstrated hydrogels capacity to control obesity-associated alterations, like body weight gain and blood glucose levels, in overweight and obese patients[162]. Indeed, in the GLOW (Gelesis Loss of Weight) study, hydrogel treatment induced greater weight loss over placebo of 2.1%. And 59% of the hydrogel-treated patients achieved a weight loss $\geq 5\%$ and 27% of the patients achieved $\geq 10\%$. Furthermore, patients with prediabetes or drug-naive type 2 diabetes had a six times higher probability of achieving $\geq 10\%$ weight loss[162]. Therefore, we wanted to better characterize the mechanism of action of this hydrogel, intensely focusing on its activity on the intestine. In particular, we wanted to understand how the hydrogel, by targeting the gastro-intestinal tract, turned out to be successful in weight management and glycemic control in obese patients.

First, we assessed the effects of hydrogel administration in a mouse model of diet-induced obesity. Through long term feeding with a 45% fat HFD, we were able to recapitulate, in mice, typical alterations occurring in overweight and obese pre-diabetic individuals, who showed the best response to hydrogel treatment[162]. Hydrogel-supplemented HFD administration prevented body weight gain, adipose tissue deposition, and adipocyte hypertrophy, together with liver triglyceride accumulation (an early alteration in NAFLD development). Hydrogel administration also had an impact on glucose homeostasis and

insulin sensitivity, which are usually impaired in T2D and NAFLD[219]. Thus, preventing mice from developing insulin resistance.

Similarly to the preventive regimen, therapeutic administration of the hydrogel in mice pre-fed a HFD (for 12 weeks, to make them obese and pre-diabetic) successfully led to significant dose-dependent body weight reduction (respectively 5 and 10% of basal), already after 4 weeks of treatment; of note, weight control lasted for over additional 8 weeks of therapy. Body weight decrease mainly happened via adipose tissue size reduction; indeed, adipose tissue enlargement is one of the first modifications induced by overfeeding in the weight gain processes[220]. We hence speculated that one of the primary mechanisms through which the hydrogel controls body weight is acting on visceral adipose tissue reserves, possibly affecting nutrient absorption and calorie intake, directly or indirectly; further studies are required to assess this point. In parallel, the amelioration of parameters related to glycemic control and insulin resistance could be explained, at least in part, by body weight loss. Nonetheless, other mechanisms are likely contributing to this phenotype. In particular, insulin resistance involves different organs[221] and has been recently linked to altered intestinal immunity and gut microbiota[222,223,224], both of which are primary targets of the hydrogel.

Conversely, therapeutic administration of the hydrogel had a mild effect on liver steatosis, which did not resolve completely, but it did not progress either in hydrogel treated animals (12 weeks of treatment). Of note, differently from humans, animals were not subjected to a concomitant reduction in caloric intake (animals were fed a HFD for the entire experiment), known to be the first line of intervention in the treatment of obesity and NAFLD/NASH[225,226]; we can speculate that a longer period of hydrogel administration is required to have a stronger impact on liver fat clearance in mice continuously fed a HFD. Interestingly, our data suggest that hepatic triglyceride clearance is presumably partly independent from body weight loss and white adipose tissue reduction.

Notably, hydrogel prophylactic administration (but not the therapeutic one) was associated with higher circulating levels of GLP-1 in mice. GLP-1 is an incretin hormone that stimulates insulin release and inhibits glucagon secretion from the pancreas in response to food ingestion, also affecting gastric emptying[227], and its activity is known to be impaired in obese and diabetic subjects[228]. GLP-1R agonists have recently been proposed as a therapeutic strategy for obesity and T2D, but are known to frequently induce side effects mainly at gastro intestinal level[229]. In addition, inhibitors of GLP-1 degradation are promising oral hypoglycemic candidates[230,231]. Even though GLP-1

levels were not assessed in humans undergoing 24 weeks of hydrogel treatment[162], these preclinical data suggest that the hydrogel could be a safer alternative strategy to modulate GLP-1 levels in obese and pre-diabetic patients.

Overall, the data we obtained strongly support that hydrogel administration induces a reduction in body weight and adiposity, paralleled by an amelioration in insulin and glucose homeostasis, in both preventive and therapeutic setting, mainly recapitulating the effects observed in human patients[162].

Since our data were fully consistent with those obtained in the clinic, we identified our diet-induced obesity model (45% fat HFD) as the most valuable to further investigate the mechanisms of action of the hydrogel in the intestine, its main target tissue. Alteration of intestinal barrier integrity and function have been extensively associated with the development of obesity and metabolic syndrome[216,232,188,155]. Indeed, intestinal barrier integrity is guaranteed through cell-cell junctions; in particular, tight junctions (TJ) protein, like occludin, claudins, and zonula occludens-1, are crucial players in the maintenance of epithelial barrier integrity, allowing transport of essential molecules and restricting the passage of harmful substances[45]. An imbalance in TJ levels, localization, or function leads to a compromised barrier selectivity and augmented permeability; these are common phenomena in a variety of pathological conditions, like IBD[233,234] , obesity[235], and metabolic disorders[86], despite the lack of a well-demonstrated causal relationship[42].

We hence hypothesized that the hydrogel exerted its beneficial effects at least in part, directly interacting with the intestinal mucosa, through the reinforcement of the intestinal barrier function, by mainly acting on epithelial tight junctions. Indeed, in long-term HFD experiments, both prophylactic and therapeutic hydrogel administration restored HFD-induced intestinal barrier impairment. Mice fed with hydrogel supplemented HFD displayed an improvement in intestinal epithelial ZO-1 protein expression whereas localization of ZO-1 at the TJ was strongly decreased -if not even under the detection limit- upon long term high-fat diet feeding. Interestingly, the rescue in ZO-1 levels at TJ of the intestinal barrier was paralleled by a reduction of barrier permeability (which was increased in HFD-fed mice), to a level equal to that of healthy mice. We can speculate that the amelioration in glycemic control and hepatic triglyceride accumulation in obese mice treated with the hydrogel is partly due to the restoration of the intestinal epithelial barrier function. Notably, the positive effect of the hydrogel on intestinal permeability and ZO-1 levels was observed also in short-term HFD fed mice, suggesting that the hydrogel efficiently prevented the development of HFD-induced alterations at its earliest

stages, together with obesity/metabolic alterations occurrence. This is particularly relevant for developing a potential intervention aimed at preventing or treating pathologies strictly associated to unhealthy dietary habits at their early stage of development. In addition, the hydrogel could be a valuable tool to better investigate early HFD-induced alteration onset and its link with intestinal barrier function.

Subsequent events following intestinal barrier impairment leading to the development of obesity and metabolic disorders are still unclear. Recent reports have shown a correlation between intestinal barrier leakiness, translocation of bacteria and/or bacterial products, and the onset of low-grade inflammation, which is believed to be at the base of metabolic disorder pathogenesis[80,152,97].

Emerging evidence from mouse models suggests that leaky gut promotes the translocation of bacterial endotoxins, fueling low-grade inflammation which in turn drives insulin resistance[152], white adipose tissue inflammation[153] together with hepatic steatosis[236,193].

Hydrogel HFD supplementation either prevented intestinal shortening or recovered intestine length, a hallmark of HFD-induced systemic low-grade inflammation[174,172]. Accordingly, the translocation of LPS into the blood circulation as a result of HFD feeding was prevented upon hydrogel administration, with the highest efficiency in the preventive regimen. These data fully agree with reports showing that bacterial LPS released by gram-negative bacteria can translocate from the gut lumen into the circulation when the intestinal barrier is damaged; in turn, circulating LPS can trigger an inflammatory response in distant organs[237]. Moreover, P.Cani and colleagues have demonstrated that exposure to a high-fat diet increases systemic endotoxin concentration[80] and that mice infused with similarly low levels of LPS show an increase of fasted glycemia and insulinemia, as well as whole-body, liver and adipose tissue weight increase to a similar extent as in HFD fed mice[152]. We must highlight that therapeutic administration of the hydrogel required a longer time to reach a block in LPS translocation, despite fully restoring intestinal barrier function: we could speculate that endotoxin clearance form blood circulation occurs quite after intestinal barrier closure.

Taken together, the data let us to conclude that the hydrogel, by restoring intestinal barrier permeability through TJ reinforcement, was able to counteract LPS translocation and subsequent low-grade inflammation promoted by HFD feeding[97]. In other words, inhibiting intestinal barrier impairment in turn would block LPS translocation, preventing endotoxemia and high fat diet-induced low-grade inflammation, which have a well-

established contribution to the pathophysiological processes underlying obesity, insulin resistance onset and steatohepatitis[97].

However, the mechanisms at the base of high-fat-induced low-grade inflammation and the role of intestinal barrier leakiness in the development of obesity and related metabolic disorders are still unclear[45,189]; interestingly, a link with the gut microbiota has been postulated[238] and obesity and metabolic disorders have been extensively associated to intestinal microbiota dysbiosis[129,132,239]. We hence hypothesized that the mechanisms of action of the hydrogel in the intestine partially rely on the modulation of the microbiota, which is known to influence both intestinal barrier and metabolic pathways. It has been reported that the microbiota can influence the integrity of the intestinal epithelium, which in turn affects gut barrier function and intestinal permeability[240]. Several reports have associated gut microbiota modifications and intestinal barrier perturbations with the onset of intestinal diseases as IBD, IBS, and celiac disease[74,197]. Of note, the causal relationship between the pathophysiological changes in the gut epithelium and altered gut microbiota (dysbiosis), and the onset of obesity have been suggested[241].

However, how dysbiosis, in diet-induced obesity, alters epithelial integrity is still an area of active investigation. Gut bacterial signals (mainly SCFA) are critical in regulating key barrier components and dysbiosis is characterized by selection for distinct types of bacteria, which may alter metabolite production as well as intestinal barrier and immune function[242]. The most compelling evidence for a pivotal role of the gut microbiota in the homeostasis of different organs and regulation of many metabolic pathways is mainly represented by experiment of Fecal Microbiota Translocation (FMT). It has been reported that the transfer of gut microbiota of lean and obese mice in healthy recipients led to the development of the metabolic features of the donors[243,244]. In a human study, the transfer of intestinal microbiota via duodenal tube from lean donors to recipient patients with metabolic syndrome resulted in an increase in insulin sensitivity within 6 weeks[245]. Furthermore, the transfer of opportunistic pathogens isolated from the gut of obese humans resulted in obesity in germ-free mice[246]. Indeed, the gut microbiota has an important role in the regulation of fat storage[247], increasing energy harvesting, and modulating storable fat synthesis[248]. In addition, gut microbiota accounts for the production of different compounds (i.e. LPS), that once absorbed into the systemic circulation are likely to contribute to the development of obesity-related alterations, increasing both tissue inflammation and insulin resistance[153]. So far, obesity-associated modifications of gut microbiota are mainly characterized by a reduction in diversity,

which in turn reduces metabolic energy consumption in comparison with that of the microbiota of lean individuals[249].

To shed light on hydrogel mechanism of action in the intestine and to assess if this involves a reshaping of the gut microbiota previously altered by HFD, we performed gut microbiota analysis of feces collected from mice preventively treated with hydrogel supplemented diets. We observed a decreased heterogenicity of community composition within individual samples (alpha-diversity) together with a shift in gut microbiota composition (beta-diversity) between mice fed with the hydrogel supplemented diets and those fed with diets lacking the hydrogel, independently from the type of diet (chow or HFD. As expected, after HFD feeding Firmicutes/Bacteroidetes ratio was altered (as in obese subjects [250,251]) with a significant increase of the *Firmicutes* and decrease of the *Bacteroidetes* in mice fed with either LFD or HFD, already after one month of feeding. Hydrogel supplementation was able to prevent the reversal of F/B ratio. In addition, mice fed with LFD and HFD, but not hydrogel treated mice, displayed an increase in *Actinobacteria*, which are known to be associated with obesity[213].

Interestingly, mice fed with hydrogel supplemented HFD displayed a microbiota enriched in *Alistipes,* associated to successful weight loss in obese humans post dietary and lifestyle interventions[214]. Furthermore, hydrogel diet supplementation induced an enrichment in *Verrucomicrobia*, in particular in *Akkermansia* genera. Several studies provided evidence for a negative correlation between *Akkermansia muciniphila* abundance and overweight, obesity and type 2 diabetes[147]. A recent study from P.Cani and his research group[146] showed that three months of administration of *A. muciniphila*, as either live or pasteurized bacteria, improved insulin sensitivity and reduced insulinemia in obese patients, while decreasing body weight and fat mass, compared to the placebo group.

We concluded that the hydrogel can preserve a "*healthy*" gut microbiota, i.e. having a composition similar to that of a physiological one, and, more interestingly, to induce the expansion of species that have been reported to be beneficial for an intact metabolic function (i.e. *Akkermanisa muciniphila).* We can also speculate that the hydrogel-shaped microbiota is a key factor for intestinal epithelial barrier function and, in the future, this could be eventually demonstrated with FMT experiments.

Targeting microbiota may represent new avenues for therapeutic interventions aimed at preventing or treating metabolic disorders; hydrogel supplementation could be used as a non-invasive strategy to both increase *A.muciniphila* abundance in gut microbiota and

revert HFD-induced gut dysbiosis, both elements participating in obesity and metabolic syndrome development.

Together our data demonstrate that hydrogel administration can prevent and treat obesity-related metabolic alterations, controlling body weight, adipose tissue deposition, insulin sensitivity, and liver steatosis. These beneficial effects are mediated by the direct action of the hydrogel on the intestine, which modulates nutrient absorption and intestinal permeability. Hydrogel supplementation protects the intestinal epithelial barrier, by increasing TJ expression and improving barrier permeability, both in healthy and obese mice. Importantly, the hydrogel prevents HFD-induced dysbiosis which precludes the translocation of bacterial antigens towards metabolically active tissues (i.e. adipose tissue, liver) and, consequently, the resulting chronically inflammatory state. This in turn prevents impairment of metabolic functions such as insulin resistance, hepatic fat deposition, and excessive adipose tissue storage.

In light of our results, we postulated that the modulation of the intestinal barrier could be the first event occurring upon hydrogel administration. This modulation can rely on two non-mutually exclusive mechanisms: directly, through the interaction of the hydrogel with the intestinal mucosa or indirectly, by hydrogel-induced gut microbiota modifications.

To better understand the existence of a link between hydrogel induced gut microbiota modification and improvement in intestinal permeability, we would like to evaluate: first, the effect of therapeutic hydrogel administration on the intestinal microbiota to comprehend whether the hydrogel can revert HFD induced dysbiosis together with the induction of an expansion of beneficial species as *Akkermansia muciniphila.*

Second, we would like to perform FMT (Fecal Microbial Transplantation) experiments to assess whether microbiota derived from animals receiving hydrogel supplemented diets is able to transfer the hydrogel effects on the intestinal barrier. In which case, this will prove an indirect link between hydrogel administration, gut microbiota modulation, and improvement of the intestinal barrier.

Further investigation is required to complete our understanding of the mechanism of action of the hydrogel in obesity and its related co-morbidities.

However, our work shows the potential of using the Gelesis hydrogel in the treatment of obesity and metabolic disorders as an effective, natural, and non-invasive therapeutic tool.

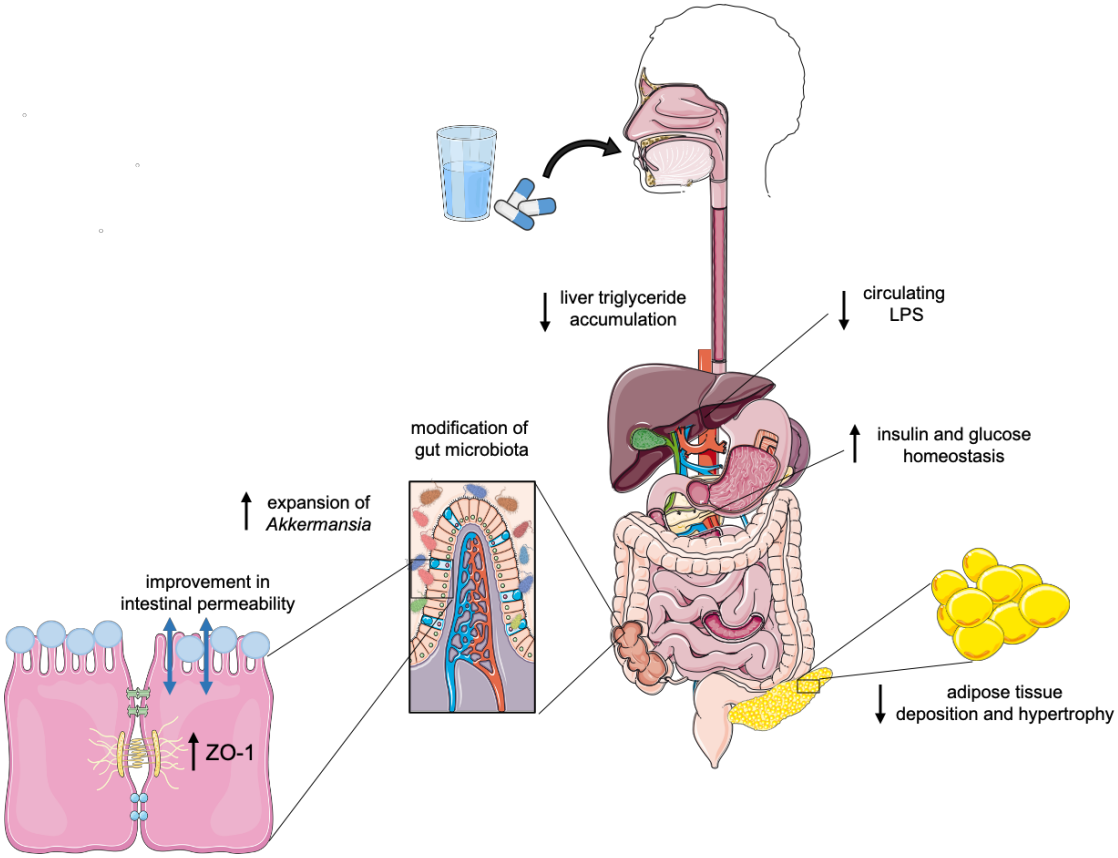

Figure 44. Proposed working model

Hydrogel administration can prevent and treat obesity-related metabolic alterations, controlling body weight, adipose tissue deposition, insulin sensitivity, and liver steatosis. These beneficial effects are mediated by hydrogel's activity on the intestine. Hydrogel supplementation protects the intestinal epithelial barrier, by increasing TJs expression, improving barrier permeability and preventing HFD-induced dysbiosis; precluding, in turn, the translocation of bacterial antigens towards metabolically active tissues (i.e. adipose tissue, liver) and, consequently shielding from the resulting chronically inflammatory state. This, in turn, prevents impairment of metabolic functions such as insulin resistance, hepatic fat deposition, and excessive adipose tissue storage.

APPENDIX

Ex-vivo preservation of intestinal tissue homeostasis depends on hydrogel elastic properties

In this work, we demonstrated the efficacy of a naturally-derived superabsorbent hydrogel in the prevention and treatment of obesity and its associated metabolic disorders. The hydrogel, designed by Gelesis, takes inspiration from some basic compositional and structural features of raw vegetables, which are known to be beneficial in weight management. Vegetables, indeed, are rich in water (about 75-95%), with insoluble cellulose being the main load-bearing fiber of the plant cell wall.

The hydrogel Gel B was designed to mimic mechanical and structural properties of high fiber vegetables, with specific reference to their dynamic-mechanical elasticity. Clinical evidence, indeed, showed that the physical form of food, (i.e. the structural or textural properties), play an important role in satiety enhancement. Due to the presence of both soluble and insoluble dietary fibers, ingested vegetables behave as semisolids, thereby showing both viscous (i.e. liquid-like) and elastic (i.e. solid-like) mechanical properties[252].

With these considerations in mind, Gelesis designed a platform of superabsorbent hydrogels with different elastic properties (stiffness), defined by the elastic modulus G', based on the ability to absorb more or less water.

Therefore, we tested in an *ex-vivo* organ culture system whether differences in the elastic or solid-like properties of the hydrogel could have a different impact on the maintenance of intestinal tissue homeostasis.

Materials and Methods

1. Ex Vivo Organ Culture (EVOC)

In order to investigate whether Gel B with different elasticity may affect the maintenance the structure of intestinal mucosa, we performed an *ex vivo* organ culture of colon tissues explanted from 8 to 12 weeks old healthy C57BL6/J male mice (n=6) (Charles River Laboratories), as previously described[253].

All experiments were performed in accordance with the guidelines established in the Principles of Laboratory Animal Care (Directive 2010/63/EU). The clean mucosal layer was washed in Dulbecco's Modified Eagle Medium (DMEM) containing 15% fetal bovine serum (FBS), glutamine (2mM), epidermal growth factor (200 ng/ml, Peprotech) and Insulin-Transferrin-Selenium-X (10 µl/ml, Gibco) and cut with sterile scalpels into 1 cm^2 pieces. A cave cylinder (borosilicate cloning cylinder, 6x6mm for mouse samples, BellCo) was glued with surgical glue (Vetbond, 3M, Milan, Italy) on the apical face of the mucosa.

The mucosa was then placed on a sterile metal grid, previously washed in FBS, in a center well organ culture dish (BD Falcon) and 1 mL of DMEM containing 15% FBS, glutamine, epidermal growth factor (200 ng/ml, Peprotech) and Insulin-Transferrin-Selenium-X (10 µl/ml, Gibco) was used to fill the center of the plate. Upon mucus reconstitution (1 hour at 37°C), colon tissues were incubated with Gel B (Figure 46b), differing for their elasticity, for 2 hours at 37°C. More precisely, Gel B samples were previously hydrated in PBS at 37°C for 30 minutes; then, colon tissues were placed in contact with the different compounds (filling the cave cylinder), only from the side which is normally exposed to the intestinal lumen. While, PBS and medium treated tissues were used as negative and positive controls, respectively. Upon incubation, tissues were fixed and embedded in paraffin to obtain tissue sections. Sections were hence stained with Alcian Blue/PAS (to visualize the mucus and mucus-secreting cells) or with Ki67 antibody (to detect cell proliferation), as briefly described in the following.

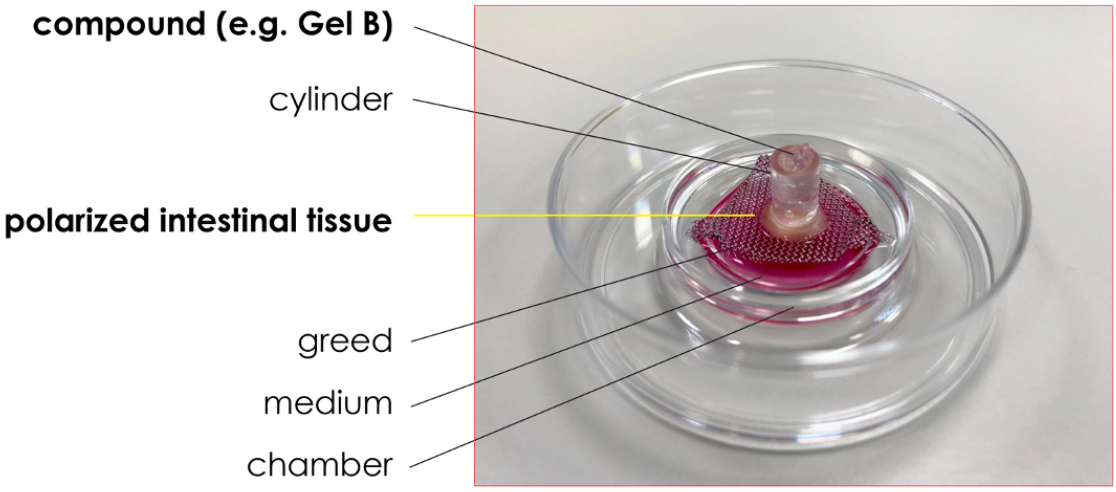

Figure 45. Ex-Vivo Organ Culture (EVOC) system

2. Carnoy's and PFA fixation

To preserve mucus layer, half of the tissue was fixed in Carnoy's fixative (Ethanol, Acetic Acid Glacial, Chloroform 6:1:3). After 2 hours of fixation, tissues were transferred in absolute ethanol and kept at +4°C for at least 72 hours, processed and paraffin embedded. To preserve the tissue structure to perform histological analysis, half of the tissue was fixed in PFA 4% (Paraformaldehyde). After overnight fixation, tissues were transferred in ethanol 70% and kept at +4°C for at least 72 hours, processed and paraffin embedded.

3. Alcian Blue-PAS mucus staining

Tissues were then stained using Alcian Blue-PAS ready to use staining kit (NovaUltra™ Alcian Blue/PAS Stain Kit, IHC WORLD) following provider's instructions. Alcian blue will stain strongly acidic mucins in blue, PAS (Periodic Acid Solution and Schiff Reagent) will stain neutral mucins in magenta. Mixtures of both acidic and neutral mucins are stained blue purple.

4. Immunohistochemistry for Ki67

Immunohistochemistry for Ki67 was performed on 4% PFA fixed paraffin-embedded tissues. Tissue sections were deparaffinized in histolemon and hydrated through graded alcohol series. Antigen unmasking was performed using Tris-EDTA pH 9 at 95°C for 50 minutes, followed by quenching of endogenous peroxidases using 3% H_2O_2. Sections were then incubated with primary rabbit polyclonal antibody against Ki67 (ab15580, ABCAM) for 2 hours at room temperature and with secondary antibody ready to use (DAKO Envision system HRP rabbit) for 20 minutes at room temperature.

Tissue sections were then washed and incubated with peroxidase (DAB, DAKO) solution. Slides were then counterstained with hematoxylin and dehydrated through graded alcohol series, washed in histolemon and mounted. Images were acquired using Olympus BX51 Widefield microscope connected to a Nikon DS-5M camera. Ki67 staining was quantified by using ImageJ software and Immunoratio plugin.

5. Statistical analysis

All data were expressed as mean ± SEM, unless otherwise noted. Statistical significance was determined by using one-way ANOVA tests, and differences were considered to be significant when p value < 0.05.

Results

We tested the ability of Gel B compounds having different elasticity, namely Gel B 01 - Gel B 04 (with Gel B 01 having the lowest and Gel B 04 the highest elasticity – Figure 46b), to preserve colonic tissue structure and homeostasis in a model of *ex-vivo* organ culture (EVOC). EVOC system is an *in-vitro* model, previously developed in our laboratory[253], allowing the maintenance of intestinal tissue polarization, thus making possible the evaluation of the effects of compounds specifically targeting the luminal side of the intestinal tissue.

As anticipated, maintenance of intestinal tissue homeostasis is guaranteed by the presence of a multilayered system of defense, encompassing the mucus layer and the continuous process of renewal of intestinal epithelial cells.

Specifically, we evaluated the ability of Gel B hydrogels having different elastic properties (G'-stiffness) to preserve tissue integrity and homeostasis, by the assessment of gut mucus layer integrity, trough Alcian Blue staining, and of the tissue proliferative niche through IHC for Ki67 (a marker of proliferation), after 2 hours of incubation of colonic tissues with the different compounds.

From our analysis it emerged that the mucus layer was better preserved when colon tissue samples were incubated with Gel B 02 or Gel B 03, in a way comparable, or even better, than the medium - our positive control (Figure 46 a,c).

Conversely, GelB01 and GelB04 failed in maintaining mucus integrity, similarly to PBS (Figure 46c), our negative control. In this regard, it is worth recalling that PBS-swollen Gel B compounds were used in the EVOC system, with PBS itself actually having a negative impact on the tissue structure. Therefore, we assumed that the effect of Gel B on the colonic mucosa was strictly related to its elastic properties, rather than its chemical nature.

To assess the integrity of the proliferative compartment, which fuels epithelial cell layer renewal, we performed Ki67 staining to visualize proliferating nuclei. In the healthy mucosa, Ki67 positive cells are abundant solely at the base of the crypt, and Ki67 positive nuclei strongly decrease in damaged tissues. In agreement with the effect on the mucus layer, GelB02 and GelB03 performed better in preserving tissue proliferative ability, similarly to the medium (brown nuclei correspond to proliferating cells, Figure 46 a; total nuclei are counterstained with hematoxylin). Conversely, the number of Ki67 positive cells (proliferative cells) was lower in tissues exposed to GelB01 or GelB04, similarly to PBS (Figure 46a; the quantification of Ki67 staining is reported in Figure 46c).

Taken together, these data suggest that both GelB02 and GelB03 have the best physical properties (i.e. elasticity) required for intestinal mucosa homeostasis preservation in an *ex vivo* system.

This suggests that the elastic properties of the hydrogel is also crucial for the maintenance of intestinal barrier health.

Taking into account these results (and other in vivo data, i.e. paragraph 1 of Results), we used an hydrogel with elastic properties at the interface between Gel B 02 and Gel B 03 in the *in vivo* experiments.. Of note, an excess of hydrogel inside the gut is able to mimic elastic properties and stiffness of compounds with higher stiffness, due to the absorption of a higher quantitative of water. In conclusion, tuning of both hydrogel's elastic properties and dosages is essential to design the compound which allow optimal preservation of intestinal tissue function and homeostasis.

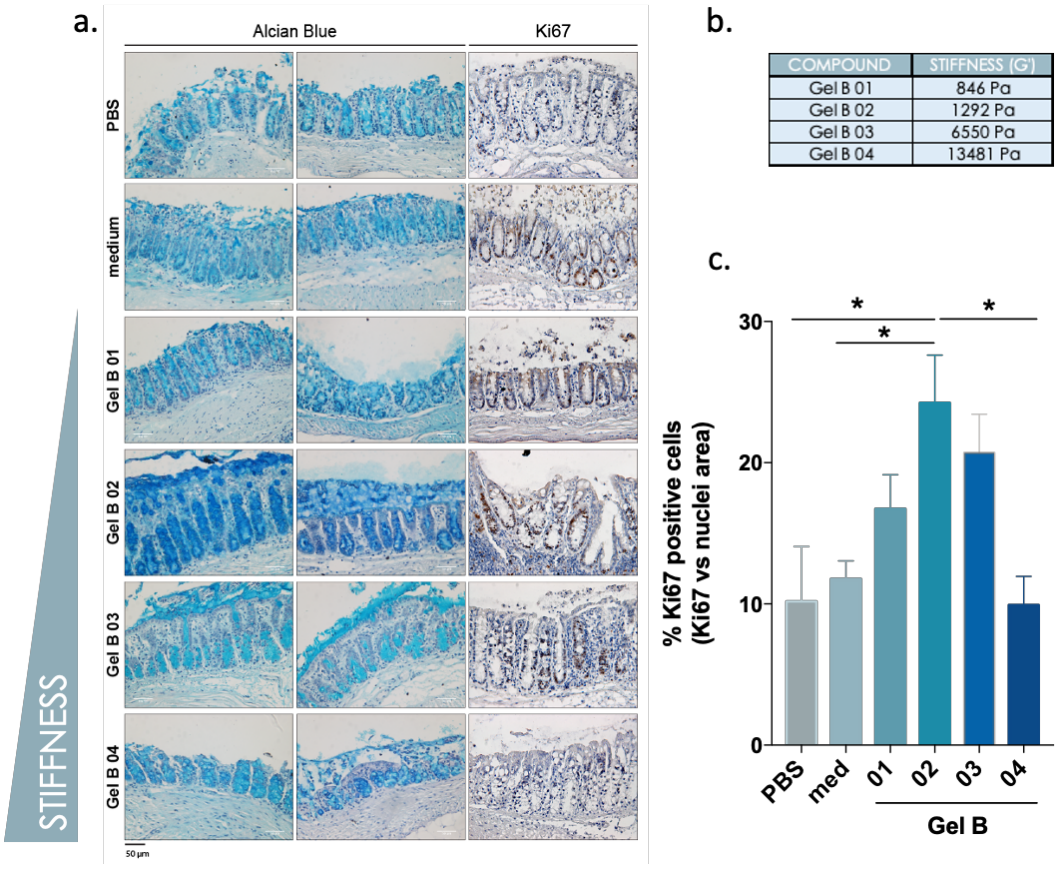

Figure 46. Hydrogel stiffness impacts intestinal tissue homeostasis in ex-vivo organ culture (EVOC)

a.Alcian Blue and Ki67 (in brown) staining of colon tissue sections. Colon tissue explants were incubated for 2 hours in an ex-vivo organ culture system with: PBS (negative control), medium (positive control) and Gel B with increasing stiffness from Gel B 01 (lowest stiffness) to Gel B 04 (highest stiffness), scale bar 50 µm; **b.** Stiffness values expressed in G' of the different Gel B variants tested in the EVOC system; **c.** Quantification of Ki67 proliferation marker, staining expressed as a percentage of Ki67 positive cells vs. nuclei positive area (* p<0,5; one-way ANOVA Tukey post-test, line at mean with SEM).

REFERENCES

1. Blüher, M. Obesity: global epidemiology and pathogenesis. *Nat. Rev. Endocrinol.* **15**, 288–298 (2019).
2. Trends in Adult Body-Mass Index in 200 Countries From 1975 to 2014: A Pooled Analysis of 1698 Population-Based Measurement Studies With 19·2 Million Participants. *Lancet (London, England)* **387**, (2016).
3. Kaur, J. A Comprehensive Review on Metabolic Syndrome. *Cardiol. Res. Pract.* **2014**, (2014).
4. Ruban, A., Stoenchev, K., Ashrafian, H. & Teare, J. Current treatments for obesity. *Clin. Med.* **19**, 205–212 (2019).
5. González-Muniesa, P. *et al.* Obesity. *Nat. Rev. Dis. Prim.* **3**, 17034 (2017).
6. San-Cristobal, R., Navas-Carretero, S., Martínez-González, M. Á., Ordovas, J. M. & Martínez, J. A. Contribution of macronutrients to obesity: implications for precision nutrition. *Nat. Rev. Endocrinol.* **16**, 305–320 (2020).
7. JA, B. *et al.* Associations of Body Mass and Fat Indexes With Cardiometabolic Traits. *J. Am. Coll. Cardiol.* **72**, (2018).
8. Li, P. *et al.* Genetic association analysis of 30 genes related to obesity in a European American population. *Int. J. Obes.* **38**, 724–729 (2014).
9. Lean, M. E. J. & Malkova, D. Altered gut and adipose tissue hormones in overweight and obese individuals: cause or consequence? *Int. J. Obes.* **40**, 622–632 (2016).
10. Khan, M. & Joseph, F. Adipose Tissue and Adipokines: The Association with and Application of Adipokines in Obesity. *Scientifica (Cairo).* **2014**, 1–7 (2014).
11. M, T. *et al.* Circulating Ghrelin Levels Are Decreased in Human Obesity. *Diabetes* **50**, (2001).
12. Suzuki, K., Jayasena, C. N. & Bloom, S. R. The Gut Hormones in Appetite Regulation. *J. Obes.* **2011**, (2011).
13. L, D. *et al.* Effect of Peptide YY3-36 on Food Intake in Humans. *Gastroenterology* **129**, (2005).
14. MA, C. *et al.* Oxyntomodulin Suppresses Appetite and Reduces Food Intake in Humans. *J. Clin. Endocrinol. Metab.* **88**, (2003).
15. MacDonald, P. E. *et al.* The Multiple Actions of GLP-1 on the Process of Glucose-Stimulated Insulin Secretion. *Diabetes* **51**, S434–S442 (2002).
16. Müller, T. D. *et al.* Glucagon-like peptide 1 (GLP-1). *Mol. Metab.* **30**, 72 (2019).

17. Collins, L. & Costello, R. A. *Glucagon-like Peptide-1 Receptor Agonists*. *StatPearls* (StatPearls Publishing, 2020).
18. 8. Obesity Management for the Treatment of Type 2 Diabetes: Standards of Medical Care in Diabetes- 2019. *Diabetes Care* **42**, (2019).
19. I, N.-V. *et al.* Insulin Resistance Associated to Obesity: The Link TNF-alpha. *Arch. Physiol. Biochem.* **114**, (2008).
20. Tzanavari, T., Giannogonas, P. & Karalis, K. P. TNF-alpha and obesity. *Curr. Dir. Autoimmun.* **11**, 145–56 (2010).
21. Eder, K., Baffy, N., Falus, A. & Fulop, A. K. The major inflammatory mediator interleukin-6 and obesity. *Inflamm. Res.* **58**, 727–36 (2009).
22. Nigro, E. *et al.* New insight into adiponectin role in obesity and obesity-related diseases. *Biomed Res. Int.* **2014**, 658913 (2014).
23. Achari, A. E. & Jain, S. K. Adiponectin, a Therapeutic Target for Obesity, Diabetes, and Endothelial Dysfunction. *Int. J. Mol. Sci.* **18**, (2017).
24. TM, M., KA, K., GM, P., JL, R. & CV, M. Transgenic Neuronal Expression of Proopiomelanocortin Attenuates Hyperphagic Response to Fasting and Reverses Metabolic Impairments in Leptin-Deficient Obese Mice. *Diabetes* **52**, (2003).
25. Myers, M. G., Leibel, R. L., Seeley, R. J., Schwartz, M. W. & Schwartz, M. W. Obesity and leptin resistance: distinguishing cause from effect. *Trends Endocrinol. Metab.* **21**, 643–51 (2010).
26. Gómez-Hernández, A., Beneit, N., Díaz-Castroverde, S. & Escribano, Ó. Differential Role of Adipose Tissues in Obesity and Related Metabolic and Vascular Complications. *Int. J. Endocrinol.* **2016**, 1216783 (2016).
27. AS, G. & MS, O. Obesity and the Role of Adipose Tissue in Inflammation and Metabolism. *Am. J. Clin. Nutr.* **83**, (2006).
28. GI, S. Ectopic Fat in Insulin Resistance, Dyslipidemia, and Cardiometabolic Disease. *N. Engl. J. Med.* **371**, (2014).
29. Haczeyni, F., Bell-Anderson, K. S. & Farrell, G. C. Causes and mechanisms of adipocyte enlargement and adipose expansion. *Obes. Rev.* **19**, 406–420 (2018).
30. ED, R. & BM, S. What We Talk About When We Talk About Fat. *Cell* **156**, (2014).
31. R, R. *et al.* Does the Relationship Between Waist Circumference, Morbidity and Mortality Depend on Measurement Protocol for Waist Circumference? *Obes. Rev.* **9**, (2008).
32. E, F. *et al.* Intrahepatic Fat, Not Visceral Fat, Is Linked With Metabolic

Complications of Obesity. *Proc. Natl. Acad. Sci. U. S. A.* **106**, (2009).

33. Ye, J. Mechanisms of insulin resistance in obesity. *Front. Med.* **7**, 14 (2013).
34. Kahn, S. E., Hull, R. L. & Utzschneider, K. M. Mechanisms linking obesity to insulin resistance and type 2 diabetes. *Nature* **444**, 840–846 (2006).
35. OT, H. *et al.* Body Mass Index-Independent Inflammation in Omental Adipose Tissue Associated With Insulin Resistance in Morbid Obesity. *Surg. Obes. Relat. Dis.* **7**, (2011).
36. J, H., Y, T., M, K., A, B. & M, S. Resolvin D1 Decreases Adipose Tissue Macrophage Accumulation and Improves Insulin Sensitivity in Obese-Diabetic Mice. *FASEB J.* **25**, (2011).
37. Hardy, O. T., Czech, M. P. & Corvera, S. What causes the insulin resistance underlying obesity? *Curr. Opin. Endocrinol. Diabetes. Obes.* **19**, 81 (2012).
38. Fabbrini, E., Sullivan, S. & Klein, S. Obesity and Nonalcoholic Fatty Liver Disease: Biochemical, Metabolic and Clinical Implications. *Hepatology* **51**, 679 (2010).
39. Z, C., R, Y., Y, X., F, D. & S, Z. A Vicious Circle Between Insulin Resistance and Inflammation in Nonalcoholic Fatty Liver Disease. *Lipids Health Dis.* **16**, (2017).
40. Divella, R., Mazzocca, A., Daniele, A., Sabbà, C. & Paradiso, A. Obesity, Nonalcoholic Fatty Liver Disease and Adipocytokines Network in Promotion of Cancer. *Int. J. Biol. Sci.* **15**, 610 (2019).
41. Chelakkot, C., Ghim, J. & Ryu, S. H. Mechanisms regulating intestinal barrier integrity and its pathological implications. *Exp. Mol. Med.* **50**, 103 (2018).
42. Vancamelbeke, M. & Vermeire, S. The intestinal barrier: a fundamental role in health and disease. *Expert Rev. Gastroenterol. Hepatol.* **11**, 821–834 (2017).
43. Artis, D. Epithelial-cell recognition of commensal bacteria and maintenance of immune homeostasis in the gut. *Nat. Rev. Immunol.* **8**, 411–420 (2008).
44. Thoo, L., Noti, M. & Krebs, P. Keep calm: the intestinal barrier at the interface of peace and war. *Cell Death Dis.* **10**, 849 (2019).
45. Chelakkot, C., Ghim, J. & Ryu, S. H. Mechanisms regulating intestinal barrier integrity and its pathological implications. *Exp. Mol. Med.* **50**, 103 (2018).
46. Deplancke, B. & Gaskins, H. R. Microbial modulation of innate defense: goblet cells and the intestinal mucus layer. *Am. J. Clin. Nutr.* **73**, 1131S-1141S (2001).
47. Van der Sluis, M. *et al.* Muc2-Deficient Mice Spontaneously Develop Colitis, Indicating That MUC2 Is Critical for Colonic Protection. *Gastroenterology* **131**, 117–129 (2006).

48. Groschwitz, K. R. & Hogan, S. P. Intestinal Barrier Function: Molecular Regulation and Disease Pathogenesis. *J. Allergy Clin. Immunol.* **124**, 3 (2009).
49. McCauley, H. A. & Guasch, G. Three cheers for the goblet cell: maintaining homeostasis in mucosal epithelia. *Trends Mol. Med.* **21**, 492–503 (2015).
50. Mabbott, N. A., Donaldson, D. S., Ohno, H., Williams, I. R. & Mahajan, A. Microfold (M) cells: important immunosurveillance posts in the intestinal epithelium. *Mucosal Immunol.* **6**, 666–677 (2013).
51. Ménard, S., Cerf-Bensussan, N. & Heyman, M. Multiple facets of intestinal permeability and epithelial handling of dietary antigens. *Mucosal Immunol.* **3**, 247–259 (2010).
52. Hollander, D. & Kaunitz, J. D. The "Leaky Gut": Tight Junctions but Loose Associations? *Dig. Dis. Sci.* **65**, 1277–1287 (2020).
53. Ménard, S., Cerf-Bensussan, N. & Heyman, M. Multiple facets of intestinal permeability and epithelial handling of dietary antigens. *Mucosal Immunol.* **3**, 247–259 (2010).
54. Hartsock, A. & Nelson, W. J. Adherens and tight junctions: Structure, function and connections to the actin cytoskeleton. *Biochim. Biophys. Acta - Biomembr.* **1778**, 660–669 (2008).
55. Hartsock, A. & Nelson, W. J. Adherens and tight junctions: Structure, function and connections to the actin cytoskeleton. *Biochim. Biophys. Acta - Biomembr.* **1778**, 660–669 (2008).
56. Ma, T. Y., Nighot, P. & Al-Sadi, R. Tight Junctions and the Intestinal Barrier. *Physiol. Gastrointest. Tract* 587–639 (2018). doi:10.1016/B978-0-12-809954-4.00025-6
57. Cardoso-Silva, D. *et al.* Intestinal Barrier Function in Gluten-Related Disorders. *Nutrients* **11**, 2325 (2019).
58. Schulzke, J. D. *et al.* Epithelial transport and barrier function in occludin-deficient mice. *Biochim. Biophys. Acta - Biomembr.* **1669**, 34–42 (2005).
59. Saitou, M. *et al.* Complex Phenotype of Mice Lacking Occludin, a Component of Tight Junction Strands. *Mol. Biol. Cell* **11**, 4131–4142 (2000).
60. Günzel, D. & Yu, A. S. L. Claudins and the Modulation of Tight Junction Permeability. *Physiol. Rev.* **93**, 525–569 (2013).
61. Zhu, L. *et al.* Claudin Family Participates in the Pathogenesis of Inflammatory Bowel Diseases and Colitis-Associated Colorectal Cancer. *Front. Immunol.* **10**, 1441 (2019).

62. Zihni, C., Mills, C., Matter, K. & Balda, M. S. Tight junctions: from simple barriers to multifunctional molecular gates. *Nat. Rev. Mol. Cell Biol.* **17**, 564–580 (2016).
63. Barmeyer, C., Schulzke, J. D. & Fromm, M. Claudin-related intestinal diseases. *Semin. Cell Dev. Biol.* **42**, 30–38 (2015).
64. DI, U., AS, F. & JM, A. Dimerization of the Scaffolding Protein ZO-1 Through the Second PDZ Domain. *J. Biol. Chem.* **281**, (2006).
65. Van Itallie, C. M., Fanning, A. S., Bridges, A. & Anderson, J. M. ZO-1 Stabilizes the Tight Junction Solute Barrier through Coupling to the Perijunctional Cytoskeleton. *Mol. Biol. Cell* **20**, 3930–3940 (2009).
66. Fanning, A. S., Itallie, C. M. Van & Anderson, J. M. A Highlights from MBoC Selection: Zonula occludens-1 and -2 regulate apical cell structure and the zonula adherens cytoskeleton in polarized epithelia. *Mol. Biol. Cell* **23**, 577 (2012).
67. Umeda, K. *et al.* ZO-1 and ZO-2 Independently Determine Where Claudins Are Polymerized in Tight-Junction Strand Formation. *Cell* **126**, 741–754 (2006).
68. Lee, S. H. Intestinal Permeability Regulation by Tight Junction: Implication on Inflammatory Bowel Diseases. *Intest. Res.* **13**, 11 (2015).
69. Heyman, M., Abed, J., Lebreton, C. & Cerf-Bensussan, N. Intestinal permeability in coeliac disease: insight into mechanisms and relevance to pathogenesis. *Gut* **61**, 1355–1364 (2012).
70. Wilbrink, J. *et al.* Intestinal barrier function in morbid obesity: results of a prospective study on the effect of sleeve gastrectomy. *Int. J. Obes.* **44**, 368–376 (2020).
71. Cox, A. J. *et al.* Increased intestinal permeability as a risk factor for type 2 diabetes. *Diabetes Metab.* **43**, 163–166 (2017).
72. Chakaroun, R. M., Massier, L. & Kovacs, P. Bacteria in Metabolic Disease : Perpetrators or Bystanders ? (2020).
73. Bischoff, S. C. *et al.* Intestinal permeability – a new target for disease prevention and therapy. *BMC Gastroenterol.* **14**, 189 (2014).
74. Natividad, J. M. M. & Verdu, E. F. Modulation of intestinal barrier by intestinal microbiota: Pathological and therapeutic implications. *Pharmacol. Res.* **69**, 42–51 (2013).
75. Brun, P. *et al.* Increased intestinal permeability in obese mice: new evidence in the pathogenesis of nonalcoholic steatohepatitis. *Am. J. Physiol. Liver Physiol.* **292**, G518–G525 (2007).
76. Damms-Machado, A. *et al.* Gut permeability is related to body weight, fatty liver

disease, and insulin resistance in obese individuals undergoing weight reduction. *Am. J. Clin. Nutr.* **105**, 127–135 (2017).

77. Tseng, C.-H. & Wu, C.-Y. The gut microbiome in obesity. *J. Formos. Med. Assoc.* **118**, S3–S9 (2019).
78. Qin, J. *et al.* A metagenome-wide association study of gut microbiota in type 2 diabetes. *Nature* **490**, 55–60 (2012).
79. Amar, J. *et al.* Intestinal mucosal adherence and translocation of commensal bacteria at the early onset of type 2 diabetes: molecular mechanisms and probiotic treatment. *EMBO Mol. Med.* **3**, 559–572 (2011).
80. Cani, P. D. *et al.* Changes in Gut Microbiota Control Metabolic Endotoxemia-Induced Inflammation in High-Fat Diet-Induced Obesity and Diabetes in Mice. *Diabetes* **57**, 1470–1481 (2008).
81. Suzuki, T. & Hara, H. Dietary fat and bile juice, but not obesity, are responsible for the increase in small intestinal permeability induced through the suppression of tight junction protein expression in LETO and OLETF rats. *Nutr. Metab. (Lond).* **7**, 19 (2010).
82. Cani, P. D. *et al.* Changes in gut microbiota control inflammation in obese mice through a mechanism involving GLP-2-driven improvement of gut permeability. *Gut* **58**, 1091 (2009).
83. Bazzoni, G. & Dejana, E. Endothelial Cell-to-Cell Junctions: Molecular Organization and Role in Vascular Homeostasis. *Physiol. Rev.* **84**, 869–901 (2004).
84. Miele, L. *et al.* Increased intestinal permeability and tight junction alterations in nonalcoholic fatty liver disease. *Hepatology* **49**, 1877–1887 (2009).
85. Vajro, P., Paolella, G. & Fasano, A. MICROBIOTA AND GUT-LIVER AXIS: A MINI-REVIEW ON THEIR INFLUENCES ON OBESITY AND OBESITY RELATED LIVER DISEASE. *J. Pediatr. Gastroenterol. Nutr.* **56**, 461 (2013).
86. Lee, B., Moon, K. M. & Kim, C. Y. Tight junction in the intestinal epithelium: Its association with diseases and regulation by phytochemicals. *J. Immunol. Res.* **2018**, (2018).
87. Burcelin, R., Crivelli, V., Dacosta, A., Roy-Tirelli, A. & Thorens, B. Heterogeneous metabolic adaptation of C57BL/6J mice to high-fat diet. *Am. J. Physiol. Metab.* **282**, E834–E842 (2002).
88. Lam, Y. Y. *et al.* Increased Gut Permeability and Microbiota Change Associate with Mesenteric Fat Inflammation and Metabolic Dysfunction in Diet-Induced

Obese Mice. *PLoS One* **7**, e34233 (2012).

89. Winer, D. A., Luck, H., Tsai, S. & Winer, S. The intestinal immune system in obesity and insulin resistance. *Cell Metab.* **23**, 413–426 (2016).
90. Richter, W. *et al.* Morphology, size distribution, and aggregate structure of lipopolysaccharide and lipid A dispersions from enterobacterial origin. *Innate Immun.* **17**, 427–438 (2011).
91. Sicard, J.-F., Le Bihan, G., Vogeleer, P., Jacques, M. & Harel, J. Interactions of Intestinal Bacteria with Components of the Intestinal Mucus. *Front. Cell. Infect. Microbiol.* **7**, 387 (2017).
92. Johansson, M. E. V *et al.* Bacteria penetrate the normally impenetrable inner colon mucus layer in both murine colitis models and patients with ulcerative colitis. *Gut* **63**, 281–291 (2014).
93. Yasuda, M. *et al.* Pseudomonas aeruginosa serA Gene Is Required for Bacterial Translocation through Caco-2 Cell Monolayers. *PLoS One* **12**, e0169367 (2017).
94. Wang, B. *et al. Lactobacillus plantarum* L9 but not *Lactobacillus acidophilus* LA reduces tumour necrosis factor induced bacterial translocation in Caco-2 cells. *Benef. Microbes* **8**, 497–505 (2017).
95. Backert, S., Boehm, M., Wessler, S. & Tegtmeyer, N. Transmigration route of Campylobacter jejuni across polarized intestinal epithelial cells: paracellular, transcellular or both? *Cell Commun. Signal.* **11**, 72 (2013).
96. Deitch, E. A. Gut-origin sepsis: Evolution of a concept. *Surg.* **10**, 350–356 (2012).
97. Cani, P. D., Osto, M., Geurts, L. & Everard, A. Involvement of gut microbiota in the development of low-grade inflammation and type 2 diabetes associated with obesity. *Gut Microbes* **3**, 279–88 (2012).
98. Thuy, S. *et al.* Nonalcoholic Fatty Liver Disease in Humans Is Associated with Increased Plasma Endotoxin and Plasminogen Activator Inhibitor 1 Concentrations and with Fructose Intake. *J. Nutr.* **138**, 1452–1455 (2008).
99. Bergheim, I. *et al.* Antibiotics protect against fructose-induced hepatic lipid accumulation in mice: Role of endotoxin. *J. Hepatol.* **48**, 983–992 (2008).
100. Nighot, M. *et al.* Lipopolysaccharide-Induced Increase in Intestinal Epithelial Tight Permeability Is Mediated by Toll-Like Receptor 4/Myeloid Differentiation Primary Response 88 (MyD88) Activation of Myosin Light Chain Kinase Expression. *Am. J. Pathol.* **187**, 2698 (2017).
101. Guo, S., Al-Sadi, R., Said, H. M. & Ma, T. Y. Lipopolysaccharide Causes an Increase in Intestinal Tight Junction Permeability in Vitro and in Vivo by Inducing

Enterocyte Membrane Expression and Localization of TLR-4 and CD14. *Am. J. Pathol.* **182**, 375–387 (2013).

102. Bischoff, S. C. *et al. Intestinal permeability-a new target for disease prevention and therapy*. (2014). doi:10.1186/s12876-014-0189-7
103. K, M., EC, D., J, W. & F, B. The Impact of Dietary Fiber on Gut Microbiota in Host Health and Disease. *Cell Host Microbe* **23**, (2018).
104. T, C. *et al.* Dietary Fibre-Based SCFA Mixtures Promote Both Protection and Repair of Intestinal Epithelial Barrier Function in a Caco-2 Cell Model. *Food Funct.* **8**, (2017).
105. Y, F., Y, W., P, W., Y, H. & F, W. Short-Chain Fatty Acids Manifest Stimulative and Protective Effects on Intestinal Barrier Function Through the Inhibition of NLRP3 Inflammasome and Autophagy. *Cell. Physiol. Biochem.* **49**, (2018).
106. VanHook, A. M. Butyrate benefits the intestinal barrier. *Sci. Signal.* **8**, ec135–ec135 (2015).
107. T, S. Stimulatory Effect of Short-Chain Fatty Acids on Epithelial Cell Proliferation in the Rat Intestine: A Possible Explanation for Trophic Effects of Fermentable Fibre, Gut Microbes and Luminal Trophic Factors. *Br. J. Nutr.* **58**, (1987).
108. H, I. & T, S. Stimulation of epithelial cell proliferation of isolated distal colon of rats by continuous colonic infusion of ammonia or short-chain fatty acids is nonadditive. *J. Nutr.* **128**, 843–847 (1998).
109. G, den B. *et al.* The Role of Short-Chain Fatty Acids in the Interplay Between Diet, Gut Microbiota, and Host Energy Metabolism. *J. Lipid Res.* **54**, (2013).
110. MS, D. *et al.* A Dietary Fiber-Deprived Gut Microbiota Degrades the Colonic Mucus Barrier and Enhances Pathogen Susceptibility. *Cell* **167**, (2016).
111. KA, E. *et al.* Quantitative Imaging of Gut Microbiota Spatial Organization. *Cell Host Microbe* **18**, (2015).
112. ME, J. *et al.* Bacteria Penetrate the Normally Impenetrable Inner Colon Mucus Layer in Both Murine Colitis Models and Patients With Ulcerative Colitis. *Gut* **63**, (2014).
113. J, Z. *et al.* Fiber-Mediated Nourishment of Gut Microbiota Protects Against Diet-Induced Obesity by Restoring IL-22-Mediated Colonic Health. *Cell Host Microbe* **23**, (2018).
114. Wannamethee, S. G., Whincup, P. H., Thomas, M. C. & Sattar, N. Associations Between Dietary Fiber and Inflammation, Hepatic Function, and Risk of Type 2 Diabetes in Older Men: Potential mechanisms for the benefits of fiber on diabetes

risk. *Diabetes Care* **32**, 1823 (2009).

115. TV, H. & T, S. Dietary Fermentable Fiber Reduces Intestinal Barrier Defects and Inflammation in Colitic Mice. *J. Nutr.* **146**, (2016).
116. TM, F. *et al.* Oral Supplementation of Butyrate Reduces Mucositis and Intestinal Permeability Associated With 5-Fluorouracil Administration. *Lipids* **47**, (2012).
117. A, F., M, M., L, C. D. & E, M. Zinc Deficiency Induces Membrane Barrier Damage and Increases Neutrophil Transmigration in Caco-2 Cells. *J. Nutr.* **138**, (2008).
118. J, K. *et al.* Novel Role of the Vitamin D Receptor in Maintaining the Integrity of the Intestinal Mucosal Barrier. *Am. J. Physiol. Gastrointest. Liver Physiol.* **294**, (2008).
119. E, A.-R., Z, U., S, C., Z, B. & R, R. Bacterial Population and Innate Immunity-Related Genes in Rat Gastrointestinal Tract Are Altered by Vitamin A-deficient Diet. *J. Nutr. Biochem.* **20**, (2009).
120. Ohland, C. L. & MacNaughton, W. K. Probiotic bacteria and intestinal epithelial barrier function. *Am. J. Physiol. Liver Physiol.* **298**, G807–G819 (2010).
121. Madsen, K. *et al.* Probiotic bacteria enhance murine and human intestinal epithelial barrier function. *Gastroenterology* **121**, 580–591 (2001).
122. Corridoni, D. *et al.* Probiotic Bacteria Regulate Intestinal Epithelial Permeability in Experimental Ileitis by a TNF-Dependent Mechanism. *PLoS One* **7**, e42067 (2012).
123. Anderson, R. C. *et al.* Lactobacillus plantarum MB452 enhances the function of the intestinal barrier by increasing the expression levels of genes involved in tight junction formation. *BMC Microbiol.* **10**, 316 (2010).
124. J, K. *et al.* Regulation of Human Epithelial Tight Junction Proteins by Lactobacillus Plantarum in Vivo and Protective Effects on the Epithelial Barrier. *Am. J. Physiol. Gastrointest. Liver Physiol.* **298**, (2010).
125. M, K., V, K.-S., AL, C., F, M. & K, C. Probiotic Mixture VSL#3 Reduces Colonic Inflammation and Improves Intestinal Barrier Function in Muc2 Mucin-Deficient Mice. *Am. J. Physiol. Gastrointest. Liver Physiol.* **312**, (2017).
126. S, R.-L. & KE, B. Probiotics and Commensals Reverse TNF-alpha- And IFN-gamma-induced Dysfunction in Human Intestinal Epithelial Cells. *Gastroenterology* **130**, (2006).
127. Sender, R., Fuchs, S. & Milo, R. Revised Estimates for the Number of Human and Bacteria Cells in the Body. *PLoS Biol.* **14**, e1002533 (2016).
128. Qin, J. *et al.* A human gut microbial gene catalogue established by metagenomic

sequencing. *Nature* **464**, 59–65 (2010).

129. Ley, R. E., Turnbaugh, P. J., Klein, S. & Gordon, J. I. Human gut microbes associated with obesity. *Nature* **444**, 1022–1023 (2006).
130. Ley, R. E. *et al.* Evolution of Mammals and Their Gut Microbes. *Science (80-.).* **320**, 1647–1651 (2008).
131. Kaplan, J. L. & Walker, W. A. Early gut colonization and subsequent obesity risk. *Curr. Opin. Clin. Nutr. Metab. Care* **15**, 278–284 (2012).
132. Cornejo-Pareja, I., Muñoz-Garach, A., Clemente-Postigo, M. & Tinahones, F. J. Importance of gut microbiota in obesity. *Eur. J. Clin. Nutr.* **72**, 26–37 (2019).
133. Zhang, H. *et al.* Human gut microbiota in obesity and after gastric bypass. *Proc. Natl. Acad. Sci.* **106**, 2365–2370 (2009).
134. Aron-Wisnewsky, J. *et al.* Gut microbiota and human NAFLD: disentangling microbial signatures from metabolic disorders. *Nat. Rev. Gastroenterol. Hepatol.* **17**, 279–297 (2020).
135. Grabherr, F., Grander, C., Effenberger, M., Adolph, T. E. & Tilg, H. Gut Dysfunction and Non-alcoholic Fatty Liver Disease. *Front. Endocrinol. (Lausanne).* **10**, 611 (2019).
136. Guinane, C. M. & Cotter, P. D. Role of the gut microbiota in health and chronic gastrointestinal disease: understanding a hidden metabolic organ. *Therap. Adv. Gastroenterol.* **6**, 295–308 (2013).
137. Meijnikman, A. S., Gerdes, V. E., Nieuwdorp, M. & Herrema, H. Evaluating Causality of Gut Microbiota in Obesity and Diabetes in Humans. *Endocr. Rev.* **39**, 133–153 (2018).
138. Schroeder, B. O. & Bäckhed, F. Signals from the gut microbiota to distant organs in physiology and disease. *Nat. Med.* **22**, 1079–1089 (2016).
139. Al-Assal, K., Martinez, A. C., Torrinhas, R. S., Cardinelli, C. & Waitzberg, D. Gut microbiota and obesity. *Clin. Nutr. Exp.* **20**, 60–64 (2018).
140. Wu, G. D. *et al.* Linking Long-Term Dietary Patterns with Gut Microbial Enterotypes. *Science (80-.).* **334**, 105–108 (2011).
141. Chakraborti, C. K. New-found link between microbiota and obesity. *World J. Gastrointest. Pathophysiol.* **6**, 110 (2015).
142. Nadal, I. *et al.* Shifts in clostridia, bacteroides and immunoglobulin-coating fecal bacteria associated with weight loss in obese adolescents. *Int. J. Obes.* **33**, 758–767 (2009).
143. Santacruz, A. *et al.* Interplay Between Weight Loss and Gut Microbiota

Composition in Overweight Adolescents. *Obesity* **17**, 1906–1915 (2009).

144. Shin, N. R. *et al.* An increase in the Akkermansia spp. population induced by metformin treatment improves glucose homeostasis in diet-induced obese mice. *Gut* **63**, 727–735 (2014).
145. Xu, Y. *et al.* Function of Akkermansia muciniphila in Obesity: Interactions With Lipid Metabolism, Immune Response and Gut Systems. *Front. Microbiol.* **11**, 219 (2020).
146. Depommier, C. *et al.* Supplementation with Akkermansia muciniphila in overweight and obese human volunteers: a proof-of-concept exploratory study. *Nature Medicine* **25**, 1096–1103 (2019).
147. Plovier, H. *et al.* A purified membrane protein from Akkermansia muciniphila or the pasteurized bacterium improves metabolism in obese and diabetic mice. *Nat. Med.* **23**, 107–113 (2017).
148. Saad, M. J. A., Santos, A. & Prada, P. O. Linking Gut Microbiota and Inflammation to Obesity and Insulin Resistance. *Physiology* **31**, 283–293 (2016).
149. Medzhitov, R. & Horng, T. Transcriptional control of the inflammatory response. *Nat. Rev. Immunol.* **9**, 692–703 (2009).
150. Shoelson, S. E. Inflammation and insulin resistance. *J. Clin. Invest.* **116**, 1793–1801 (2006).
151. Blüher, M. Adipose tissue inflammation: a cause or consequence of obesity-related insulin resistance? *Clin. Sci.* **130**, 1603–1614 (2016).
152. Cani, P. D. *et al.* Metabolic endotoxemia initiates obesity and insulin resistance. *Diabetes* **56**, 1761–72 (2007).
153. Hersoug, L.-G., Møller, P. & Loft, S. Gut microbiota-derived lipopolysaccharide uptake and trafficking to adipose tissue: implications for inflammation and obesity. *Obes. Rev.* **17**, 297–312 (2016).
154. Burcelin, R., Garidou, L. & Pomié, C. Immuno-microbiota cross and talk: The new paradigm of metabolic diseases. *Semin. Immunol.* **24**, 67–74 (2012).
155. Teixeira, T. F. S. *et al.* Intestinal permeability parameters in obese patients are correlated with metabolic syndrome risk factors. *Clin. Nutr.* **31**, 735–740 (2012).
156. Parada Venegas, D. *et al.* Short Chain Fatty Acids (SCFAs)-Mediated Gut Epithelial and Immune Regulation and Its Relevance for Inflammatory Bowel Diseases. *Front. Immunol.* **10**, 277 (2019).
157. Everard, A. & Cani, P. D. Diabetes, obesity and gut microbiota. *Best Pract. Res. Clin. Gastroenterol.* **27**, 73–83 (2013).

158. E, B., P, H. & KL, P. Determinants of Adherence to Lifestyle Intervention in Adults With Obesity: A Systematic Review. *Clin. Obes.* **7**, (2017).
159. Cheung, B. M. Y., Cheung, T. T. & Samaranayake, N. R. Safety of antiobesity drugs. *Ther. Adv. Drug Saf.* **4**, 171 (2013).
160. Pories, W. J. Bariatric Surgery: Risks and Rewards. *J. Clin. Endocrinol. Metab.* **93**, S89 (2008).
161. *DEN180060-Debbie Koeneman*. (2016).
162. Greenway, F. L. *et al.* A Randomized, Double-Blind, Placebo-Controlled Study of Gelesis100: A Novel Nonsystemic Oral Hydrogel for Weight Loss. *Obesity* **27**, 205–216 (2019).
163. Demitri, C. *et al.* Novel superabsorbent cellulose-based hydrogels crosslinked with citric acid. *J. Appl. Polym. Sci.* **110**, 2453–2460 (2008).
164. Galarraga, M. *et al.* Adiposoft: Automated software for the analysis of white adipose tissue cellularity in histological sections. *J. Lipid Res.* **53**, 2791–2796 (2012).
165. KJ, L. & TD, S. Analysis of Relative Gene Expression Data Using Real-Time Quantitative PCR and the 2(-Delta Delta C(T)) Method. *Methods* **25**, (2001).
166. Canfora, E. E., Meex, R. C. R., Venema, K. & Blaak, E. E. Gut microbial metabolites in obesity, NAFLD and T2DM. *Nat. Rev. Endocrinol.* **15**, 261–273 (2019).
167. Citi, S. Intestinal barriers protect against disease. *Science (80-.).* **359**, 1097–1098 (2018).
168. Giordano, A. *et al.* Obese adipocytes show ultrastructural features of stressed cells and die of pyroptosis. *J. Lipid Res.* **54**, 2423–2436 (2013).
169. Ziegler, A. K. *et al.* An anti-inflammatory phenotype in visceral adipose tissue of old lean mice, augmented by exercise. *Sci. Rep.* **9**, 12069 (2019).
170. Duan, Y. *et al.* Inflammatory links between high fat diets and diseases. *Front. Immunol.* **9**, (2018).
171. Tilg, H., Zmora, N., Adolph, T. E. & Elinav, E. The intestinal microbiota fuelling metabolic inflammation. *Nat. Rev. Immunol.* (2019). doi:10.1038/s41577-019-0198-4
172. Soares, A., Beraldi, E. J., Ferreira, P. E. B., Bazotte, R. B. & Buttow, N. C. Intestinal and neuronal myenteric adaptations in the small intestine induced by a high-fat diet in mice. *BMC Gastroenterol.* **15**, 3 (2015).
173. Ding, S. *et al.* High-Fat Diet: Bacteria Interactions Promote Intestinal

Inflammation Which Precedes and Correlates with Obesity and Insulin Resistance in Mouse. *PLoS One* **5**, e12191 (2010).

174. Chassaing, B. *et al.* Lack of soluble fiber drives diet-induced adiposity in mice. *Am. J. Physiol. Gastrointest. Liver Physiol.* **309**, G528-41 (2015).
175. Hoffler, U. *et al.* Diet-induced obesity is associated with hyperleptinemia, hyperinsulinemia, hepatic steatosis, and glomerulopathy in C57Bl/6J mice. *Endocrine* **36**, 311–25 (2009).
176. Kanno, A. *et al.* Compensatory hyperinsulinemia in high-fat diet-induced obese mice is associated with enhanced insulin translation in islets. *Biochem. Biophys. Res. Commun.* **458**, 681–686 (2015).
177. MacDonald, P. E. *et al.* The Multiple Actions of GLP-1 on the Process of Glucose-Stimulated Insulin Secretion. *Diabetes* **51**, S434–S442 (2002).
178. Holst, J. J. From the Incretin Concept and the Discovery of GLP-1 to Today's Diabetes Therapy. *Front. Endocrinol. (Lausanne).* **10**, (2019).
179. Polyzos, S. A., Kountouras, J. & Mantzoros, C. S. Obesity and nonalcoholic fatty liver disease: From pathophysiology to therapeutics. *Metabolism.* **92**, 82–97 (2019).
180. Herck, M. A. Van, Vonghia, L. & Francque, S. M. Animal Models of Nonalcoholic Fatty Liver Disease—A Starter's Guide. *Nutrients* **9**, (2017).
181. Fraulob, J. C., Ogg-Diamantino, R., Fernandes-Santos, C., Aguila, M. B. & Mandarim-de-Lacerda, C. A. A Mouse Model of Metabolic Syndrome: Insulin Resistance, Fatty Liver and Non-Alcoholic Fatty Pancreas Disease (NAFPD) in C57BL/6 Mice Fed a High Fat Diet. *J. Clin. Biochem. Nutr.* **46**, 212–23 (2010).
182. Ullah, R. *et al.* Role of nutrition in the pathogenesis and prevention of non-alcoholic fatty liver disease: Recent updates. *International Journal of Biological Sciences* **15**, 265–276 (2019).
183. Van Herck, M. A., Vonghia, L. & Francque, S. M. Animal models of nonalcoholic fatty liver disease—a starter's guide. *Nutrients* **9**, 1–13 (2017).
184. Tiniakos, D. G., Vos, M. B. & Brunt, E. M. Nonalcoholic Fatty Liver Disease: Pathology and Pathogenesis. *Annu. Rev. Pathol. Mech. Dis.* **5**, 145–171 (2010).
185. Richards, P. *et al.* High fat diet impairs the function of glucagon-like peptide-1 producing L-cells. *Peptides* **77**, 21 (2016).
186. Sun, Y. *et al.* Restoration of GLP-1 secretion by Berberine is associated with protection of colon enterocytes from mitochondrial overheating in diet-induced obese mice. *Nutr. Diabetes* **8**, 53 (2018).

187. Chakaroun, R. M., Massier, L. & Kovacs, P. Gut Microbiome, Intestinal Permeability, and Tissue Bacteria in Metabolic Disease: Perpetrators or Bystanders? *Nutrients* **12**, 1082 (2020).
188. Teixeira, T. F. S., Collado, M. C., Ferreira, C. L. L. F., Bressan, J. & Peluzio, M. do C. G. Potential mechanisms for the emerging link between obesity and increased intestinal permeability. *Nutr. Res.* **32**, 637–647 (2012).
189. Fukui, H. Increased Intestinal Permeability and Decreased Barrier Function: Does It Really Influence the Risk of Inflammation? *Inflamm. Intest. Dis.* **1**, 135 (2016).
190. Nagpal, R. & Yadav, H. Bacterial Translocation from the Gut to the Distant Organs: An Overview. *Ann. Nutr. Metab.* **71**, 11–16 (2017).
191. Luca, C. de & Olefsky, J. M. Inflammation and Insulin Resistance. *FEBS Lett.* **582**, 97 (2008).
192. Tarantino, G., Savastano, S. & Colao, A. Hepatic steatosis, low-grade chronic inflammation and hormone/growth factor/adipokine imbalance. *World J. Gastroenterol.* **16**, 4773 (2010).
193. Mouries, J. *et al.* Microbiota-driven gut vascular barrier disruption is a prerequisite for non-alcoholic steatohepatitis development. *J. Hepatol.* (2019). doi:10.1016/j.jhep.2019.08.005
194. Thaiss, C. A. *et al.* Hyperglycemia drives intestinal barrier dysfunction and risk for enteric infection. **1383**, 1376–1383 (2018).
195. Tomas, J. *et al.* High-fat diet modifies the PPAR-γ pathway leading to disruption of microbial and physiological ecosystem in murine small intestine. *Proc. Natl. Acad. Sci. U. S. A.* **113**, E5934–E5943 (2016).
196. Tanaka, S. *et al.* High-fat diet-derived free fatty acids impair the intestinal immune system and increase sensitivity to intestinal epithelial damage. *Biochem. Biophys. Res. Commun.* **522**, 971–977 (2020).
197. Odenwald, M. A. & Turner, J. R. The intestinal epithelial barrier: A therapeutic target? *Nat. Rev. Gastroenterol. Hepatol.* **14**, 9–21 (2017).
198. Al-Sadi, R. *et al.* Occludin regulates macromolecule flux across the intestinal epithelial tight junction barrier. *Am. J. Physiol. Liver Physiol.* **300**, G1054–G1064 (2011).
199. Pope, J. L. *et al.* Claudin-1 regulates intestinal epithelial homeostasis through the modulation of Notch-signalling. *Gut* **63**, 622–634 (2014).
200. Luettig, J., Rosenthal, R., Barmeyer, C. & Schulzke, J. Claudin-2 as a mediator of leaky gut barrier during intestinal inflammation. *Tissue Barriers* **3**, (2015).

201. Olefsky, J. M. & Glass, C. K. Macrophages, Inflammation, and Insulin Resistance. *Annu. Rev. Physiol.* **72**, 219–246 (2010).
202. Draisma, A., Pickkers, P., Bouw, M. P. W. J. M. & van der Hoeven, J. G. Development of endotoxin tolerance in humans in vivo. *Crit. Care Med.* **37**, 1261–7 (2009).
203. Kuwabara, W. M. T., Yokota, C. N. F., Curi, R. & Alba-Loureiro, T. C. Obesity and Type 2 Diabetes mellitus induce lipopolysaccharide tolerance in rat neutrophils. *Sci. Rep.* **8**, 17534 (2018).
204. Han, J. M. & Levings, M. K. Adipose Inflammation Immune Regulation in Obesity-Associated. (2020). doi:10.4049/jimmunol.1301035
205. Dabke, K., Hendrick, G. & Devkota, S. The gut microbiome and metabolic syndrome. *J. Clin. Invest.* **129**, 4050–4057 (2019).
206. Frazier, T. H., DiBaise, J. K. & McClain, C. J. Gut Microbiota, Intestinal Permeability, Obesity-Induced Inflammation, and Liver Injury. *J. Parenter. Enter. Nutr.* **35**, 14S-20S (2011).
207. Teixeira, T. F. S., Collado, M. C., Ferreira, C. L. L. F., Bressan, J. & Peluzio, M. do C. G. Potential mechanisms for the emerging link between obesity and increased intestinal permeability. *Nutr. Res.* **32**, 637–647 (2012).
208. Murphy, E. A., Velazquez, K. T. & Herbert, K. M. Influence of High-Fat-Diet on Gut Microbiota: A Driving Force for Chronic Disease Risk. doi:10.1097/MCO
209. Davis, C. D. The Gut Microbiome and Its Role in Obesity. *Nutr. Today* **51**, 167–174 (2016).
210. Sun, L. *et al.* Insights into the role of gut microbiota in obesity: pathogenesis, mechanisms, and therapeutic perspectives. *Protein Cell* **9**, 397–403 (2018).
211. Leocádio, P. C. L., Oriá, R. B., Crespo-Lopez, M. E. & Alvarez-Leite, J. I. Obesity: More Than an Inflammatory, an Infectious Disease? *Front. Immunol.* **10**, 3092 (2020).
212. Ley, R. E. *et al.* Obesity alters gut microbial ecology. *Proc. Natl. Acad. Sci. U. S. A.* **102**, 11070–11075 (2005).
213. Turnbaugh, P. J. *et al.* A core gut microbiome between lean and obesity twins. *Nature* **457**, 222–227 (2009).
214. Louis, S., Tappu, R.-M., Damms-Machado, A., Huson, D. H. & Bischoff, S. C. Characterization of the Gut Microbial Community of Obese Patients Following a Weight-Loss Intervention Using Whole Metagenome Shotgun Sequencing. *PLoS One* **11**, e0149564 (2016).

215. Cani, P. D. & de Vos, W. M. Next-generation beneficial microbes: The case of Akkermansia muciniphila. *Frontiers in Microbiology* **8**, (2017).
216. Teixeira, T. F. S., Collado, M. C., Ferreira, C. L. L. F., Bressan, J. & Peluzio, M. do C. G. Potential mechanisms for the emerging link between obesity and increased intestinal permeability. *Nutr. Res.* **32**, 637–647 (2012).
217. Genser, L. *et al.* Increased jejunal permeability in human obesity is revealed by a lipid challenge and is linked to inflammation and type 2 diabetes. *J. Pathol.* **246**, 217–230 (2018).
218. Thaiss, C. A. *et al.* Hyperglycemia drives intestinal barrier dysfunction and risk for enteric infection. *Science (80-.).* **359**, 1376–1383 (2018).
219. Czech, M. P. Insulin action and resistance in obesity and type 2 diabetes. *Nat. Med.* **23**, 804 (2017).
220. Alligier, M. *et al.* Subcutaneous Adipose Tissue Remodeling during the Initial Phase of Weight Gain Induced by Overfeeding in Humans. *J. Clin. Endocrinol. Metab.* **97**, E183–E192 (2012).
221. Petersen, M. C. & Shulman, G. I. Mechanisms of Insulin Action and Insulin Resistance. *Physiol. Rev.* **98**, 2133–2223 (2018).
222. Thaiss, C. A. *et al.* Hyperglycemia drives intestinal barrier dysfunction and risk for enteric infection. *Science (80-.).* **359**, 1376–1383 (2018).
223. Winer, D. A., Luck, H., Tsai, S. & Winer, S. The Intestinal Immune System in Obesity and Insulin Resistance. *Cell Metab.* **23**, 413–426 (2016).
224. Xiao, H. & Kang, S. The Role of the Gut Microbiome in Energy Balance With a Focus on the Gut-Adipose Tissue Axis. *Front. Genet.* **11**, 297 (2020).
225. Obesity Management Interventions Delivered in Primary Care for Patients with Hypertension or Cardiovascular Disease: A Review of Clinical Effectiveness. (2014).
226. Promrat, K. *et al.* Randomized Controlled Trial Testing the Effects of Weight Loss on Nonalcoholic Steatohepatitis (NASH). *Hepatology* **51**, 121 (2010).
227. Madsbad, S. The role of glucagon-like peptide-1 impairment in obesity and potential therapeutic implications. *Diabetes, Obesity and Metabolism* **16**, 9–21 (2014).
228. Anandhakrishnan, A. & Korbonits, M. Glucagon-like peptide 1 in the pathophysiology and pharmacotherapy of clinical obesity. *World J. Diabetes* **7**, 572 (2016).
229. Filippatos, T. D., Panagiotopoulou, T. V. & Elisaf, M. S. Adverse Effects of GLP-

1 Receptor Agonists. *Rev. Diabet. Stud.* **11**, 202 (2014).

230. Rosenstock, J. & Zinman, B. Dipeptidyl peptidase-4 inhibitors and the management of type 2 diabetes mellitus. *Curr. Opin. Endocrinol. Diabetes Obes.* **14**, 98–107 (2007).
231. Gallwitz, B. Clinical Use of DPP-4 Inhibitors. *Front. Endocrinol. (Lausanne).* **10**, 389 (2019).
232. Bischoff, S. C. *et al.* Intestinal permeability – a new target for disease prevention and therapy. *BMC Gastroenterol.* **14**, (2014).
233. Schulzke, J. D. *et al.* Epithelial Tight Junctions in Intestinal Inflammation. *Ann. N. Y. Acad. Sci.* **1165**, 294–300 (2009).
234. Blander, J. M. A new approach for inflammatory bowel disease therapy. *Nat. Med.* **25**, 545–546 (2019).
235. Ahmad, R., Rah, B., Bastola, D., Dhawan, P. & Singh, A. B. Obesity-induces Organ and Tissue Specific Tight Junction Restructuring and Barrier Deregulation by Claudin Switching. *Sci. Rep.* **7**, 5125 (2017).
236. N, M. *et al.* Effect of Lipopolysaccharide on the Progression of Non-Alcoholic Fatty Liver Disease in High Caloric Diet-Fed Mice. *Scand. J. Immunol.* **83**, (2016).
237. Al-Attas, O. S. *et al.* Changes in endotoxin levels in T2DM subjects on anti-diabetic therapies. *Cardiovasc. Diabetol.* **8**, 20 (2009).
238. Laugerette, F., Vors, C., Peretti, N. & Michalski, M.-C. Complex links between dietary lipids, endogenous endotoxins and metabolic inflammation. *Biochimie* **93**, 39–45 (2011).
239. Mazidi, M., Rezaie, P., Kengne, A. P., Mobarhan, M. G. & Ferns, G. A. Gut microbiome and metabolic syndrome. *Diabetes Metab. Syndr. Clin. Res. Rev.* **10**, S150–S157 (2016).
240. Takiishi, T., Fenero, C. I. M. & Câmara, N. O. S. Intestinal barrier and gut microbiota: Shaping our immune responses throughout life. *Tissue Barriers* **5**, (2017).
241. Hamilton, M. K., Boudry, G., Lemay, D. G. & Raybould, H. E. Changes in intestinal barrier function and gut microbiota in high-fat diet-fed rats are dynamic and region dependent. *Am. J. Physiol. Liver Physiol.* **308**, G840–G851 (2015).
242. Rooks, M. G. & Garrett, W. S. Gut microbiota, metabolites and host immunity. *Nat. Rev. Immunol.* **16**, 341 (2016).
243. Kulecka, M. *et al.* Prolonged transfer of feces from the lean mice modulates gut microbiota in obese mice. *Nutr. Metab. (Lond).* **13**, 57 (2016).

244. Ellekilde, M. *et al.* Transfer of gut microbiota from lean and obese mice to antibiotic-treated mice. *Sci. Rep.* **4**, (2014).
245. A, V. *et al.* Transfer of Intestinal Microbiota From Lean Donors Increases Insulin Sensitivity in Individuals With Metabolic Syndrome. *Gastroenterology* **143**, (2012).
246. Fei, N. & Zhao, L. An opportunistic pathogen isolated from the gut of an obese human causes obesity in germfree mice. *ISME J.* **7**, 880–884 (2013).
247. F, B. *et al.* The Gut Microbiota as an Environmental Factor That Regulates Fat Storage. *Proc. Natl. Acad. Sci. U. S. A.* **101**, (2004).
248. Turnbaugh, P. J. *et al.* An obesity-associated gut microbiome with increased capacity for energy harvest. *Nature* **444**, 1027–1031 (2006).
249. Muscogiuri, G. *et al.* Gut microbiota: a new path to treat obesity. *Int. J. Obes. Suppl.* **9**, 10–19 (2019).
250. Castaner, O. *et al.* The gut microbiome profile in obesity: A systematic review. *Int. J. Endocrinol.* **2018**, (2018).
251. Koliada, A. *et al.* Association between body mass index and Firmicutes/Bacteroidetes ratio in an adult Ukrainian population. *BMC Microbiol.* **17**, (2017).
252. Almiron-Roig, E. *et al.* Factors that determine energy compensation: a systematic review of preload studies. *Nutr. Rev.* **71**, 458–473 (2013).
253. Tsilingiri, K., Sonzogni, A., Caprioli, F. & Rescigno, M. A novel method for the culture and polarized stimulation of human intestinal mucosa explants. *J. Vis. Exp.* e4368 (2013). doi:10.3791/4368